LEABHARLANN CHOLÁISTE NA TRÍONÓIDE, BAILE ÁTHA CLIATH | TRINITY COLLEGE LIBRARY DUBLIN
Ollscoil Átha Cliath | The University of Dublin

Terms and Conditions of Use of Digitised Theses from Trinity College Library Dublin

Copyright statement

All material supplied by Trinity College Library is protected by copyright (under the Copyright and Related Rights Act, 2000 as amended) and other relevant Intellectual Property Rights. By accessing and using a Digitised Thesis from Trinity College Library you acknowledge that all Intellectual Property Rights in any Works supplied are the sole and exclusive property of the copyright and/or other IPR holder. Specific copyright holders may not be explicitly identified. Use of materials from other sources within a thesis should not be construed as a claim over them.

A non-exclusive, non-transferable licence is hereby granted to those using or reproducing, in whole or in part, the material for valid purposes, providing the copyright owners are acknowledged using the normal conventions. Where specific permission to use material is required, this is identified and such permission must be sought from the copyright holder or agency cited.

Liability statement

By using a Digitised Thesis, I accept that Trinity College Dublin bears no legal responsibility for the accuracy, legality or comprehensiveness of materials contained within the thesis, and that Trinity College Dublin accepts no liability for indirect, consequential, or incidental, damages or losses arising from use of the thesis for whatever reason. Information located in a thesis may be subject to specific use constraints, details of which may not be explicitly described. It is the responsibility of potential and actual users to be aware of such constraints and to abide by them. By making use of material from a digitised thesis, you accept these copyright and disclaimer provisions. Where it is brought to the attention of Trinity College Library that there may be a breach of copyright or other restraint, it is the policy to withdraw or take down access to a thesis while the issue is being resolved.

Access Agreement

By using a Digitised Thesis from Trinity College Library you are bound by the following Terms & Conditions. Please read them carefully.

I have read and I understand the following statement: All material supplied via a Digitised Thesis from Trinity College Library is protected by copyright and other intellectual property rights, and duplication or sale of all or part of any of a thesis is not permitted, except that material may be duplicated by you for your research use or for educational purposes in electronic or print form providing the copyright owners are acknowledged using the normal conventions. You must obtain permission for any other use. Electronic or print copies may not be offered, whether for sale or otherwise to anyone. This copy has been supplied on the understanding that it is copyright material and that no quotation from the thesis may be published without proper acknowledgement.

Exploring the function of *SUPERMAN*, and the repression of the trichome initiation pathway, during *Arabidopsis* flower development

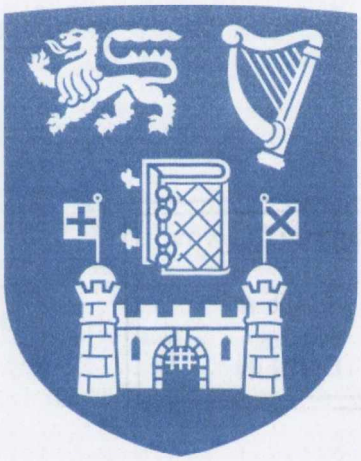

Trinity College Dublin

The University of Dublin

A thesis submitted to The University of Dublin for the degree of Doctor in Philosophy by Darragh Stewart, 2017.

Thesis supervisor: Prof. Frank Wellmer
Smurfit institute of genetics
Dublin University
Trinity College

TRINITY LIBRARY
0 8 AUG 2017
DUBLIN

Thesis 11403

Declaration

I declare that this thesis has not been submitted as an exercise for a degree at this or any other university and it is entirely my own work.

I agree to deposit this thesis in the University's open access institutional repository or allow the Library to do so on my behalf, subject to Irish Copyright Legislation and Trinity College's conditions of use and acknowledgement.

Summary

The notion that flowers are in essence modified leaves was hypothesized as far back as 1790. Supporting this early hypothesis, genetic analyses of floral organ identity genes in the model plant *Arabidopsis thaliana* showed that the combined loss of their activities leads to the conversion of floral organs into leaf-like structures. However, how these regulators act to suppress leaf development and control the formation of floral organs is currently not well understood. To address this knowledge gap, I used trichome initiation as a proxy for the leaf developmental program and investigated the genetic mechanisms that contribute to the suppression of trichome formation in flowers. To this end, I employed mainly a combination of mutant analyses and gene perturbation experiments. My work showed that the floral organ identity factors are directly linked, in several positions, into the regulatory network that controls trichome formation throughout plant development. It further revealed that the control of this key feature of leaf development is mediated by both independent and interacting pathways, which appear to act in a partially redundant manner. Thus, the repression of trichome initiation is a surprisingly complex regulatory process, suggesting that the suppression of other leaf features during flower development might be equally intricate.

In the second part of this thesis, the function of the gene *SUPERMAN* (*SUP*) during early flower development was investigated. *SUP* encodes a zinc-finger domain-containing transcription factor, which is known to be involved in regulating the boundary between the third and fourth floral whorls in *Arabidopsis*. However, the genes which are both indirectly and directly regulated by SUP, and the processes it controls, have remained largely elusive. To better understand SUP's function, I used transcriptomics approaches and genetic analyses and identified promising candidate genes, whose mis-expression likely contributes to the expression of the *sup* mutant phenotype, which is chiefly characterised by the formation of supernumerary stamens.

Acknowledgments

First I'd like to thank Prof. Frank Wellmer for the opportunities he gave me to work in the laboratory over the years, and for guiding me through my doctorate. For his patience, advice, and kind words, for without him I wouldn't be the geneticist I am today.

I'd also like to thank everyone who I worked with closely in the laboratory. Kamila who listened to me behind her over the 4 years. To Bennett for keeping me sane in the lab and pushing me along For Bei Bei's smile greeting me every morning, and also Dr. Pat Ryan for all the help with the data analysis. I'd especially like to thank all previous members of the laboratory, in particular Dr. Diarmuid Ó'Maoiléidigh, who was a steady guide and tutor to my work even from afar.

Where I got today wouldn't have been possible without the unrelenting support from my family. I'd like to thank my Mum and Dad who gave me so much support, especially when times got really hard, and my brothers Jamie and Cameron, and sister Daneka. To my loving one of a kind Nan, who passed away during my time in the laboratory. I know she was looking down on me at the toughest times giving me her blessings.

Finally, I'd like to thank my friends and my wonderful girlfriend Aoife. Without their love, support, encouragement, and positive energy, I wouldn't have gotten half as far as I have today.

Publications

Stewart, D., Graciet, E., and Wellmer, F. (2016). **Molecular and regulatory mechanisms controlling floral organ development.** *FEBS Journal* **283**, 1823–1830.

Diarmuid S. Ó'Maoiléidigh [§], Darragh Stewart [§] and Frank Wellmer. (2016) **The successive initiation and convergence of transcriptional networks underlies the metamorphosis of leaves to flowers** (In preparation).

[§] Equal contribution

LIST OF ABBREVIATIONS

$35S_{PRO}$ – Cauliflower Mosaic Virus 35S promoter
AG – AGAMOUS
amiRNA – artificial micro-RNA
AP1 – APETALA1
AP2 – APETALA2
AP3 – APETALA3
bHLH – basic Helix–Loop–Helix
BLAST – Basic Local Alignment Search Tool
bp – base pairs
C2H2 – Cys_2His_2
CAL – CAULIFLOWER
cDNA – complementary deoxyribonucleic acid
CDS – coding DNA sequence
ChIP – chromatin Immunoprecipitation
CPC - CAPRICE
CRISPR - Clustered regularly interspaced short palindromic repeats
DEG – Differentially expressed genes
DNA – Deoxyribonucleic acid
DRN – DORNROSCHEN
DRNL- DORNROSCHEN-LIKE
EAR – Ethylene responsive element binding factor associated Amphiphilic Repression
EtOH – ethanol
FIS – Floral Induction system
GFP – Green Fluorescent Protein
GIS - GLABROUS INFLORESCENCE STEMS
GL – GLABRA
GO - Gene Ontology
GR – Glucocorticoid Receptor
h - hours
KAN – KANADI
L–*er* – Landsberg *erecta*
LFY - LEAFY
mRNA – messenger ribonucleic acid
PI – PISTILLATA
PCR – polymerase chain reaction
qPCR – quantitative polymerase chain reaction
MBW – single repeat R2R3 MYB, basic Helix-Loop-Helix, Wd-40 repeat
mRNA – messenger ribonucleic acid

ORF – Open Reading Frame
PCR – Polymerase Chain Reaction
qPCR – quantitative polymerase chain reaction
RGEN - RNA-guided endo-nuclease
RT-PCR – reverse transcription polymerase chain reaction
SAM – Shoot Apical Meristem
SEP - SEPALLATA
SHP - SHATTERPROOF
SPL- SQUAMOSA PROMOTER BINDING PROTEIN-LIKE
SRDX – repressor domain derived from the SUPERMAN protein
SUP – SUPERMAN
T0 – unselected transformed seeds
T1 – The first progeny that is derived from a transformed plant
T-DNA – Transfer DNA
TAIR – The Arabidopsis Information Resource
TCL – TRICHOMELESS
TF – Transcription factor
TRY – TRIPTYCHON
TTG - TRANSPARENT TESTA GLABRA
UFO - UNUSUAL FLORAL ORGANS
ZFP – ZINC FINGER PROTEIN

Table of contents

TABLE OF CONTENTS 1

LIST OF FIGURES 4

LIST OF TABLES 8

CHAPTER 1 – INTRODUCTION 9

1.1 *ARABIDOPSIS THALIANA* AS A MODEL ORGANISM FOR STUDYING REPRODUCTIVE DEVELOPMENT IN PLANTS. 9

1.2 INTRODUCTION TO FLOWER DEVELOPMENT 11

1.3 EARLY STEPS DURING FLOWER DEVELOPMENT 12

1.4 THE ABCE MODEL FOR FLORAL ORGAN IDENTITY SPECIFICATION 15

1.5 GENOME-WIDE IDENTIFICATION OF GENES ACTING DOWNSTREAM OF THE FLORAL ORGAN IDENTITY FACTORS 23

1.6 MODERN APPROACHES FOR STUDYING THE GENE REGULATORY NETWORK UNDERLYING FLOWER DEVELOPMENT 28

1.7 PROJECT OUTLINES AND AIMS OF THIS THESIS. 36

CHAPTER 2 - MATERIALS AND METHODS 38

2.1 STRAINS AND GROWTH CONDITIONS 38

2.1.1 Published plant lines 38

2.1.2 Bacterial strains 39

2.1.3 Plant growth media 40

2.1.4 Bacterial growth media 40

2.2 CONSTRUCT CLONING AND GENOTYPING 40

2.2.1 Plasmid DNA preparation 40

2.2.2 FAST EXTRACTION OF *ARABIDOPSIS* GENOMIC DNA 40

2.2.3 CTAB method to extract Genomic DNA 41

2.2.4 Preparation and transformation of chemically competent Escherichia coli cells 41

2.2.5 Preparation and transformation of competent Agrobacterium tumefaciens cells 42

2.2.6 RNA extraction and cDNA synthesis 43

2.3 PLANT TRANSFORMATION AND ISOLATING TRANSFORMED PLANTS 43

2.3.1 Plant transformation and seed sterilization 43
2.3.2 Isolating transgenic plants 44
2.4 Microscopy techniques 44
2.4.1 Light microscope 44
2.4.2 Cryogenic Scanning Electron microscopy (S.E.M.) 45
2.5 Treatment of transgenic lines with inducible promoter systems 45
2.5.1 Ethanol induction of plants 45
2.5.2 Dexamethasone induction of plants 45
2.5.3 Collection of induced tissue 46
2.6 Cloning of artificial-miRNAs 46
2.7 Cloning of CRISPR constructs 47
2.8 Quantitative real-time PCR 47
2.12 GUS staining of plant tissue 48
2.12.1 Staining of Arabidopsis tissue 48
2.12.2 Fixation of tissue 49
2.12.3 Sectioning and slide preparation of tissue 49
2.13 Generation of transgenic lines 49
2.13.1 Generation of a constitutive amiRNA targeting SUP mRNA 49
2.13.2 Generation and expression of an inducible amiRNA targeting SUP mRNA 50
2.13.3 Generation and expression of Inducible over-expression lines of the SUP coding sequence 50
2.13.4 Generation of lines carrying the SUPpro::SUP-GFP rescue construct 51
2.13.5 Crossing the SUPpro::SUP-GFP sup-5 lines into the FIS 52
2.13.6 Generation of lines affecting Cytokinin synthesis 52
2.13.7 Generation and expression of the inducible SHP2-GFP construct 53
2.13.8 Generation of GUS reporter lines 53
CHAPTER 3 – INVESTIGATING THE REPRESSION OF THE TRICHOME INITIATION PATHWAY IN FLORAL REPRODUCTIVE ORGANS **54**
3.1 Introduction 54
3.1.1 The control of trichome Initiation in Arabidopsis thaliana 57
3.1.2 The Lateral Inhibition Model 58
3.1.3 The SQUAMOSA PROMOTER BINDING PROTEIN-LIKE genes regulate trichome formation 61

3.1.4 Role of phytohormones in trichome initiation *62*

3.1.5 Suppression of the leaf developmental programs by AG, AP3, and PI. *63*

3.1.5.1 The $35S_{PRO}$:AlcR/$AlcA_{PRO}$:AG-amiRNA system 66

3.1.5.2 *AG* regulates genes involved in trichome formation 67

3.1.5.3 Other MADS-domain transcription factors supress trichome formation in flowers with *AG* 70

3.1.5.4 *TRY* suppresses trichome initiation in parallel with *AG* 71

3.2 RESULTS 73

3.2.1 AG suppresses the formation of trichomes on carpel valves in parallel with TRY *73*

3.2.2 The known leaf trichome activation complex is required for ectopic trichome initiation on floral organs *75*

3.2.3 The SHATTERPROOF genes regulate trichome formation in flowers together with AG *77*

3.2.4 The SQUAMOSA PROMOTER BINDING PROTEIN-LIKE genes redundantly regulate trichome initiation on carpels *82*

3.2.5 TRY and CPC suppress trichome formation on floral organs *84*

3.2.6 AG acts as negative regulator of cytokinin signalling to repress trichome formation on flowers *94*

3.2.7 CPC and TRY act as negative regulators of cytokinin signalling to prevent trichome formation in flowers *99*

3.2.8 CPC and TRY act antagonistically to pattern the gynoecium *105*

3.2.9 KANADI1 and AG suppress the formation of trichomes and control the growth of the gynoecium *111*

3.3 DISCUSSION 113

3.3.1 AG suppresses trichome formation in flowers with the help of other MADS-domain transcription factors *115*

3.3.2 The SPLs repress trichome formation in flowers in parallel with AG *115*

3.3.3 Regulation of cytokinin sensitivity is key to supressing trichome formation in flowers and the regulation of carpel patterning *117*

3.3.4 Floral trichomes as a possible new avenue for crop protection *118*

CHAPTER 4 - INVESTIGATING THE GENE REGULATORY NETWORK DOWNSTREAM OF THE ZINC-FINGER TRANSCRIPTION FACTOR SUPERMAN 120

4.1 INTRODUCTION 120

4.2 RESULTS 126

4.2.1 Phenotypic variation between mutant alleles of SUP *126*
4.2.2 Generation of an amiRNA targeting SUP *129*
4.2.3 Generation of an inducible amiRNA against SUP *132*
4.2.4 Generation of a stable knockout of SUPERMAN using CRISPR/Cas9 technology *135*
4.2.5 Genes acting downstream of SUP *136*
4.2.6 Mutations in DORNROESCHEN and DORNROESCHEN-LIKE partially rescue the sup mutant phenotype *144*
4.2.7 Genes directly regulated by SUP *147*
4.2.8 Generation of inducible SUP-GFP overexpression lines *149*
4.2.9 Generation of a construct for the overexpression of a dominant negative version of SUP *154*
4.2.10 Exogenous cytokinin treatment causes a partial rescue of the SUP mutant phenotype *.155*
4.2.11 Partial rescue of sup by overexpression of a known cytokinin biosynthesis gene *158*
4.3 DISCUSSION 160
4.3.1 The role of SUP in flower development *160*
4.3.2 Genes and processes regulated by SUP *162*
4.2.3 SUP's role in regulating phytohormone-dependent processes *164*
CHAPTER 5 – GENERAL DISCUSSION AND FUTURE WORK 166
REFERENCES 170
APPENDIX 185

List of figures

Chapter 1

Figure 1.1: Life cycle of Arabidopsis thaliana 10
Figure 1.2: An Arabidopsis thaliana flower 13
Figure 1.3: ABCE model of floral organ identity specification 17
Figure 1.4: Working model for the activities of floral organ identity factor complexes. 23
Figure 1.5: A system for the induction of synchronous flower development 30
Figure 1.6: CRISPR/Cas9 system for genome editing 33

Chapter 3

Figure 3. 1 The lateral inhibition model 59
Figure 3. 2 Global expression patterns of genes controlled by B and C function regulators. ..65
Figure 3. 3 Molecular and phenotypic characteristics of AG perturbation..... 69
Figure 3.4: *AG* suppresses the formation of trichomes on carpel valves in parallel with *TRY*. 74
Figure 3.5: The leaf trichome activation complex is needed for trichomes to form on floral organs. 76
Figure 3.6: The SHP genes redundantly regulate trichome formation with AG. 78
Figure 3.7: Over-expression of SHP2 rescues the ag mutant phenotype..... 79
Figure 3.8: Over-expression of SHP2 can partially repress trichome initiation caused by an AG knockdown. 81
Figure 3.9: The SPL genes redundantly regulate trichome initiation on carpels with AG. 84
Figure 3.10: TRY represses trichome initiation in parallel with AG..... 85
Figure 3.11: CPC represses trichome initiation together with AG. 87
Figure 3.12: CPC and TRY together contribute to the suppression of floral trichomes..... 88
Figure 3.13: TRY and CPC represses trichome formation with AG. 89
Figure 3.14: Trichomes form on the abaxial side of EtOH-treated AlcA:AG-amiRNA try-29760 cpc-1 flowers..... 91
Figure 3.15: Trichomes form on the adaxial side of EtOH-treated AlcA:AG-amiRNA try-29760 cpc-1 flowers..... 92
Figure 3.16: AG, AP3, TRY, and CPC redundantly repress trichome initiation on the abaxial side of anthers. 94
Figure 3.17: Loss of AG activity leads to increased phytohormone sensitivity and trichome formation on carpel valves..... 96
Figure 3.18: Loss of AG activity leads to cytokinin sensitivity and trichome formation on carpel valves..... 97
Figure 3.19: GIS2 is required for trichome formation on carpels and ZFP8 is downstream of AG to prevent trichome initiation. 98
Figure 3.20: The loss of TRY and CPC activity results in enhanced cytokinin sensitivity in wild-type and AG knockdown lines. 100

Figure 3.21: Quantification of trichomes per carpel valves after EtOH and BAP treatments. 101
Figure 3.22: SEMs of trichome phenotype on try cpc double mutants and AG knockdown lines. 102
Figure 3.23: Trichomes form on the tips of carpels of BAP-treated try cpc flowers after an AG knockdown 103
Figure 3.24: Trichomes form on the tips and abaxial side of anthers, and the adaxial side of carpels, in try cpc and AG knockdown lines treated with BAP 104
Figure 3.25: Trichomes form on the tips of floral organs in the try mutant background. 105
Figure 3.26: TRY and AG suppress cytokinin induced medial gyneoecial tissue outgrows.. 106
Figure 3.27: SEMs of try and AG knockdown lines after 2 weeks of treatments. 108
Figure 3.28: CPC is required for the formation of cytokinin-induced medial gynoecial tissue outgrowths 110
Figure 3.29: AG interacts with KAN1 to suppress trichome formation on carpel valves and medial outgrowths 112
Figure 3.30: SEMs of kan1 mutant flowers following perturbation of AG. 113
Figure 3. 31 Current model for the control of trichomes on floral organs 119

Chapter 4

Figure 4.1: *SUP* expression pattern during flower development and schematic representation of the *SUP* locus 122
Figure 4.2: Mutations in SUP result in supernumerary stamens and extra carpel tissue. 127
Figure 4.3: Defects of sup mutant flowers are allele-dependent. 128
Figure 4.4: Isolation of a functional artificial microRNA against SUP 130
Figure 4.5: Characterization of 35S:$_{PRO}$SUP-amiRNA3-4 plants 132
Figure 4.6: Generation of an inducible amiRNA against SUP. 133
Figure 4.7: Defects observed in flowers of OP$_{PRO}$:SUP-amiRNA3 plants 135
Figure 4.8: Microarray data from the comparison of the transcriptomes of sup-5 FIS vs. pooled wild-type and sup-5 heterozygous FIS 137
Figure 4.9: Analysis of microarray data for sup-5 FIS vs. pooled wild-type and sup-5 heterozygous FIS. 139
Figure 4.10 MA plots of differentially expressed genes of 3.5 d time-point vs. 5 d. 142

Figure 4.11: qRT- PCR on $35S_{PRO}$:AP1-GR ap1 cal sup-5 5 d time-point. 143
Figure 4.12: Loss of DRNL causes partial rescue of the sup-5 mutant phenotype. 145
Figure 4.13: Loss of DRN causes partial rescue of the sup-5 mutant phenotype. 146
Figure 4.14: Loss of DRN rescues the supernumerary stamen phenotype of sup-5.....147
Figure 4.15: Generation of a SUP_{PRO}:SUP-GFP-3'UTR rescue construct. 149
Figure 4.16: Generation of an inducible SUP over-expression line. 151
Figure 4.17: Generation of a dexamethasone-inducible SUP over-expression line. 153
Figure 4.18: Characterization of a construct over-expressing SUP with its repressor domain deleted. 155
Figure 4.19: Exogenous cytokinin treatment can cause a partial rescue of the sup-5 mutant phenotype. 156
Figure 4.20: Exogenous cytokinin treatment restores carpel growth in sup-2 and sup-3 mutant plants. 157
Figure 4.21: Overexpression of ISOPENTENYLTRANSFERASES8 (IPT8) results in a partial rescue of the sup-5 mutant phenotype. 159

Appendix

Supplementary figure 1.1: Schematic of the *SUP* locus depicting mutation sites for the alleles used in this study and their putative protein products.....185

List of tables

Chapter 4

Table 4.1: Selected genes identified as differentially expressed in early stage sup-5 flowers. 141

Appendix

Supplementary Table 1: List of primers used in this study 186

Supplementary Table 2 SUP-amiRNA target sequences 190

Supplementary Table 3: SUPERMAN CRISPR/Cas target sequence 190

Chapter 1 – Introduction

This chapter is based in part on the following article:

Stewart, D., Graciet, E., and Wellmer, F. (2016). Molecular and regulatory mechanisms controlling floral organ development. *FEBS Journal* **283**, 1823–1830.

1.1 *Arabidopsis thaliana* as a model organism for studying reproductive development in plants

Historically, the field of plant research has focused primarily on crop plants due to their pivotal relevance for society. However, most of these plants proved difficult to work with due to their often large and polyploid genomes, long generation times and size. In the mid 1980s, *Arabidopsis thaliana,* a member of the Brassicaceae family, was introduced as a model organism for plant research by Pruitt, Meyerowitz and others (Meyerowitz et al. 1985). *Arabidopsis* has a diploid genome, a short generation time of 6-8 weeks (Fig. 1.1), and its small size allows researchers to grow thousands of plants in the limited space of a laboratory (Meyerowitz et al., 1985). It also has no barrier to self-fertilization and each plant can produce a very large quantity of seeds per generation. *Arabidopsis* was also found to be easily transformed via the 'floral dip' method using *Agrobacterium tumefaciens*, a bacterium used for its Transfer-DNA (T-DNA) integration properties (Clough and Bent, 1998), with a reasonably high rate of efficiency.

Arabidopsis was the first higher plant whose genome was fully sequenced. This success was made possible by the *Arabidopsis* Genome Initiative (AGI), which published the genome sequence in the year 2000 (AGI, 2000). The *Arabidopsis* genome is roughly 120 Mb in size and contains approximately 27,000 genes. The comparison with other angiosperm

genomes revealed that the *Arabidopsis* genome is comparatively small and exhibits a high gene density. Thus, it is ideal for an analysis of plant biology through genetic analyses.

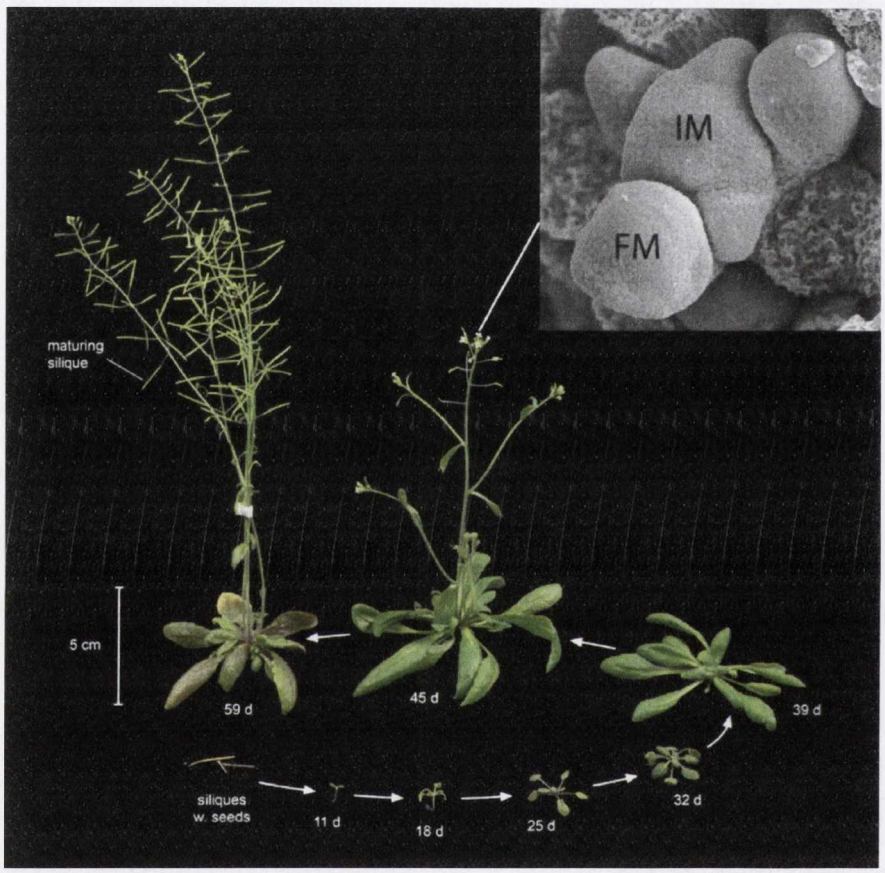

Figure 1.1: Life cycle of *Arabidopsis thaliana*.

The life cycle of *Arabidopsis* starts with the germination of a seed, resulting in the formation of a seedling. The continuous initiation of leaves from the shoot apical meristem leads to the formation of a rosette. Once certain environmental and endogenous conditions have been met the plant switches from vegetative to reproductive growth. Floral meristems (FM) form on the flanks of the inflorescence meristem (IM) in a sequential manner (inset shows a scanning electron micrograph of a inflorescence apex). Once fertilization of the ovules occurs, the gynoecium elongates and forms a silique, in which the seeds develop and mature. The siliques then dry and release the seeds. Under laboratory conditions, it takes roughly 8 weeks in-between generations. Figure modified from Green et al., 2005; Kramer, 2015.

Over the past 25 years, a large number of key regulators of *Arabidopsis* development have been identified mainly through the use of forward and reverse genetics approaches. These include many genes involved in the control of plant reproduction, which is the focus of this thesis.

1.2 Introduction to flower development

Over the past three decades, flower development has served as one of the main model systems to study the genetic and molecular mechanisms that control organogenesis in plants. This work has attracted much attention for at least three reasons. Firstly, flowers contain the reproductive organs of angiosperms, the largest group of land plants, and thus are of pivotal importance for biology. Secondly, because much of the food humans and their livestock consume is directly produced by flowers, they are of considerable agricultural and economic importance so that research on flowers has substantial translational potential. Lastly, although a common blueprint underlies the structure of flowers and the different organ types they contain are largely conserved, flowers of different angiosperms do exhibit a great degree of variation in size, symmetry (which can be radial or bilateral), organ number, organ arrangement (either in a whorled or in a spiral pattern), as well as organ morphology. Therefore, in addition to being an excellent model for studying the genetic principles that underlie plant development, research into flower formation also allows to investigate and to elucidate the evolutionary mechanisms that act upon developmental processes. This is especially relevant in light of the enigmatic evolutionary origin of flowers and the dramatic diversification of angiosperms during the early Cretaceous, which is thought to have been

driven at least in part by the emergence of new floral traits (Armbruster, 2014; Soltis and Soltis, 2014).

Research on flower development was initially based almost exclusively on genetics and molecular biology methods and led to the identification of many key floral regulators, most of which encode transcription factors. In recent years, this work has been complemented by a wide range of additional approaches, including (gen)omic technologies, live imaging and mathematical modelling, resulting in a broad overview of the composition and the structure of the gene regulatory networks that control flower formation. Much of this research has focused on early flower development when floral primordia are initiated on the flanks of an inflorescence meristem and different types of floral organs begin to form from these primordia in a characteristic pattern. However, later-occurring processes such as pollen, ovule and fruit development have also received much attention and work in these areas has resulted in an ever more detailed understanding of the underlying genetic mechanisms (*e.g.*, Causier and Davies, 2014; Hirano et al., 2014; O'Maoileidigh et al., 2014; Pajoro et al., 2014; Prunet and Jack, 2014; Wellmer et al., 2014; Sablowski, 2015).

1.3 Early steps during flower development

Arabidopsis flowers are composed of four organ types: sepals, petals, stamens, and carpels. (Fig. 1.2), which are radially patterned into four distinct whorls. There are four sepals in the outermost whorl, followed by 4 petals in the second whorl, 6 stamens in the third whorl and 2 carpels in the centremost whorl, which fuse to form the gynoecium (Hawkins and Liu, 2014).

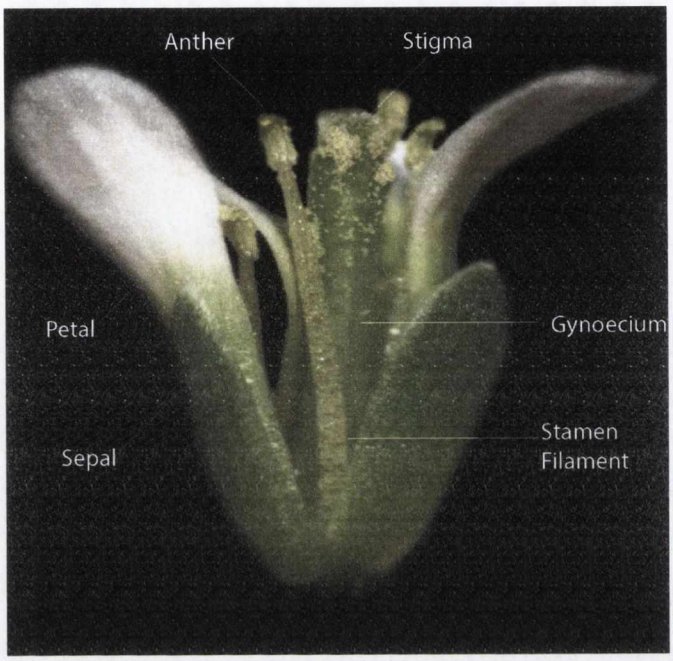

Figure 1.2: An *Arabidopsis thaliana* flower.

Each flower has four sepals in the outermost whorl. This is followed by four petals in the second whorl, and six stamens in the third whorl. A stamen is composed of a filament and an anther, which produces pollen. In the innermost whorl, two carpels fuse together to form the gynoecium (with stigmatic tissue at the apex), where the ovules are contained.

Flower development follows the switch from the vegetative to the reproductive phase of plant development, which involves the transformation of the shoot apical meristem (SAM) into an inflorescence meristem (IM) that produces floral primordia on its flanks in a sequential manner (Wellmer and Riechmann, 2010) (Fig. 1.1 inset). The onset of flowering is tightly controlled by floral pathway integrator genes (for review see: Komeda, 2004; Pajoro et al., 2014). The activities of these genes is controlled by complex regulatory pathways in response to certain environmental cues such as light and temperature, but also by endogenous factors such as the age of the plant (Jack, 2004).

Floral primordia consist of initially undifferentiated cells, which are then programmed by the activated floral meristem identity genes to enter into a developmental program initiating the formation of flowers. The main floral meristem identity genes are *LEAFY* (*LFY*) (Weigel et al., 1992), *APETALA1* (*AP1*) (Mandel et al., 1992), and the *AP1* paralog, *CAULIFOWER* (*CAL*) (Kempin et al., 1995). These transcriptional regulators are thought to act through two independent mechanisms: firstly, they suppress the expression of floral repressors such as *FLOWERING LOCUS C* (*FLC*) and *TERMINAL FLOWER 1* (*TFL1*).

, allowing the flower development program to commence (Kaufmann et al., 2010). Secondly, they act in concert with additional regulators to activate the expression of floral organ identity genes in specific regions of the developing floral bud (Lohmann and Weigel, 2002; Parcy et al., 1998).

The *lfy* null mutation causes a transformation of the first few flowers into leaves and later-arising flowers are replaced by leaf-like bracts with abnormal flowers forming from the base of these bracts (Parcy et al., 1998). *LFY* is directly upstream of *AP1* activating it early on (Wagner et al., 1999). *LFY* has also been shown to be sufficient in determining floral fate in the lateral shoot meristems (Liljegren et al., 1999; Parcy et al., 1998; Weigel and Nilsson, 1995). Early experiments also showed that the interaction of *LFY* with a *LFY*-responsive enhancer in the floral organ identity gene AGAMOUS (*AG*) was required for *AG* activity in plants, proving *LFY* was indeed upstream to the floral organ identity genes (Busch et al., 1999).

LFY is thought to have several co-factors, in part because a fusion of LFY to the activation domain from the viral transcription factor VP16 (LFY:VP16) was seen to be sufficient for floral development. Here, the other proteins were thought to be functionally

replaced by the VP16 domain (Parcy et al., 1998). One of these co-factors was found to be the floral organ identity factor SEPALLATA3 (SEP3) (see also next section). These plants which constitutively expressed both LFY and SEP3 were shown to develop ectopic petals, carpels and ovules on rosette leaves and on the axils of cauline leaves phenocopying LFY:VP16 plants (Castillejo et al., 2005). Another gene known to function with *LFY* in activating the floral organ identity genes is *UNUSUAL FLORAL ORGANS* (*UFO*) (Lee et al., 1997). *UFO* encodes an F-box protein with a likely function in protein degradation and has been shown to physically interact with LFY (Chae et al., 2008).

The stem cell regulator WUSCHEL (WUS) was also found to work in concert with LFY to activate *AG* (Lohmann et al., 2001; Lenhard et al., 2001). *WUS* is expressed in the developing floral meristem cells that will eventually form the carpels and stamens, it is known to also maintain the pluripotent cells of the floral meristem (Mayer et al., 1998). It was also found that a negative feedback loop exists between AG and *WUS*. In wild-type flowers, *WUS* expression is turned off at stage 6 in the centre of the flower where the floral stem cell niche is abolished in the formation of the central gynoecium (Mayer et al., 1998). However, in the *ag* mutant background *WUS* expression was seen to be still active in the meristem of these flowers, which results in the hallmark indeterminate flower of *ag* (Lohmann et al., 2001; Lenhard et al., 2001).

1.4 The ABCE model for floral organ identity specification

Floral organs are specified by the combined activities of floral organ identity genes. These genes were initially identified based on floral mutants that show homeotic transformations, *i.e.* the conversion of certain types of floral organs into others. Based on these mutant

phenotypes and the genetic interactions between the individual mutants, it was proposed in the so-called ABC model that: i) 'A function' gene activity alone leads to the formation of sepals; ii) the combined activities of A and B function genes result in petal development; iii) B and C gene activities together are sufficient for stamen formation; iv) C function activity alone specifies carpels; and v) A and C function activities act in a mutually antagonistic manner to suppress each others function (Bowman et al., 1989, 1991; Coen and Meyerowitz, 1991). The ABC model was later extended to include E function genes, which were found to be important for the formation of all floral organ types (Pelaz et al., 2000; Ditta et al., 2004). Further to the E function genes, D function genes were proposed to be required for ovule development (Colombo et al., 1995; Pinyopich et al., 2003). The genes found to be necessary for ovule development were *SEEDSTICK* (*STK*), which controls ovule identity and seed coat development (Colombo et al., 2008), and *SHATTERPROOF1* (*SHP1*) and *SHATTERPROOF*2 (*SHP*2), which redundantly regulate carpel margin meristem lignification (Colombo et al., 2010; Pinyopich et al., 2003). Ectopically expressing the *SHP* genes in sepals is sufficient to transform them into carpeloid organs, which can produce ovules (Favaro et al., 2003).

Although the ideas central to the ABCDE model have been largely confirmed through a wide range of experimental approaches, the original concept of A function gene activity has been put into doubt because corresponding mutants could not be identified in most of the species that have been investigated in this regard. Also, *APETALA2* (*AP2*), one of the A function genes in *Arabidopsis*, was found to be only indirectly involved in organ specification and to instead contribute to the proper patterning of emerging floral primordia (Krogan et al., 2012). However, *AP2* does mediate part of the antagonism between A and C function activities and thus fulfils one of the tenets of the ABC model. To reconcile the data obtained

from studying flower development in different species, it has been proposed that A function is mediated by genes that also confer identity to floral primordia (Causier et al., 2010). Thus, one may view sepals (which according to the ABC model are specified by A function genes) as the default state of a floral organ that is then modified by the activities of the other floral organ identity genes to give rise to petals, stamens and carpels.

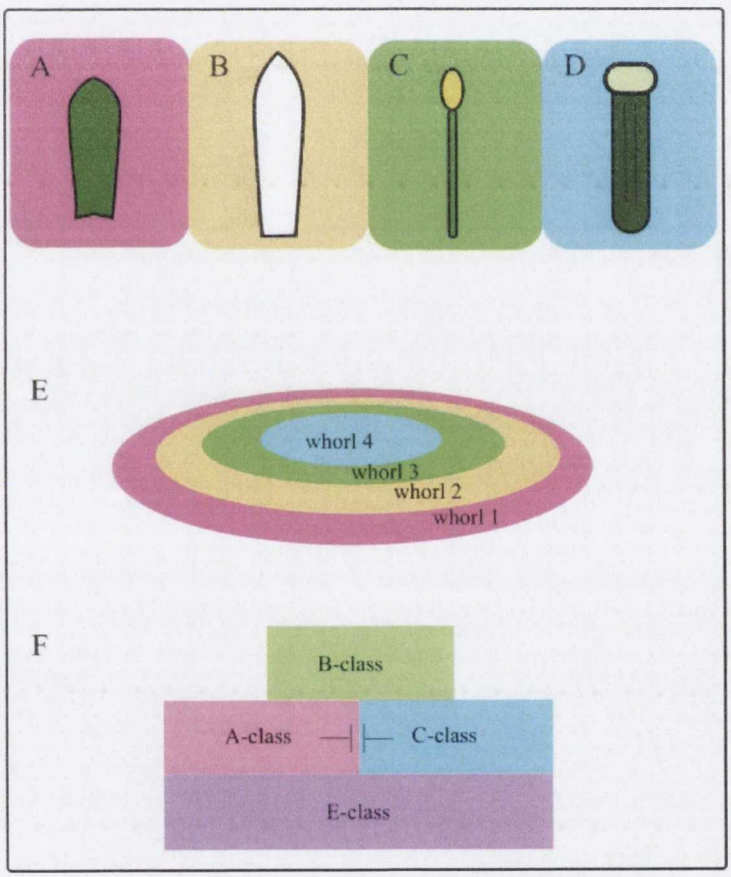

Figure 1.3: ABCE model of floral organ identity specification.

The floral organ identity factors are classed into different groups and are responsible for the development of sepals (A), petals (B), stamens (C) and carpels (D). (E) In the first whorl (pink) the A class genes are expressed, producing sepals. In the second whorl (orange) the A and B (green) genes are co-expressed, resulting in the formation of petals. In the third whorl (green) the B class genes and

C class genes (blue) function together to give stamens. In the innermost fourth whorl, C functions alone produces carpels. (F) Mutual antagonism is predicted in the ABC model between the A and C classes, denoted by the repression lines. The E class genes (purple) provide the ground state throughout all 4 whorls.

As has been shown in a wide range of angiosperm species, floral organ identity genes encode members of the family of MADS-domain transcription factors ('MADS' is derived from the names of four of the founding members of this family: *MCM1* from *Saccharomyces cerevisiae*, *AGAMOUS* from *Arabidopsis*, *DEFICIENS* from *Antirrhinum majus*, and *Serum Response Factor* from humans), which is much enlarged in plants when compared to other eukaryotes (Gramzow and Theissen, 2010). Though initially thought to act as dimers, it was proposed in the so-called 'quartet model' that the floral organ identity factors form tetramers in specific combinations to give rise to four different regulatory complexes that mediate the specification of the four types of floral organs. While the existence of these different complexes has now been experimentally confirmed (Smaczniak et al., 2012), there is strong evidence to suggest that they contain additional, as-of-yet unidentified co-factors with unknown functions necessary for the overall activities of the floral organ identity factors.

Through inducible gene perturbation experiments it was shown that the floral organ identity genes are not only involved in the specification of floral organ primordia during the earliest stages of flower development, but also directly in many aspects of floral organ morphogenesis (Ito et al., 2007; Wuest et al., 2012; O Maoileidigh et al., 2013). This result is in agreement with the observation that the expression of these genes occurs in floral organ primordia throughout most of their development (Krizek and Fletcher, 2005). Thus, in order to understand the function of these transcriptional regulators, their activities must be analysed

over a prolonged time period spanning most of floral organ development, which in the case of *Arabidopsis* takes almost two weeks to complete (Smyth et al., 1990).

To identify the genes directly or indirectly regulated by the different floral organ identity factors on a global scale, a combination of genome-wide localization studies and gene perturbation assays coupled to transcriptomics approaches were employed in recent years (Kaufmann et al., 2009; Kaufmann et al., 2010; Wuest et al., 2012; O Maoileidigh et al., 2013; Pajoro et al., 2014). This work complemented and confirmed the results of older studies, in which selected target genes had been identified through molecular methods. It was found that the floral organ identity factors bind to thousands of sites in the *Arabidopsis* genome, and that, as expected, the bound regions are strongly enriched for CArG-box–like sequences (consensus: 5'-CC(A/T)$_6$GG-3'), the canonical binding sites of MADS-domain proteins. A comparison of the binding patterns for different floral organ identity factors revealed that they share many and perhaps most of their binding sites, even in cases where the proteins are not thought to be members of the same higher-order complexes (O Maoileidigh et al., 2013). Thus, it appears that these factors may bind largely indiscriminately to accessible sites in the genome and consequently, that binding activities alone are insufficient to explain the different regulatory functions of these transcription factors. In agreement with this idea it was found that only a subset of genes bound by the floral organ identity factors respond transcriptionally to a perturbation of their activities. What's more, despite their similar binding patterns, the sets of genes that are regulated by the different proteins exhibit considerable differences. Taken together, these results highlight one of the most pressing open questions in the field of flower development, namely the current lack of understanding as to

why one gene that is bound by a MADS-domain protein complex responds to its activity whereas another one does not.

Over the past few years, several studies have provided data that will likely serve as stepping-stones in the further functional characterization of the floral organ identity factors. For example, it has been shown that the binding of a tetrameric MADS-domain protein complex to two adjacent CArG-boxes can lead to short-range DNA looping, which may be of general importance for the regulation of target genes (Mendes et al., 2013). Furthermore, through gel filtration experiments, it was shown that protein complexes containing the *Arabidopsis* E function factor SEP3 have a molecular weight of around 670 kDa and thus are considerably larger than what would be expected for a MADS-domain protein tetramer (~120 kDa) (Smaczniak et al., 2012). Thus, in all probability, additional proteins are associated with the floral organ identity factors. While the exact nature of these proteins is currently unknown, several interacting proteins have been reported. For example, it has been shown that BASIC PENTACYSTEINE (BPC) transcription factors, which appear to be active throughout the plant, can interact with a MADS-domain complex and may be generally required for their function (Simonini et al., 2012). Also, proteins involved in the epigenetic control of gene expression have been shown to bind to at least some of the floral organ identity factors. An example is a transcriptional co-repressor complex composed of two proteins, SEUSS (SEU) and LEUNIG (LEU), which is thought to recruit histone deacetylases that suppress gene expression by reducing chromatin accessibility (Sridhar et al., 2004; Gonzalez et al., 2007).

To identify proteins associated with floral organ identity complexes, a large-scale proteomics study was recently carried out (Smaczniak et al., 2012). This work yielded a

number of promising candidate proteins, which include both transcription factors from different families and proteins with known or predicted functions in the regulation of chromatin. The likely association of other transcription factors with MADS-domain protein complexes is in agreement with the observation that several known or putative *cis*-regulatory elements are strongly enriched within or around regions bound by the floral organ identity factors. These include G-boxes (consensus: 5'-CACGTG-3'), a frequently utilized motif in the regulation of gene expression in plants, which is bound by basic leucine zipper or basic helix-loop-helix proteins (Wuest et al., 2012). However, despite these recent advances, the exact nature of the proteins that may act as co-factors of the floral organ identity complexes has yet to be determined. Given how successful mutant screens have been in the identification of floral regulators, one can only wonder about why these putative co-factors have not been isolated as of yet.

One possibility is that they belong to a group of functionally redundant proteins so that the inactivation of a single family member has no phenotypic consequences (*e.g.*, members of the large family of REPRODUCTIVE MERISTEM (REM) proteins, which show highly specific expression patterns in flowers and appear to exhibit a high degree of redundancy; Mantegazza et al., 2014). Alternatively, co-factors of the floral organ identity complexes may have ubiquitous functions in the plant (such as the BPC proteins mentioned above) and their inactivation may lead to embryo lethality or other severe developmental defects that preclude the characterization of their functions during flower development. Either way, the requirement for co-factor binding to *cis*-regulatory elements in the vicinity of CArG-boxes may explain why some genes do not respond to MADS-domain protein binding: in those cases, CArG-boxes may simply lie outside of functional *cis*-regulatory modules. Another important idea

that has been recently put forward for floral organ identity factor function is that these regulators may act as 'pioneer factors' and prepare the chromatin landscape for the activation of specific gene expression programs. In agreement with this idea, delayed changes in chromatin accessibility in response to DNA binding have been identified for some floral organ identity factors (Pajoro et al., 2014).

Based on the results outlined above, a good working model for the function of the floral organ identity factors may be the one shown in Figure 1.4. MADS-domain protein dimers bind to accessible CArG-boxes in the genome and, in some cases, this might trigger the formation of tetrameric complexes between adjacent DNA-bound dimers, resulting in DNA looping. The MADS-domain proteins may then act as anchors to recruit, through protein-protein interactions, additional transcription factors that bind to *cis*-regulatory elements in the vicinity of the CArG-box sequences. The resulting higher-order complexes would then recruit proteins involved in chromatin remodelling and the epigenetic control of gene expression, leading to changes in chromatin conformation and to an activation or repression of gene activities, respectively.

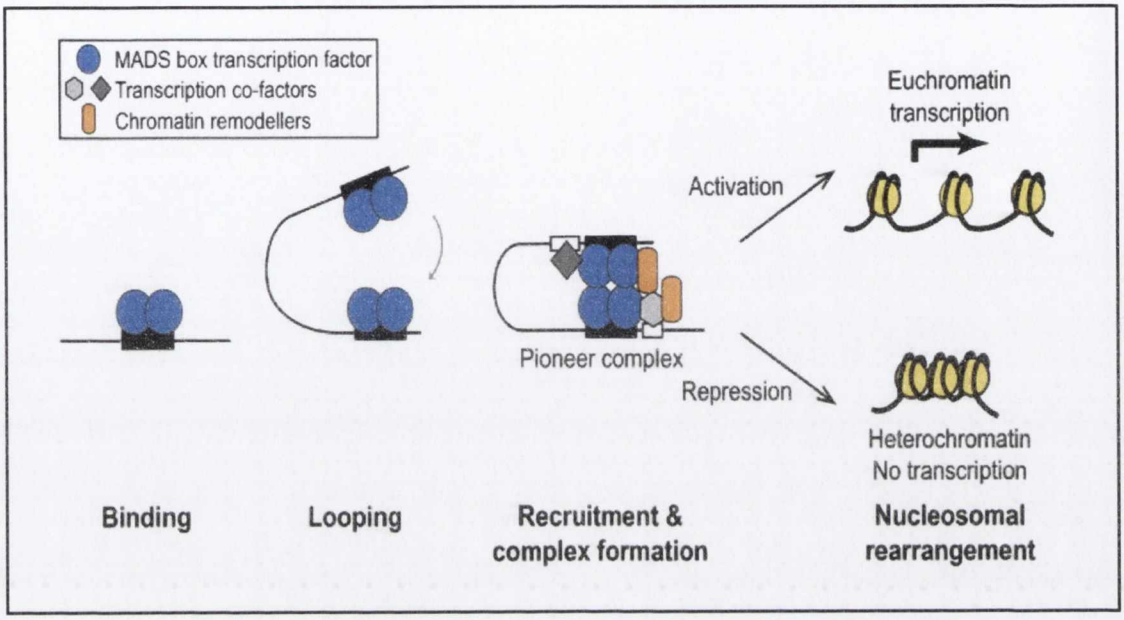

Figure 1.4: Working model for the activities of floral organ identity factor complexes.

Left to right: two MADS-domain transcription factors dimerize and bind to a CArG-box sequence (black rectangles); through the interaction between two DNA-bound MADS-domain protein dimers, DNA looping occurs; the MADS-domain transcription factors recruit transcriptional co-factors to additional *cis*-regulatory elements (white rectangles) as well as chromatin remodelers possibly forming a 'pioneer complex'; the transcription factor complex can then alter chromatin accessibility, resulting in the formation of euchromatin or heterochromatin and in the activation and repression of gene expression, respectively.

1.5 Genome-wide identification of genes acting downstream of the floral organ identity factors

Over many years, research into flower development has primarily focused on how the floral organ identity genes are activated and how they interact with each other to pattern the flower (Honma and Goto 2000; Lohmann et al., 2001; Lenhard et al., 2001; Mayer et al., 1998). This work has lead to accepted models of flower initiation and patterning at early stages of

development (Parcy et al., 1998). In contrast, the gene regulatory network (GRN) of the genes acting downstream of these key regulators has largely remained elusive. This has been due to the nature of the technologies available at the time with a classical approach to analysis of knockout lines, overexpression of key regulators and the analysis of their expression patterns. However, as described above, target genes for the different floral organ identity factors have been recently identified through a combination of genome-wide localization studies such as chromatin immunoprecipitation and subsequent gene perturbation assays using microarrays. From this work it appears that these transcription factors have at least a few hundred direct target genes each, and that the expression of many more genes depends indirectly, and often in a stage-specific manner, on their activities. Also, they seem to mediate both the repression and activation of target genes, suggesting that they act as bifunctional transcription factors.

What have we learned to date from the long lists of target genes that were identified for the different floral organ identity factors? As one would perhaps expect from proteins that act as developmental master regulators, one observation that was made in several independent studies was that genes encoding other transcription factors are strongly enriched among their targets (Kaufmann et al., 2009; Kaufmann et al., 2010; Wuest et al., 2012; O Maoileidigh et al., 2013; Pajoro et al., 2014). In fact, as much as 50% of their target genes may encode proteins with regulatory potential. Thus, the floral organ identity factors appear to mediate organ development to a large extent by controlling the expression of other regulatory genes. Arguably the best example for this to date is the gene *NOZZLE/SPOROCYTELESS* (*NZZ/SPL*), which encodes a key regulator of sporogenesis in *Arabidopsis*. *NZZ/SPL* expression is induced by the combined activities of the B function regulators APETALA3 (AP3) and PISTILLATA (PI) and the C function regulator AGAMOUS (AG) (Ito et al., 2004;

Wuest et al., 2012; O Maoileidigh et al., 2013). Subsequently, *NZZ/SPL* functions independently of the floral organ identity factors to control sporogenesis (Ito et al., 2004). Thus, it appears that in at least in some cases, the floral organ identity factors can trigger an entire developmental process by activating one or a small number of regulatory genes. However, in other cases, a continued direct input of the floral organ identity factors may be required. This idea is supported by the results from these inducible knockdown experiments mentioned above, which showed that there is the need for a prolonged activity of these transcription factors during organ morphogenesis.

In addition to genes encoding transcription factors, another group of genes that is enriched among targets of the floral organ identity factors encodes proteins involved in hormone metabolism or response (these also include some transcriptional regulators). Given the pivotal roles that phytohormones play in the control of plant development these genes are of particular interest on the context of floral organ morphogenesis. For example, auxin is a universal growth hormone that is involved in a myriad of processes from body plan establishment during embryogenesis, to the regulation of apical dominance, and the positioning of organs along the stem. In flowers, auxin signalling contributes to the patterning of floral meristems, the outgrowth of floral organ primordia, and to different morphogenetic events during floral organ formation (Cheng and Zhao, 2007). Similar to auxin, cytokinins also function throughout the plant's life cycle but often act antagonistically to auxin. They play particularly important roles in the maintenance of meristems (including floral meristems), which harbour the stem cell populations of the plant (Bartrina et al., 2011). Several other hormone classes, such as gibberellins and jasmonates, have also been implicated in flower development (Chandler, 2011). The floral organ identity factors have been shown to

target genes involved in the metabolism of, or the response to, these different phytohormones (summarized in: Pajoro et al., 2014), but no coherent picture has emerged yet that would explain how hormone activities are controlled during floral organ development. What's more, there is now ample evidence that different hormones affect the expression of floral organ identity genes (*e.g.*, Yu et al., 2004), strongly suggesting that there is extensive feedback between flower-specific regulators and the more universal hormone pathways. A challenge for future research in the field of flower development will thus be to decipher these regulatory interactions and to better understand when, where and to what extent different hormones accumulate during the formation of flowers and how the corresponding signalling pathways are integrated into the flowering gene regulatory network. In this context, an exciting recent discovery was the identification of Auxin Response Factors (ARFs), which control auxin-dependent gene expression, as direct interaction partners of floral MADS-domain transcription factors (Ripoll et al., 2015). This finding offers the intriguing possibility that plants directly integrate growth promoting signals (*i.e.* auxin) with specific gene expression programs to drive the formation of the different types of floral organs.

As predicted by the ABCE model, different floral organ identity factors often have overlapping activities and target genes. However, it has also been shown that they can act antagonistically at least in some cases. For example, while the C function regulator AG activates genes required for carpel development in the centre of floral meristems, the B function factors AP3 and PI repress the same genes in the adjacent floral whorl, which gives rise to stamens (Wuest et al., 2012; O Maoileidigh et al., 2013). Thus, it seems that the antagonistic activities of these transcription factors ensure that the developmental programs required for the formation of the male and female reproductive organs are non-overlapping,

and it has been suggested that the emergence of this antagonism may have been a key step in the evolution of sex determination in flowering plants. However, the molecular mechanism underlying these antagonistic activities is currently unknown.

Another emerging theme among the genes that act downstream of the floral organ identity factors relates to genes with known functions during leaf development. There is now ample experimental evidence to show that floral organs are derived from leaves as originally hypothesised by Goethe (1790) and thus, their development requires not only that specific gene sets are switched on that can then drive morphogenesis, but also that the developmental program for leaf formation is suppressed or overwritten. First insights into how the latter may be achieved stems from genes involved in the control of trichome formation. Trichomes, or hairs, are typically formed in the epidermis of leaves and have a variety of functions, including the regulation of transpiration and defence against insect pests. Floral organ identity factors have been shown to inhibit trichome formation on floral organs in part by directly controlling the expression of key trichome regulators (O Maoileidigh et al., 2013). Thus, they suppress a morphological feature of leaves as part of the developmental program leading to floral organ formation. The link between floral organ identity factor function and trichome formation is one of the main topics of this thesis (see Chapter 3).

In addition to suppressing certain aspects of leaf development, there is emerging evidence that the floral organ identity factors may also activate regulatory genes involved in other developmental processes and modify their activities to bring about floral organ formation. Of particular interest in this context are genes involved in the control of organ polarity such as *KANADI4* (*KAN4*) and *REVOLUTA* (*REV*), which are often directly regulated by the floral MADS-domain complexes (Wuest et al., 2012; O Maoileidigh et al., 2013).

Together with the abovementioned hormone pathways, the control of these genes may be especially important to sculpt the different types of floral organs. If true, the considerable differences in floral organ morphologies found among the angiosperms could be explained by evolutionary changes in the regulatory code that drives the expression of these genes.

1.6 Modern approaches for studying the gene regulatory network underlying flower development

With the advent of the -omic technologies the use of high-throughput approaches allowed for the first time to elucidate links between the floral organ identity factors and a plethora of other genes known to be involved in flower development (Alvez-Ferreira et al., 2007; Ito et al., 2007; Kaufmann et al., 2009; Wellmer et al., 2004). However, one of the main problems that plagued the flower development field was that each floral primordium is at a distinct developmental stage because flowers are initiated sequentially (Smyth et al., 1990) (Fig. 1.5 K). Therefore, the collection of sufficient amounts of plant tissue to study a specific developmental stage was extremely challenging as the floral buds (especially at early stages) are minute and difficult to dissect. To circumvent this limitation, a "floral induction system" (FIS) was developed, which is based on *ap1 cal* double-mutant plants (Fig. 1.5 A) (Wellmer et al., 2006). When *AP1* and its paralog *CAL* are knocked out a massive over-proliferation of inflorescence-like meristems occurs, leading to a cauliflower-like appearance (Ferrandiz et al., 2000). Synchronization of flower development could be genetically induced in this background by expressing a translational fusion between AP1 and the rat glucocorticoid receptor (GR) ligand binding domain (denoted: AP1-GR). Treatment of *ap1 cal* $35S_{pro}$:AP1-

GR inflorescences with the glucocorticoid dexamethasone led to a transformation of the inflorescence-like meristems into floral meristems and thus, to synchronized flower development (Wellmer et al., 2006) (Fig. 1.5 L). This synchronization system allows for the collection of large quantities of floral buds that are approximately at the same stage of development, thus facilitating high-throughput approaches such as global gene expression profiling or genome-wide localization studies. This system has been expanded on over the years, with different inducible promoter systems, and the replacement of the constitutive 35S promoter with the endogenous AP1 promoter to better mimic the expression pattern of the AP1 fusion protein (O'Maoileidigh et al., 2015).

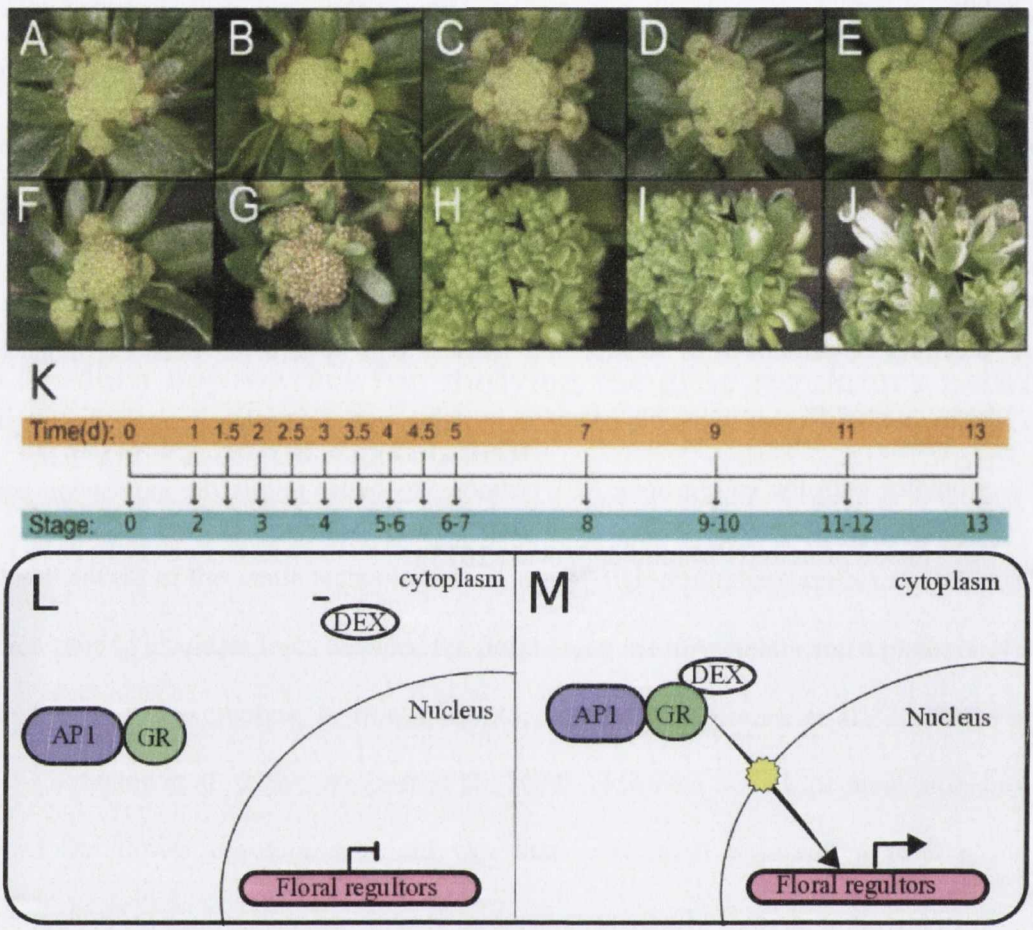

Figure 1.5: A system for the induction of synchronous flower development.

(A-J) $AP1_{pro}$:AP1-GR *ap1-1 cal-1* plants after dexamethasone (DEX) treatment. Flowers begin to form in a synchronous manner upon treatment. (A) 0 d time-point, and (B) 1 d, (C) 2 d, (D) 3 d, (E) 4 d, (F) 5 d, (G) 7 d, (H) 9 d, (I) 11 d, and (J) 13 d after treatment with a solution containing 10 μM DEX. (K) Time in days after activation of flower formation with correlating floral stage. (L) In the absence of DEX, the AP1-GR protein is retained in the cytoplasm and thus inactive. Once plants are treated with DEX the AP1-GR fusion protein translocates to the nucleus and becomes active, leading to the induction of flower formation. Figure modified from Ryan et al. (2015).

Perturbing gene functions classically relied on the generation of null alleles, or the use of T-DNA insertions, but these techniques were cumbersome and limited in availability. Other

tools such as artificial microRNAs (amiRNA) have proved extremely useful in the plant development field, particularly to overcome developmental epistasis (the requirement of a gene at different developmental stages) by using them to knock down genes at the different stages. MicroRNAs (miRNAs) are known to be essential throughout animal and plant development (Bartel and Bartel 2003; Kozomara and Griffiths-Jones 2011), including flower formation (Chen, 2005). MiRNAs are transcribed by RNA polymerase II to create a RNA hairpin which is then processed by DICER-LIKE (DCL1) and HYPONASTIC WAVES (HYL1) to form the miRNA duplex (Mallory et al., 2008) (Fig. 1.6). Methylation of the duplex then occurs on the ribose at the 3' nucleotide by the methyltransferase HEN1 (HUA ENHANCER 1), which prevents its degradation (Chen, 2005). Following this the RNA transporter HASTY relocates the miRNA duplex, or single-stranded miRNA, to the cytoplasm where the correct ARGONAUTE protein binds to the more stable miRNA strand forming the RNA-induced silencing complex (RISC), which activates and cleaves the miRNA. This complex then associates with its target mRNA sequence causing it to be cleaved (Mallory et al., 2008; Mi et al., 2008).

The utility of this system as a tool to investigate different gene functions was first put forward by Schwab et al., and has proven to work quite successfully in disrupted varying genes throughout development by generating artificial miRNAS (amiRNA) against your gene of interest (Schwab et al., 2006). The benefits and reliability of this system has been proved over the years following its publication, including the coupling of them to inducible promoter systems. (O'Maoileidigh et al., 2013; Ossawski et al., 2008; Stahle et al., 2009; Wuest et al., 2012). Furthermore, the development and updating of the web-based amiRNA design

software, and the ease of designing and cloning multiple amiRNAs, allows for high-throughput knockdown experiments to characterize gene functions with ease.

Quite recently a new strategy to perturbing gene function by site directed mutagenesis has been published, known as the Clustered Regularly Interspaced Short Palindromic Repeats/CRISPR-associated (CRISPR/Cas). This system has been shown to successfully knockout a gene of interest in bacterial and human cells without any off-target effects (Cong et al., 2013; Jinek et al., 2013; Qi et al., 2013; Mali et al., 2013) and also more recently in plants (Hyun et al., 2015). The CRISPR/Cas system is a natural prokaryotic immune system that grants resistance to foreign DNA from within plasmids and phages, providing an acquired immunity to the bacterium. In short the CRISPR/Cas system works by cleaving DNA by RNA-guided endo-nuclease (RGEN) activity (Bhaya et al., 2011). This system has been modified to allow specific targeted gene editing. The CRISPR system consists of three genes: the Cas9 nuclease, and two noncoding RNAs; trans-activating crRNA (tracrRNA) and a precursor crRNA (pre-crRNA) containing the guide target sequence. The pre-crRNA is further processed and its this which forms the RNA-protein complex between the tracrRNA and the Cas9 endonuclease (Hyun et al., 2015). A chimeric fusion between the tracrRNA and the crRNA has been developed into a single transcriptional unit known as the single guide RNA (sgRNA), and has been shown to effectively guide the Cas9 nuclease to the target of interest (Jinek et al., 2012). This also has a 3' protospacer adjacent motif (PAM) comprising an NGG nucleotide sequence, which is responsible for target site verification by Cas9 (Fig. 1.7). After recognition of the PAM motif, the sgRNA-Cas9 complex binds to it's target site

and induces DNA cleavage (Sternberg et al., 2014). This system causes double strand breaks in the DNA and relies on non-homologous end joining to introduce errors in the DNA.

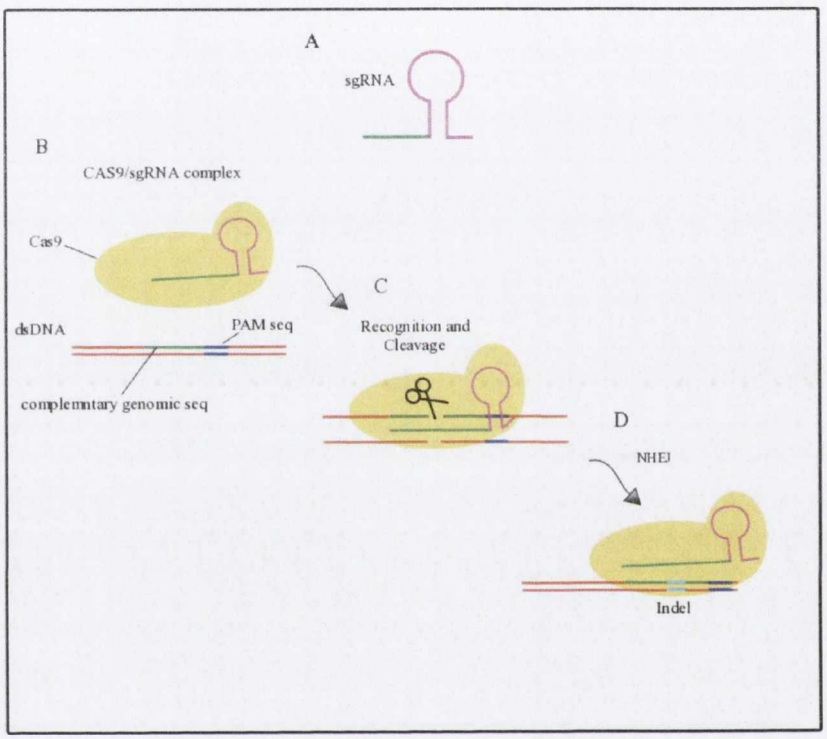

Figure 1.6: CRISPR/Cas9 system for genome editing.

Using the online CRISPR finder web tool a genomic sequence complementary to the gene of interest is generated. This sequence is then cloned into a plasmid to form a chimera with the transactivating CRISPR RNA (trcrRNA) forming the single guide RNA (sgRNA) (A). The sgRNA then forms a complex with the Cas9 protein (B) and recognizes DNA with the guide sequence with an adjacent 3' protospacer adjacent motif (PAM) comprising of an NGG nucleotide sequence. PAM is essential for target site verification by Cas9. Cas9 then induces DNA cleavage after recognition of the PAM site. When the sgRNA/Cas9 complex binds to the target site it induces double strand breaks (DSB) (C). Once a DSB has occurred the DNA repair system activates and repairs it by non-homologus end joining (NHEJ) (D) NHEJ is error prone and during this process nucleotide exchange, insertions, or deletions happen at low frequencies, causing the gene to become inactive in a portion of cells.

One of the early problems with RGEN in human cell populations was that it induced mutations only in a few cells (Cong et al. 2013; Mali et al. 2013) and the same problems occurred in higher plants with a portion of cells only being affected. In the experiments using tobacco and rice, mutant plants were generated from RGEN-applied callus cultures after the isolation of mutated plantlets (Li et al. 2013; Nekrasov et al. 2013; Shan et al. 2013). This method is cumbersome, and in *Arabidopsis* transformation is normally carried out by the floral dip method, which allows for the selection of mutant plants without a requirement for callus culture or plantlet regeneration (Clough and Bent 1998). This problem was circumvented by Hyun et al. (2015). They introduced the CRISPR/Cas system in *Arabidopsis* to create a heritable site-directed mutagenesis system. They coupled Cas9 to the promoter of *INCURVATA2* (*ICU2*), which encodes a catalytic subunit of DNA polymerase alpha in *Arabidopsis*. This promoter is highly active in cells that frequently divide, including those in meristems, proliferating primordia, the vegetative shoot, inflorescences, and flowers (Hyun et al., 2013). This results in highly efficient somatic mutagenesis at their targets in transgenic plants, and the mutant polymorphism is passed on to the next generation with a high frequency of them showing the expected mutant phenotype (Hyun et al., 2015).

The scope of the CRISPR/Cas system is only now becoming known. With the availability of different CRISPR/Cas plasmids between labs and the development of new CRISPR/Cas systems with different, more effective nucleases (Fonfara et al., 2016), the possibility of using CRISPR/Cas for genome editing is become more efficient and widespread. One interesting aspect of using the CRISPR/Cas system in plants is that once the T-DNA of the *Agrobacterium* used to transform is outcrossed, there is no foreign DNA left in

the plant. As there is no foreign DNA in this genetically modified plant it will not be under the remit of European Union or national genetically modified legislature. This has already been the case in the United States of America, where plant pathologist Dr. Yinong Yang, working on the white button mushroom (*Agaricus bisporus*), has edited a gene encoding the enzyme polyphenol oxidase (PPO). Abolishment of this gene results in the mushroom resisting browning, hence looking more appetising for longer. Furthermore, it was judged to be unregulated by The US Department of Agriculture as it doesn't fall under their legislature.

Another technique that has proved invaluable and has given information on direct protein-DNA interactions in flower development is chromatin immunoprecipitation coupled to ultra high-throughout DNA sequencing (ChIP-Seq). ChIP is a molecular technique used for testing binding of proteins to DNA *in vivo* at a given time (Park, 2009). With the advent of next-generation sequencing and the constantly declining cost, ChIP experiments can then be totally sequenced to check for all of the DNA or RNA in a sample on a genome-wide scale. ChIP has to be carried out with an antibody that specifically recognizes the protein of interest (Lee et al., 2006). The protein of interest can be fused to an epitope tag or an antibody can be raised against the protein. With the latter being more expensive most ChIP experiments are carried out with commercially available epitope tags such as HA (Human Influenza Hemagglutinin), FLAG or GFP (Green Fluorescent Protein) tags. ChIP-Seq is widely used in the plant community and has become the gold standard in examining the direct interactions of transcription factors with DNA (O'Maoileidigh et al., 2013; Wuest et al., 2012; Valouev et al., 2008). It has also been effectively used to identify epigenetic modifications, in both humans and plants (Barski et al., 2007; Bastow et al., 2004), but the only drawback is that it can only be carried out on organisms whose whole genome has been sequenced.

1.7 Project outlines and aims of this thesis.

The main aim of this thesis is to add to the growing body of knowledge of the genetic network underlying flower development in the model plant *Arabidopsis thaliana*. Furthermore, the work investigates the evolution of flower development, and specifically how floral organs were formed from leaf-like precursors. As mentioned before (section 1.3), the hypothesis that flowers are in essence modified leaves is now supported by ample genetic and molecular evidence. However, how this transformation process occurs is still not fully understood, and the genetic network which supresses the leaf developmental program in flowers is only starting to come to light. In this thesis, using trichome distribution and initiation as a proxy for leaf development, the role of the floral organ identity factors in this process was analysed. Their genetic interaction with other known regulators of trichome initiation was investigated through the use of a wide range of methods, including inducible perturbation and over-expression, phytohormone treatments, and the analysis of genetic interactions between known floral regulators and regulators of trichome initiation. The results of these analyses and their interpretation is presented in Chapter 3.

In a second project, I have focused my efforts on the gene *SUPERMAN* (*SUP*), which was originally described as *FLO10* (*FLORAL MUTANT 10*) (Schultz et al., 1991). *Sup* mutants have a striking phenotype with supernumerary stamens in the third whorl encroaching on the fourth whorl, and a decrease or increase in carpel tissue in the centre of the flower depending on the allele (Bowman et al., 1992). Due to these phenotypes *SUP* is thought to regulate the boundary between the third and fourth whorl and also regulate cell division or differentiation in the floral meristem. Several models of *SUP*'s function have been put forward, yet which genes and molecular processes it regulates are still unknown (Breuil-Broyer et al., 2016). To

address this knowledge gap, I tried to uncover the main functions of *SUP* in early flower development through perturbation experiments, inducible over-expression, microarray analysis, genetic interaction analyses, genome-wide binding studies and the analysis of the interplay of SUP with the phytohormone cytokinin. The results from these experiments and the interpretation of the data obtained is the focus of Chapter 4.

Chapter 2 - Materials and Methods

2.1 Strains and growth conditions

2.1.1 Published plant lines

The previously published plant lines used in this study are:

$35S_{pro}$:AlcR/$AlcA_{pro}$:AG-amiRNA (Ó'Maoiléidigh et al., 2013)

$35S_{pro}$:AlcR/$AlcA_{pro}$:AG-amiRNA *try-29760* (Ó'Maoiléidigh et al., 2013)

$35S_{pro}$:AP1-GR *ap1-1 cal-1* (Wellmer et al., 2006)

$35S_{pro}$:LhG4-GR/N6xOP_{pro}:AP3-amiRNA (Wuest et al., 2012)

$35S_{pro}$:MIM-156 (Franco-Zorrilla et al., 2007)

$35S_{pro}$:miR156f (Wang et al., 2008)

ag-1 (Bowman et al., 1989)

ag-10 (Bowman et al., 1989)

ap1-1 cal-1 (Bowman et al., 1993)

$AP1_{pro}$:AP1-GR *ap1-1 cal-1 ag-1* (Ó'Maoiléidigh et al., 2013)

Columbia (*Col-0)* wild-type

cpc-1 (Wada et al., 1997)

drn-1 (Chandler et al., 2007)

drnl-1 (Chandler et al., 2007)

gis2-1 (Gan et al., 2007)

gl1-20990 (Oppenheimer et al., 1991)

gl2-1 (Koorneef, 1981)

gl3-1 egl3-1 (Koorneef, 1981)

kan1-11 (Kerstetter et al., 2001)

kan2-5 (Huang et al., 2014)

Landsberg *erecta* (L-*er)* wild-type

shp1-1 shp2-1 (Liljegren et al., 2000)

spl9-4 spl15-1 (Schwatz et al., 2009)

$SPL9_{pro}$:GFP-rSPL9 (Wang et al., 2008)

sup-1 (Bowman et al., 1992)

sup-2 (Bowman et al., 1992)

sup-3 (Bowman et al., 1992)

sup-5 (Gaiser et al., 1995)

try-29760 (Esch et al., 2003)

ttg1-1 (Galway et al., 1994)

zfp8-1 (Gan et al., 2007)

2.1.2 Bacterial strains

***Escherichia coli* strain XL1-Blue** – Genotype recA1 endA1 gyrA96 thi-1 hsdR17 supE44 relA1 lac [F' proAB lacIZ"M15 Tn10 (Tet)] (Stratagene).

***Escherichia coli* strain Tp611** – Genotype recBC hsdRM cya610 pcn–12 (Glaser et al., 1993).

***Escherichia coli* strain STBL2** – Genotype F- endA1 glnV44 thi-1 recA1 gyrA96 relA1 Δ(lac-proAB) mcrA Δ(mcrBC-hsdRMS-mrr) λ- (Invitrogen).

***Agrobacterium tumefaciens* strain C58 pGV2260** (McBride and Summerfelt, 1990)

2.1.3 Plant growth media

All plants were grown in a mixture consisting of compost, perlite and vermiculite (NAD, Dublin) in a ration of 3:1:1 (V:V:V).

0.5xMS agar plates (Murashige and Skoog medium) consisted of 2.2g/L MS salts, pH5.7, 6g/L agar.

2.1.4 Bacterial growth media

All bacteria were grown in LB (Luria-Bertani medium) consisting of 10g/L bacto-tryptone, 5 g/L bacto-yeast extract and 10g/L NaCL.

LB agar plates – 15g/L agar was added to make LB plates.

2.2 Construct cloning and genotyping

2.2.1 Plasmid DNA preparation

All plasmids were extracted from XL1-Blue, Tp611, and STBL2 *E. coli* cultures using the E.Z.N.A DNA plasmid mini kit (VWR) according to the manufacturer's instructions.

2.2.2 Fast extraction of *Arabidopsis* genomic DNA

Genomic DNA was routinely extracted using the procedure described in Edwards et al. (1991). The DNA from Edwards preparations was then used in genotyping assays.

2.2.3 CTAB method to extract Genomic DNA

This method was used to extract contaminant-free genomic DNA from plant tissue, buffers and unwanted salts solutions, which was then used to clone genes with their genomic sequences. 500 mg of plant tissue was ground in liquid nitrogen, then CTAB buffer (100 mM Tris-HCl pH8.0, 20 mM EDTA, 1.4 M NaCl

2% (w/v) CTAB (cetyltrimethyl ammonium bromide – nonionic detergent), facultative 1% PVP 40,000 (polyvinyl pyrrolidone) was added and the sample vortexed and incubated for 10 minutes at 65°C. The DNA was then purified by phenol-chloroform extraction with phase-lock tubes (5-prime) twice. The DNA was precipitated using isopropanol and resuspended in molecular biology grade water once the isopropanol had evaporated.

2.2.4 Preparation and transformation of chemically competent *Escherichia coli* cells

Two different protocols were used to generate chemically competent *E. coli.* XL1- Blue and STBL2 were generated using protocol 1. Competent Tp611 was generated using protocol 2.

Protocol 1: Competent cells were generated as described in Inoue et al. (1990).

Protocol 2: The Tp611 strain was streaked on a LB agar plate and incubated at 37°C over-night. The following day, a single colony was grown at 37°C in 3 mL LB. This pre-culture was used to inoculate 40 mL of LB and incubated at 37°C until an OD600 of 0.5 was reached. The culture was then chilled on ice for 10 min, and centrifuged at 4,000 rpm for 6 min at 4°C. The pellet was then resuspended in 20 mL of an ice-cold solution containing 100 mM $CaCl_2$ and 25% glycerol, and incubated on ice for 20 min. The cell suspension was then centrifuged

at 4,000 rpm for 6 min at 4°C and resuspended in 1 mL of an ice-cold solution containing 100 mM $CaCl_2$, 25% (v/v) glycerol. Aliquots of 200 µL were frozen in liquid nitrogen and stored at -80°C for future use.

All competent cells were transformed using the Heat Shock method. Cells were thawed on ice, and incubated for 10 min with the plasmid of interest on ice. Afterwards the cells were incubated at 42°C for 1 min in a heat block. The cells were then incubated at 37°C for 1 h with 1 mL of LB. After incubation 200 µL of the transformed cells were plated on an LB agar plate containing the appropriate antibiotic(s). If the plasmid of interest was known to have a low copy number the transformed cells were pelleted, the supernatant was removed and the pellet was resuspended in 200 µL LB before plating. Plates were then incubated overnight at 37°C.

2.2.5 Preparation and transformation of competent *Agrobacterium tumefaciens* cells

To generate competent *Agrobacterium* cells, a 5 mL LB culture was grown overnight at 28°C. Next 250 mL of LB supplemented with 0.2 g/L $MgSO_4$ was inoculated with 0.5 mL of the 5 mL culture. This culture was then grown at 28°C until an OD_{600} between 1 and 2.5 was reached. The cells were then pelleted by centrifugation and washed with ice-cold $CaCl_2$. Subsequently, the suspension was then pelleted and resuspended in 4 mL ice-cold $CaCl_2$. 100 µL aliquots were made and frozen in liquid nitrogen for future use. Plasmids were transformed into *Agrobacterium* using the snap-freeze method. An aliquot of cells was thawed on ice. The plasmid of interest was then added and snap frozen for 5 min in liquid nitrogen. The cell suspension was then thawed at room temperature and 1 mL of LB was added. The cell suspen-

sions were then immediately incubated at 28°C for 3-4 h. After incubation the cells were pelleted though centrifugation and the pellet was resuspended in 500 µL LB. An aliquot was then plated on an LB agar plate containing rifampicin (50 µg/mL), and other relevant antibiotics. Plates were incubated at 28°C for approximately 2-3 days.

2.2.6 RNA extraction and cDNA synthesis

RNA was extracted form the relevant plant tissue using the Spectrum Plant Total RNA kit (Sigma-Aldrich) as per the manufacturer's guidelines. DNase treatment of RNA was also run on the extraction column where appropriate. cDNA was then transcribed from the RNA using oligo$(dT)_{18}$ primers (Thermoscientific) and RevertAid H Minus reverse transcriptase (Thermoscientific) according to the manufacturer's protocol. cDNA generated from this reaction was then used for PCR or quantitative real-time PCR.

2.3 Plant transformation and isolating transformed plants

2.3.1 Plant transformation and seed sterilization

All plants were transformed using the floral dip method as described in (Clough and Bent 1998). If the selection of transformants was to be done on MS agar plates, the resulting seeds from the transformed plants were collected and sterilized in a airtight chamber using chlorine gas. This was generated by adding 3 mL concentrated hydrochloric acid to 100 mL of bleach (Domestos). The sterilization was performed for 3-4 hours.

2.3.2 Isolating transgenic plants

To select for transformants which successful took up a construct with an ammonium-glufosinate (BASTA) resistance gene, seeds were germinated on soil and the seedlings were sprayed three times every third day with a 0.15% (v/v) BASTA (Bayer) solution. Seedlings which survived all three sprayings and continued to grow were transplanted to fresh individual pots and genotyped for the presence of the correct transgene, to ensure no cross contamination of seeds.

2.3.3 Trichome counts

EtOH treated AG-amiRNA^{AlcR} carpel valves, and mutant crosses with or without hormone treatments, were monitored at anthesis for the presence of trichomes several days after ethanol vapour treatment, until trichomes no longer formed on successive flowers. The full activation of the AG-amiRNA was determined by the presence of other *ag*-like phenotypes such as bent gynoecia, shortened stamens and floral meristem indeterminacy.

2.4 Microscopy techniques

2.4.1 Light microscope

Dissection and photographing of flowers and plant tissue was performed using an Optika SZM-LED2 trinocular stereozoom microscope equipped with a Optika SRL camera.

2.4.2 Cryogenic Scanning Electron microscopy (S.E.M.)

Floral organs were dissected from the main inflorescence and mounted on a glue and graphene mixture 1:1 (V:V). The tissue was then immersed in liquid nitrogen for up to 1 min in a vacuum before being transferred to an air tight S.E.M. Cryo chamber (-140°C). The sample was sublimed for 30 s to – 80°C to remove excess surface water. The sample was then chilled to -140°C and sputtered with gold for imaging. All images were acquired using a Zeiss Ultra Plus S.E.M. Assistance was provided by the Centre for Microscopy and Analysis (Trinity College Dublin, Ireland).

2.5 Treatment of transgenic lines with inducible promoter systems

2.5.1 Ethanol induction of plants

Plants to be treated were sealed inside an artificial greenhouse chamber with two 50 mL falcon tubes (Corning) with 10 mL 100% ethanol in each. Each of the tubes were secured to opposite ends of the chamber to allow for homogenous dispersal of ethanol vapour. For mock treatments the same procedure was followed except the ethanol was replaced with ddH_2O.

2.5.2 Dexamethasone induction of plants

Once plants had bolted to roughly 1 cm, the main inflorescence meristem of the plant was treated using a Pasteur pipette of a solution containing 10 μM dexamethasone (Sigma), 0.1% (v/v) ethanol, and 0.015% (v/v) Silwett-77.

2.5.3 Collection of induced tissue

After the required time following induction, plants with wild-type inflorescences, of up to stage 9 flowers from the main treated inflorescence meristem, were collected in a tube in liquid nitrogen. For tissue collected from the FIS the induced buds from the main inflorescence meristem were scraped off and placed into a tube in liquid nitrogen. Tissue was then stored at -80°C until used.

2.6 Cloning of artificial-miRNAs

The amiRNAs were designed using the Web microRNA designer (http://wmd3.weigelworld.org). In short, the Arabidopsis Genome Initiative (AGI) number of the gene of interest was entered to the online database and a list of microRNAs were presented which have the potential of targeting the mRNA of the gene of interest. These amiRNAs are ranked by various criteria such as amiRNA sequence composition; mismatch positions, hybridization energy when paired to intended targets, number of other genes that have 5 or less mismatches to the amiRNA, and hybridization energies of other genes with 5 or less mismatches to the amiRNA. The ranking system ranks the potentially functional amiRNAs into four different color-coded classes. The amiRNAs predicted to perturb gene function most efficiently are colored in green, followed by the next ideal ones in yellow and orange, and the remaining least effective in red.

Once an amiRNA sequence is chosen, an Oligo Designer tool (http://wmd3.weigelworld.org) generated oligonucleotides that allowed site-directed mutagenesis to be performed on the pRS300 plasmid, which contains a copy of the endogenous *Arabidopsis* miRNA miR319a (At4g23713) (Palatnik et al., 2003). Overlapping PCR was used to generate the amiRNA pre-

cursor and the final PCR product was digested with *BamHI* and *EcoRI*, and ligated to a vector (pBJ36) containing either the CaMV 35S promoter or the $6xOP_{Pro}$ dexamethasone-inducible promoter. After verifying the sequence of the amiRNA, a fragment containing the promoter and the amiRNA was sub-cloned into either of the binary vectors pML-BART using *NotI* sites. This vector was then used to transform plants as described in Section 2.3.1.

2.7 Cloning of CRISPR constructs

First the guide sequence against your gene of interest (*sgRNA*) is generated using the Cas-designer tool at www.rgenome.net. This generates an optimal target sequence which oligos are then designed for to create the $U6_{pro}$:sgRNA cassette. Two separate PCR products are then amplified. The first from genomic DNA with a forward oligo designed in the *U6* promoter (Hyun et al., 2015) and the reverse with the guide DNA sequence. The second reaction is done with pRG2 plasmid (Hyun et al., 2015) as template, with the forward guide DNA oligo and a reverse oligo designed in the *U6* promoter. In a second round of PCR, the two PCR products are annealed by overlapping PCR to create the $U6_{pro}$:sgRNA cassette. This product is then digested with *SpeI* and ligated into pGREEN0029-$ICU2_{pro}$:CAS9-NLS-HA and transformed into *Agrobacterium* with the helper plasmid pSOUP.

2.8 Quantitative real-time PCR

Oligos for qPCR should have a strict melting temperature (Tm) of 60±1°C. Each oligo pair used in this study did not vary in annealing temperature by more than 1°C. Each primer pair amplifying cDNA was generated to span exon-exon boundaries where possible and were as

close to the 3' end of the coding sequence as possible. The annealing temperature and dimerization potentials of the primer pairs were checked using the thermodynamic oligo software, Oligo Analyzer, on the Integrated DNA technologies website (http://eu.idtdna.com). The Lightcycler 480 (Roche) with SYBR green master 1 (Roche) was then used to quantify relative enrichments of cDNA. Each reaction mix contained 5μL of 2x SYBR green master 1, 1μL cDNA, 1 μL of 10μM primer mix and 3uL of molecular biology grade water. Each amplicon was designed to be no less than 120bp and an extension time of 60 s per 1kb of DNA was used. The enrichment observed was then calculated relative to the input sample. For each gene analyzed the enrichment was could then be calculated using the formula: $2^{\wedge(CP(REF)-CP(GENE)}$, where CP is the crossing point calculated by the Lightcycler 480, CP(REF) is the CP value for the chosen reference gene and CP(GENE) is the CP value for the chosen target gene. The reference gene used for qPCR *PROTEIN PHOSPHATASE 2A*, was chosen from (Czechowski et al., 2005).

2.12 GUS staining of plant tissue

2.12.1 Staining of *Arabidopsis* tissue

Plant tissue to be examined was placed in 90% acetone in H_2O on ice for 10 minutes once picked. The tissue was then transferred to a staining solution without X-gluc (0.2% Triton, 50 mM NaPi, 2 mM potassium ferro/ferricyanide, H_2O and rinsed. The solution was then replaced with an X-gluc staining solution (0.2% Triton, 50 mM NaPi, 2 mM potassium ferro/ferricyanide, H_2O, 2mM X-gluc) and vacuum infiltrated one or more times until all air left the tissue. Tissue was then incubated at 37°C for up to 24 hours, or until blue staining was visible

2.12.2 Fixation of tissue

Tissue was first dehydrated using an Ethanol series: 20%, 35%, 50% in H_2O (30 min each at RT with slow agitation). Post-fixation was done for 30 min in FAA at RT with slow agitation. A further Ethanol series was done: 70%, 80%, 90%, overnight in 95% with eosin Y at RT (stains tissue and allows easier positioning of the resin block on microtome). Dehydration was finished with a 2x 100% ethanol at RT (30 min each). Tissue was then cleared with 25% Tert-butanol (TBA) in ethanol (30 min each time), followed by 50% TBA in ethanol, and 100% TBA at 60°C for 6 h to o/n. Tissue was then incubated in 50% paraplast in TBA o/n at 60°C. Paraplast was then replaced with 100% paraplast at 60°C for several hours, then poured into a plastic weighing boat. Tissue was kept at 4°C until sectioning (up to several months).

2.12.3 Sectioning and slide preparation of tissue

Sectioning of tissue was done at 8 to 10 μm. Strips were placed on water on a glass slide at 42°C. Once set the water was removed and the slides were dried at 40°C overnight. The paraffin was removed with 2x 10 min washes in Histoclear.

2.13 Generation of transgenic lines

2.13.1 Generation of a constitutive amiRNA targeting *SUP* mRNA

A detailed description of how amiRNAs are designed, cloned and expressed in *Arabidopsis* is available in Section 2.6. Sequences of primers used are available in supplementary table 1. To generate the $35S_{pro}$:SUP-amiRNA construct, amiRNAs were amplified, digested and ligated

into the pBJ36 vector with the *CaMV 35S* promoter. Once verified by colony PCR the promoter-amiRNA fragment was then digested using NotI and ligated into the binary vector pML-BART, which was digested with the same restriction enzyme and treated with alkaline phosphatase. The construct was then transformed into *Arabidopsis* plants via *Agrobacterium*-mediated transformation. Plants were then genotyped for the construct.

2.13.2 Generation and expression of an inducible amiRNA targeting *SUP* mRNA

Once a constitutive overexpression construct was found to be functional against the *SUP* mRNA, this sequence was put under the control of an inducible promoter system. The SUP-amiRNA sequence was cut using *MluI* and *Acc65I,* and ligated into pBJ36-6xOP$_{pro}$ cut with the same restriction enzymes. Once verified by colony PCR the construct containing the promoter amiRNA fragment was then digested with *NotI* and subcloned into pML-BART-35S$_{pro}$:LhG4-GR, which was digested with the same restriction enzyme and treated with alkaline phosphatase. The construct was then transformed into *Arabidopsis* plants via *Agrobacterium*-mediated transformation. Plants were then genotyped for the construct. A working line was selected based upon DEX treatment and the correct phenotype being scored.

2.13.3 Generation and expression of Inducible over-expression lines of the *SUP* coding sequence

The SUP-GFP fragment was cut from pAR301 using *Xho1* and *Xba1* and cloned into either a pBJ36 vector containing the 35S$_{pro}$:*AlcA* promoter, or the 6xOP promoter sequence cut with

the same restriction enzymes. Once verified by colony PCR the construct containing the promoter-amiRNA fragment was then digested with *NotI* into pML-BART-$35S_{pro}$:AlcR or pML-BART-$35S_{pro}$:LhG4-GR, which were digested with the same restriction enzyme and treated with alkaline phosphatase. The constructs were then transformed into *Arabidopsis* plants via *Agrobacterium*-mediated transformation. Plants were then genotyped for the corresponding construct. A working line was selected based upon DEX/EtOH treatment and the correct phenotype being scored.

2.13.4 Generation of lines carrying the SUPpro::SUP-GFP rescue construct

To generate the SUP_{pro}::SUP-GFP construct, the 5' *SUP* promoter and coding sequence were amplified from *Arabidopsis* Colombia genomic DNA using the primers oDS1/oDS2. The genomic fragment was digested using *A*cc651 and ligated into pBJ36-GFP cleaved with the same restriction enzymes. The 3' untranslated region of the *SUP* locus was amplified from ecotype *Columbia* genomic DNA using the primers oDS3/4. The fragment was then cut with *HpaI* and *BamI* and ligated into pBJ36-5'SUP_{pro}:SUP-GFP cut with the same restriction enzymes. Once verified by colony PCR the construct containing the promoter-SUP-GFP-3'UTR fragment was then digested with *NotI* into pML-BART, which was digested with the same restriction enzyme and treated with alkaline phosphatase. The construct was then transformed into *Arabidopsis* plants via *Agrobacterium*-mediated transformation. Plants were then genotyped for the construct. A line was then selected based upon a rescue of the *sup* floral mutant phenotype.

2.13.5 Crossing the SUPpro::SUP-GFP *sup*-5 lines into the FIS

Pollen from a $AP1_{pro}$:AP1-GR *ap1-1 cal-1 sup-5* plant was used to fertilize emasculated flowers from a SUP_{pro}:SUP-GFP *sup-5* plant. F_1 plants were then genotyped for the presence of the GFP sequence, and seeds were collected from these plants. F_2 plants that exhibited an *ap1 cal* mutant phenotype were then treated with DEX to check for the presence of the $AP1_{pro}$:AP1-GR transgene by activation of flowering. F_3 plants that were homozygous for all transgenes and for the T-DNA harboring $AP1_{PRO}$:AP1-GR were isolated. Since no positional genotyping assay was available for the T-DNA encoding the SUP_{pro}:SUP-GFP fusion, a segregation analysis had to be carried out on the offspring of individual F_3 plants in order to isolate a line that was homozygous for the GFP sequence.

2.13.6 Generation of lines affecting Cytokinin synthesis

To clone the inducible $35S_{pro}$:LhG4-GR/$6xOP_{pro}$:IPT8 construct, the *ISOPENTYL TRANSFERASE8* sequence was cloned by PCR using primers oDS96/97 from cDNA derived from RNA extracts of Arabidopsis Col-0 flowers. The PCR fragment was then digested using the enzymes *MluI* and *Xho1*, and ligated into pBJ36-$6xOP_{pro}$ which had been cleaved with the same restriction enzymes. Once verified by colony PCR the construct containing the promoter and *IPT8* sequence was then digested with *NotI* and ligated into pML-BART-$35S_{pro}$:LhG4-GR, which was digested with the same restriction enzyme and treated with alkaline phosphatase. The verified construct was then transformed into *Arabidopsis* plants via *Agrobacterium*-mediated transformation.

2.13.7 Generation and expression of the inducible SHP2-GFP construct

To generate the $6xOP_{pro}$:SHP2-GFP/$35S_{pro}$:GR-LhG4 construct, cDNA derived from RNA extracts of *Arabidopsis* L-*er* flowers were amplified using primers DM722 and DM723. This PCR fragment was restriction digested with *Sal*I and *Mlu*I and ligated to pBJ36-GFP, which was cut with the same enzymes, to generate pBJ36-SHP2-GFP. The SHP2-GFP fragments was then subcloned to downstream of the 6xOP promoter in pBJ36-$6xOP_{pro}$ using *Xho*I and *BamH*I. To generate the final binary vector, the $6xOP_{pro}$:SHP2-GFP fragment was subcloned into pML-BART-$35S_{pro}$:GR-LhG4 using *Not*I. The construct was then transformed into *Arabidopsis* plants via *Agrobacterium*-mediated transformation.

2.13.8 Generation of GUS reporter lines

To generate the various GUS reporter systems in this study, the promoters of interest were amplified form genomic DNA derived from extracts of *Arabidopsis* L-*er* flowers, and amplified using primers designed against the gene of interest (see supplementary table 1). The promoter was then cut and ligated into pBJ36-GUS-3'OCS. Once verified by colony PCR the construct containing the promoter fragment of interest was then digested with *Not*I and subcloned into pML-BART, which was digested with the same restriction enzyme and treated with alkaline phosphatase. The construct was then transformed into *Arabidopsis* plants via *Agrobacterium*-mediated transformation. Plants were then genotyped for for the presence of the GUS sequence using primers oDS73/74.

Chapter 3 – Investigating the repression of the trichome initiation pathway in floral reproductive organs

3.1 Introduction

As mentioned previously (section 1.3), Johann Wolfgang von Goethe hypothesized that floral organs are in essence modified leaves (von Goethe, 1790) and this idea has resonated with plant biologists ever since. Charles Darwin also commented on the sudden appearance of flowers in the fossil record with little evidence of a gradual modification, calling it an "abominable mystery" (Crepet, 2000). In recent decades this hypothesis was readdressed with a variety of experimental approaches, most notably genetic analyses, supporting the idea that flowers are indeed composed of modified leaves. Goethe's hypothesis was validated when the floral homeotic regulators were discovered, which culminated in the establishment of the ABC model of floral organ identity specification (Coen and Meyerowitz, 1991) (Section 1.3). The ABC model of flower development shows that the overlapping activities of three classes of genes are sufficient to specify the four floral organ types. When a single class of gene is inactivated, a floral homeotic conversions occurs. For example, *agamous* (*ag*) mutants in *Arabidopsis* lack stamens and carpels, and the positions that are normally occupied by these organs are filled by sepals and petals (Bowman et al., 1989). Furthermore, when all ABC genes are inactivated at once, floral organs transform into leaf-like structures (Bowman et al., 1991). Subsequently, it was also shown that the ABC genes are sufficient to confer floral identity, however, this discovery hinged on the of identification of the E function genes, known as the *SEPELLATA* (*SEP*) genes. When all four *SEP* genes are knocked out, leaves are

seen to form in the place of floral organs (Ditta et al., 2004) Further to this it was found that ectopic expression of the ABC genes alone failed to convert leaves to floral organs. However, with the addition of the *SEP* genes leaves were readily transformed (Honma and Goto 2001; Pelaz et al., 2001). These experiments show that the floral organ identity genes are not only necessary but also sufficient for floral organ formation.

Since these early discoveries, much experimental research has been done on understanding the molecular activities of the ABCE genes, all of which encode MADS-domain containing transcription factors with the exception of *APETALA2* (*AP2*) (Theissen et al., 2001). The identification of direct targets of the homeotic proteins was slow at first. However, the availability and cost effectiveness of high-throughput approaches has resulted in rapid progress. For example, *AG* has been shown to promote the expression of many genes that are required specifically for floral organ development, such as *CRABS CLAW,* which is required for gynoecium development, and *SPOROCYTELESS,* which is involved in stamen development (Ito et al., 2004; O' Maoileidigh et al., 2013). Both of these genes encode transcription factors and through their activation, and many other transcription factors, this is how it is thought *AG* regulates stamen and carpel development.

The emerging picture of how leaves evolved into flowers is one in which these MADS-domain transcription factors regulate the expression of a plethora of genes involved in development of the specialised tissues and structures of the floral organs, while the addition of other regulators fine-tuned the activity of genes with general roles in organ development (Sablowski, 2010). Until recently an unsolved question has been whether the floral organ

identity genes actively supress an underlying leaf development program and then activate floral organ development. There is little evidence how the MADS-domain proteins influence leaf development, but recent work has opened up an avenue to explore this using trichome formation as a proxy for control of these programs. Recent transcriptomics data shows that the suppression of the leaf developmental program occurs in flowers, as there was an activation of genes whose peak expression normally occurs in leaf tissue, was observed in early-stage *ag* and *pi* mutant flowers (Fig. 3.2 (C)) (O' Maoileidigh et al., 2013).. Many of these genes are known to participate in photosynthetic processes but binding of AG to the *cis*-elements of these genes was not observed in accompanying ChIP-Seq data. The ChIP-Seq data did identify regulators of trichome initiation, such as *GLABRA1* (*GL1*) and *CAPRICE* (*CPC*) as direct targets, and *CYTOKININ OXIDASE 6* (*CKX6*), a gene known to be involved in the catabolism of CYTOKININ (CK), which is essential for trichome formation (Steiner et al., 2012).

Expression analysis of these genes after perturbation of *AG* activity, using an inducible artificial microRNA (amiRNA) that specifically targets *AG* (AG-amiRNA), showed that *GL1* expression is normally suppressed by *AG* while *CPC* expression is normally activated (Fig. 3.3 (C)). These responses indicated that *AG* normally represses the trichome initiation pathway. Finally, through the use of the inducible AG-amiRNA, it was shown that the perturbation of *AG* activity during intermediate stages of flower development resulted in the initiation of branched trichomes on the carpels valves (Fig 3.3 (B)).

This chapter focuses on the role that *AG* plays during trichome initiation. To improve our understanding of these roles, we analysed *AG*'s interactions with other known regulators of trichome initiation on a genetic level. The results of these analyses and my interpretation of the data is presented below. Prior to this, however, I will describe the distribution of trichomes during Arabidopsis development and the molecular mechanisms that are known to control it.

3.1.1 The control of trichome Initiation in *Arabidopsis thaliana*

Plant trichomes (Fig 1.4) are specialized epidermal protrusions, which are present on the surfaces of most vascular plants. *Arabidopsis* bears eglandular (non-secreting) trichomes that are thought to perform several specific functions, such as protection of the plant from UV light, reducing water loss, and protection against herbivores (Traw and Bergelson, 2003; Olsson et al., 2009). It has also been shown that upon biotic damage plants can increase the number and density of trichomes on the next generation of leaves to aid in their protection (Hanley et al., 2007; Traw and Bergelson, 2003; War et al., 2012).

Trichomes initially form in a regularly spaced manner on the adaxial side of rosette leaves. These trichomes are normally two-branched and three-branched (stellate). Trichomes do not form on the abaxial sides of the first few rosette leaves, and it is the absence of these trichomes that is often used to define the juvenile stage of development. Adult rosette leaves are defined by the presence of both abaxial and adaxial trichomes. After the floral transition, cauline leaves bear two-branched trichomes, which form more densely on the adaxial sides of

early arising leaves than later-arising adaxial trichomes. Conversely, the abaxial sides of early arising cauline leaves bear fewer trichomes than later-arising leaves. Stems primarily bear simple (non-branched) trichomes which are less densely initiated with each successive internode. Similarly, the sepals of early arising flowers bear simple trichomes while later arising flowers have glabrous (hairless) sepals. Notably, the petals, stamens, and gynoecia of *Arabidopsis* are normally glabrous. How this is regulated in *Arabidopsis* has been researched in detail and I will discuss this next.

3.1.2 The Lateral Inhibition Model

The gene regulatory network underlying trichome formation and patterning has been intensively studied as a model for cellular differentiation. From these analyses, a model based upon an immobile activating protein complex being regulated by mobile inhibitors was proposed, which can account for the regular spacing of trichomes on the leaf epidermis (Fig. 3.1) (Lee and Schiefelbein 2002; Pattanaik et al., 2014; Schnittger et al., 1999). In this lateral inhibition model, the development of trichomes is promoted by the activating complex (the MBW complex), which contains three groups of transcription factors: The R2R3 MYB-type, GLABRA1 (GL1); the Basic Helix-Loop-Helix GLABRA 3 (GL3), or ENHANCER OF TRY AND CPC 3 (EGL3); and a WD40-repeat containing protein TRANSPARENT TESTA GLABRA 1 (TTG1) (Bernhardt et al., 2005; Pattanaik et al., 2014). This complex activates the expression of *GL2,* a homeo-domain containing protein which is the limiting factor in whether a trichome forms or not (Szymanski et al., 1998). Mutations in any of these genes

lead to a dramatic loss in trichome density or glabrous plants (Payne et al., 200; Bernhardt et al., 2005). The complex also activates a number of genes that encode single-repeat R3-MYB proteins, which inhibit the activity of the complex in a non-cell autonomous manner. These proteins move from the trichome-forming cell to their neighbouring cells, where they then compete with GL1 in the activator complex, rendering it inactive and unable to induce *GL2* expression (Wang and Chen, 2014).

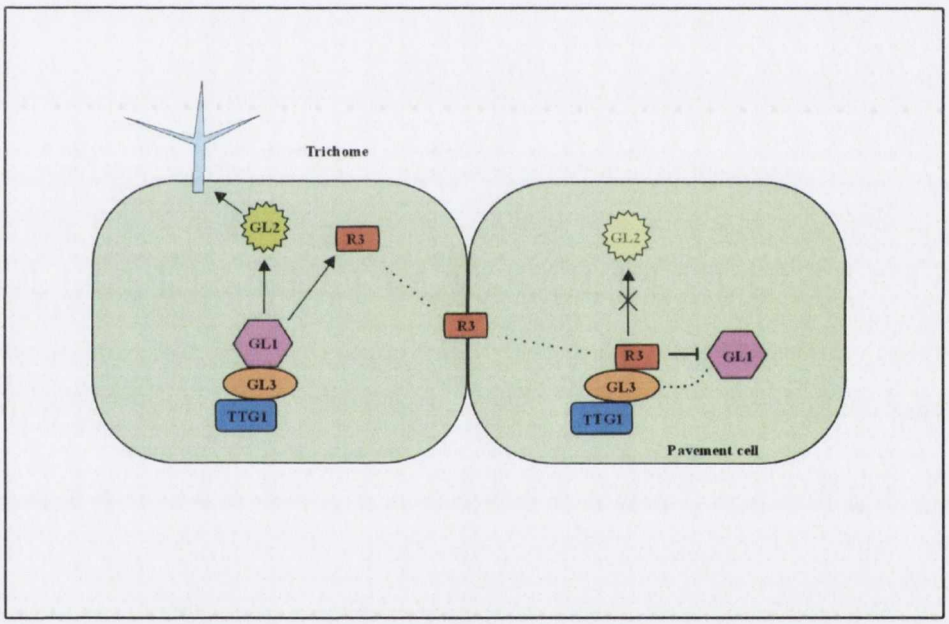

Figure 3.1 The lateral inhibition model.

The lateral inhibition model is based on cell-to-cell communication by movement of single-repeat R3 MYB proteins (R3). The activator complex consists of TTG1, GL3, and GL1. This complex initiates the expression of *GL2,* which promotes trichome development. In addition, it activates the expression of R3 MYB repressor proteins. These proteins translocate to adjacent cells where they compete with GL1 for binding to the activator complex while also inhibiting its expression. This results in the activator complex becoming inactive, leading to the suppression of trichome formation.

There are seven known small single-repeat R3 MYB proteins that act in a highly redundant manner as inhibitors of trichome initiation in *Arabidopsis*: *TRIPTYCHON* (*TRY*), *CAPRICE* (*CPC*), *TRICHOMELESS 1* (*TCL1*) and *TCL2*, *ENHANCER OF TRIPTYCHON AND CAPRICE 1* (*ETC1*), *ETC2* and *ETC3*. All of them are involved in the repression of trichome formation as their over-expression leads to a reduction in trichome number (Schnittger et al., 1998; Schellmann et al., 2002; Wada et al., 2002; Kirik et al., 2004; Wang et al., 2007). With the exception of TCL1, they have all been shown to move to neighbouring cells to carry out their functions (Wang and Chen, 2014).

Although all are involved in the repression of trichome formation, single mutant analyses of these genes showed that they can vary in their primary function. For instance, *try* mutants exhibit an increase in trichome clustering, while *cpc* mutants bear more trichomes on leaves. Other MYBs such as *TCL1* and *TCL2*, control trichome initiation on stems, but not on leaves, most likely due to the proteins having different biochemical properties compared to the other MYBs (Gan et al., 2011;Wang et al., 2007).

In summary, these genes form a regulatory loop containing activators and repressors, which regulate the expression of their downstream targets, resulting in the control of eglandular trichome formation in *Arabidopsis*.

3.1.3 The *SQUAMOSA PROMOTER BINDING PROTEIN-LIKE* genes regulate trichome formation

The lateral inhibition model describes the core machinery required to initiate trichomes in a regular pattern on the epidermis of the leaf. Several transcription factors are known to regulate expression of the genes encoding components of this core machinery. For example, the *SQUAMOSA PROMOTER BINDING PROTEIN-LIKE* (*SPL*) genes, which are known to be involved in controlling flowering time, also regulate trichome formation (Wang et al., 2008). In *spl9-1 spl15-1* double mutant plants there are higher numbers of trichomes found on rosette leaves compared to the wild type (Schwarz et al., 2008). In addition, ectopic expression of *miR156*, which targets the mRNAs of many of the *SPL*s, increases the number of trichomes on stems (Wang et al., 2008). Conversely, plants with more *SPL* activity due to an over-expression of a mimicry target of *miR156*, MIM156, which causes the inactivation of miR156, have fewer trichomes on stems than the wild type (Wang et al., 2008). More evidence for their involvement in the repression of trichome formation stems from transgenic plants expressing a miR156-resistant form of *SPL* (*rSPL*), which results in suppression of trichomes on stems (Wang et al., 2008; Yu et al., 2010). The *SPL*s have been shown to directly enhance the negative regulators of trichome formation, particularly *TRY* and *TCL1* (Yu et al., 2010). As the levels of the *SPL* genes are known to increase as the plants ages, this was the first identification of an age-dependant mechanism controlling trichome development.

3.1.4 Role of phytohormones in trichome initiation

Plant hormones are also known to play an essential role in trichome initiation by controlling many downstream targets (Schellmann et al., 2002; Gan et al., 2006; Zhao et al., 2008). Jasmonic acid (JA), gibberellins (GA), and cytokinin (CK) can influence trichome numbers across *Arabidopsis* and this has been studied in-depth (Matías-Hernández et al., 2016; Traw and Bergelson, 2003). It has been shown that the biosynthesis and signalling of GA, JA, and CK, is essential for trichome formation, as when genes involved in their biosynthesis and signalling pathways are disrupted plants become glabrous. However, trichome formation can easily be restored in these mutants with exogenous application of the correct hormone and many of the key regulatory genes have identified through these screens (Maes et al., 2008; Perazza et al., 1998; Qi et al., 2014). Other phytohormones, such as brassinosteriods, ethylene, and salicylic acid, affect trichome formation. Most of the studies involving the formation of trichomes in response to the different phytohormones have been done on rosette leaves, cauline leaves, and stems, but there has been little research performed on the regulation of trichome formation on sepals, the only floral organ where they appear.

Recently, three genes encoding C2H2 transcription factors, *GLABROUS INFLORESCENCE STEMS* (*GIS*), *GIS2,* and *ZINC FINGER PROTEIN 8* (*ZFP8*), have been shown to integrate GA and CK signalling processes. Gan *et* al. (2006) and (2007) report that all three genes are responsive to exogenous GA treatments in the sensitized background of GA-deficient plants while only *GIS2* is responsive to exogenous CK application. In contrast, Yu *et al.* (2010) report that all three genes are responsive to exogenous CK applications while also showing

that this response is independent of *SPL* activity. Both are expressed in early plant development, with *GIS2* being strongly expressed in inflorescence meristems, and *ZFP8* most highly in cauline leaves (Gan et al., 2007). *zfp* mutants bear fewer trichomes on the adaxial surfaces of cauline leaves, while *gis2* mutants bear fewer trichomes forming on the abaxial side of sepals (Gan et al., 2007). Constitutive overexpression of *GIS, GI2,* or *ZFP8,* causes an increase in trichome density on leaves and stems compared to wild-type plants. Further to this, their overexpression is also sufficient to cause trichome initiation on carpel valves (Gan et al., 2007). Overall, the function of *GIS, GIS2,* and *ZFP8,* seems to be in the regulation of specific epidermal responses through the integration of the CK and GA pathways. Their targets are yet unknown, but both pathways act at least on *GL1* to promote activation of trichome initiation (Gan et al., 2007; Szymanski et al., 1998; Lin and Aoyama, 2012).

In conclusion, phytohormones play an essential role in regulating trichome formation. The phytohormones are known to act synergistically or antagonistically throughout plant development, and future work is being carried out on how the different hormonal pathways interact to regulate trichome formation. Further to these pathways regulating trichome initiation, it has also been shown that the homeotic genes actively regulate some of the genes involved in these processes, and this will be discussed in the next section.

3.1.5 Suppression of the leaf developmental programs by *AG, AP3,* and *PI.*

As mentioned in section 3.1 recent work in the Wellmer laboratory has started to uncover the developmental processes that are directly regulated by *AP1, AG, AP3,* and *PI.* This previously published work showed that the expression of the leaf developmental programs are regulated

in part by *AG* and *PI,* and this lays the foundation for this chapter (Wuest et al., 2012; O' Maoileidigh et al., 2013). This work was primarily done through the use of an inducible promoter system driving the expression of an amiRNA against *AG* mRNA and this system will be discussed next.

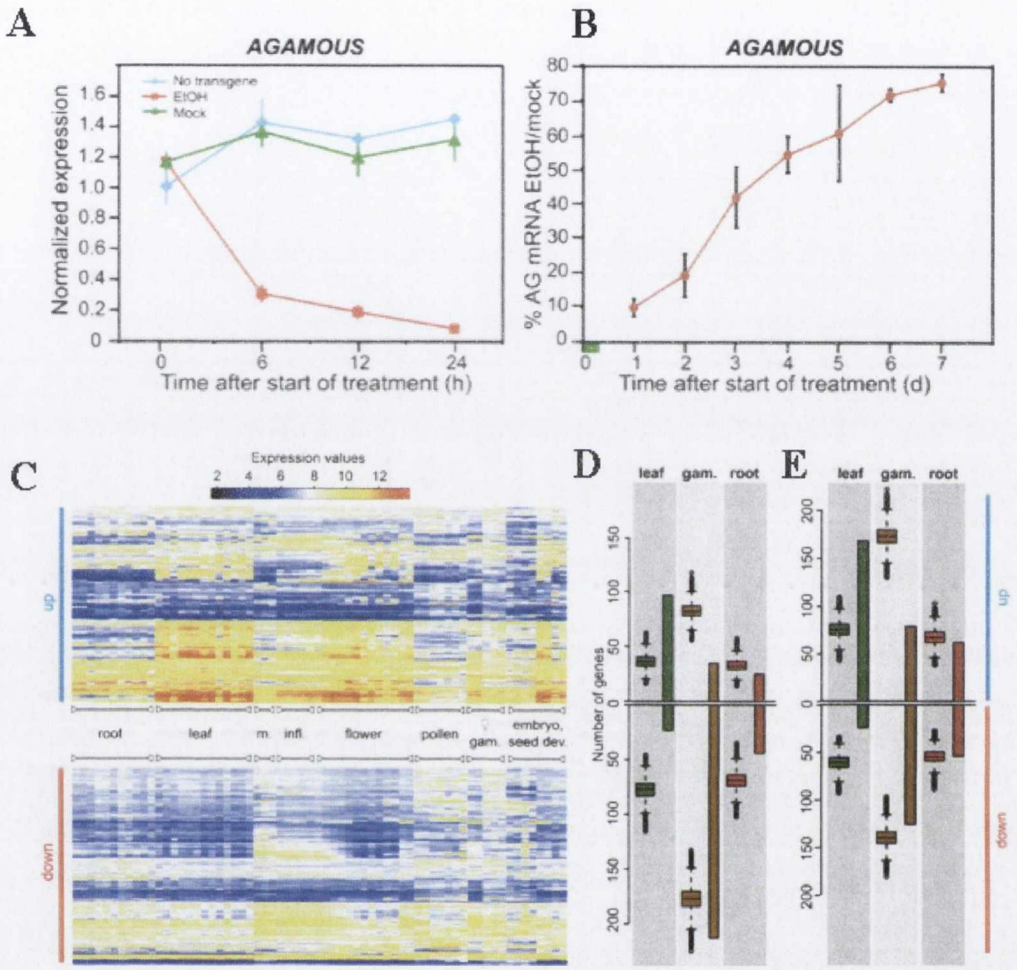

Figure 3.2 Global expression patterns of genes controlled by B and C function regulators.

(A) Induction of the the AG-amiRNA with EtOH results in strong knockdowns of *AG* mRNA after 6h of treatment (B) *AG* mRNA in the plants recovering gradually back to normal levels 1 week after treatment of 6 hours (green bar). (C) The expression levels of genes identified as upregulated (upper panel) or downregulated (lower) in *ag-1*, compared to wild-type, from 65 different *Arabidopsis* tissue samples. Transcriptomics data was grouped into 8 clusters from this experiment: root, leaf, meristem (m.), inflorescence (infl.), flower, pollen, female gametophyte (♀ gam.), and embryo and seed development. The enrichment for genes being upregulated in leaves, flowers, and embryo and seed development is evident in the upper panel indicated by the redder colours. (D-E) The number of genes identified as upregulated (top) or downregulated (lower) in the *ag-1* (D) and *pi-1* (E) microarrays that showed their peak expression in leaves, gametophytic tissues (gam), or roots, are annotated through

coloured bars. To understand the significant enrichment of these genes in the data sets, 100,000 equally sized sets of randomly selected *Arabidopsis* genes were further analysed, and the results are visualized through the use of box and whisker plots. From this analysis the genes in leaves are mostly upregulated in these mutant backgrounds, and in the gamete and root to a lesser extent. (Figure adapted from O' Maoileidigh et al., 2013)

3.1.5.1 The $35S_{PRO}$:AlcR/$AlcA_{PRO}$:AG-amiRNA system

Many of the experiments in this chapter rely on the characterization of genetic interactions between regulators of trichome initiation and *AG*. To perform these experiments, an inducible version of the AG-amiRNA was used, which was designed to specifically target the *AG* mRNA. The inducible system used constitutively expresses the ethanol responsive AlcR transcription factor from the the Cauliflower Mosaic Virus (CaMV) 35S promoter ($35S_{PRO}$). This transcription factor can directly bind and activate the expression of genes that are downstream of the *AlcA* promoter. The *AlcA* promoter is inactive unless the AlcR transcription factor binds to it and AlcR can only bind and activate the AlcA promoter in the presence of EtOH vapour (Roslan et al., 2001). Expression of the AG-amiRNA from the AlcA promoter after AlcR activation *via* EtOH vapour treatments resulted in the rapid reduction of *AG* mRNA levels, which recovered several days after the treatment (Fig. 3.2 (A-B)). Furthermore, known targets of AG were also rapidly downregulated. Induction of the amiRNA also led to the appearance of flowers that phenocopied strong *ag* mutants. However, given the sequential initiation of flowers from the inflorescence meristem of *Arabidopsis*, the severity of the phenotypes produced were dependent on the developmental stage of a given flower when EtOH vapour was applied. For example, when the AG-amiRNA was activated at late stages of flower development, flowers with misshapen carpels, and smaller stamens and

petals were observed, suggesting AG is required for organ growth (O' Maoileidigh et al., 2013).

3.1.5.2 *AG* regulates genes involved in trichome formation

As mentioned in Section 3.1, transcriptomics studies identified genes, whose peak expression is normally in leaves, being upregulated in *ag* flowers. ChIP-Seq experiments also identified *AG* binding to a few of the genes involved in trichome formation eg CPC, GL1 and CKX6. . To see if *AG* was really controlling these regulators of trichome initiation the inducible AG-amiRNA was then used to check their expression levels by perturbing *AG* activity. qPCR analyses have shown that some of the activators of trichome initiation (*GL1* and *ZFP8*) were upregulated upon *AG* knockdown at early stages of flower development. On the other hand some of the repressors of trichome initiation, were downregulated (*TCL1*, *CPC*, *CKX6*), but another known regulator, *TRY*, seemed to be largely unaffected (Fig.3.3 (C)). These results demonstrated that in early flower development *AG* downregulates the activators and upregulates the repressors of the genes involved in trichome formation, with other factors possibly regulating *TRY*.

It was then tested whether the AG-dependant transcriptional control of these genes might lead to an apperance of trichomes on the normally trichomeless floral organs. This was done by using the inducible AG-amiRNA and assessing the floral mutant phenotypes at different stages of flower development. In the flowers where *AG* had been knocked down at intermediate stages by treating the plants with EtOH vapour, trichomes were seen to be

forming on the valves of the (Fig 3.3 (A-B)). This was in agreement with the differential expression of the regulators of trichome initiation observed in the molecular experiments.

The visible trichomes were seen to be branched on occasion, which is a hallmark of leaf development, rather than unbranched sepal trichomes, suggesting that this transformation of carpel tissue was most likely to leaf tissue rather than sepal. This hypothesis is further supported by the fact that in the *sep1/sep2/sep3/sep4* quadruple mutant, where sepals are more leaf-like with abaxial epidermal cells resembling leaf cells, the trichomes are predominantly branched or stellate (Ditta et al., 2004). The cellular structure of the carpel was then analysed, and in keeping with the idea that this was a conversion to leaf tissue, the cellular structure often resembled that of a leaf (Fig. 3.3 (D-G)).

Overall these results showed that *AG* directly regulates the expression of the genes involved in trichome initiation and disruption of its activity is sufficient to convert carpel tissue into leaf tissue, with a hallmark of leaf development – trichomes - being able to form there.

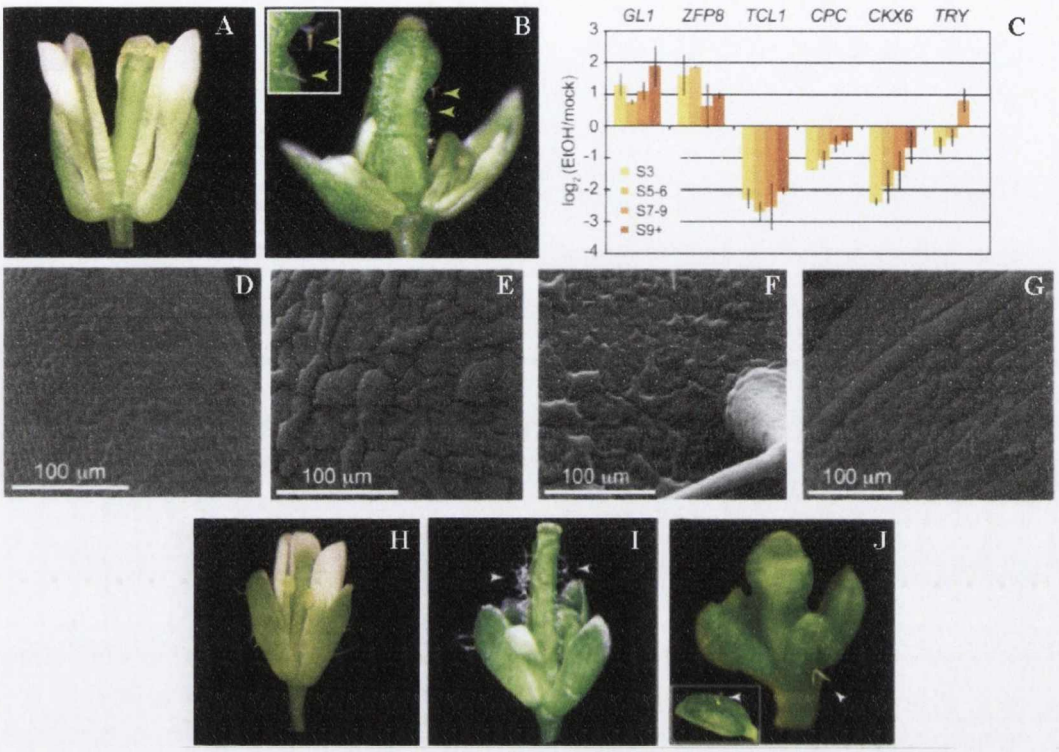

Figure 3.3 Molecular and phenotypic characteristics of AG perturbation.

(A) A wild-type flower. (B) Flower of an AG-amiRNA plant treated with EtOH, with visible branched trichomes forming on the carpel valves. (C) Response of genes involved in trichome development due to activation of the AG-amiRNA with EtOH across 1, 3, 5, 7 day time points compared to mock treated plants. Upregulation of *GL1* and *ZFP8*, activators of trichome initiation, can been seen across the time points, while the repressors *TCL1*, *CPC,* and *CKX6,* are downregulated across all time points. *TRY* remains unchanged, suggesting its expression is regulated by other means. (D) Wild-type carpel valve epidermis cellular structure. (E) EtOH treated AG-amiRNA carpel valve. (F) Wild-type rosette leaf and (G) abaxial surface of a sepal. When *AG* is knocked down the carpel epidermis transforms to a leaf-like cells rather than sepal-like. (H) AG-amiRNA *try-29760* plant untreated and (I) a treated plant with higher numbers of trichomes forming on the carpel valves compared to wild-type. (J) Knockdown of *AG* function and *PI* function simultaneously, through the use of amiRNAs, results in the formation of trichomes on carpel valves and on the abaxial surface of the anthers. (Figure adapted from O' Maoileidigh et al., 2013)

3.1.5.3 Other MADS-domain transcription factors supress trichome formation in flowers with *AG*

One interesting observation was that trichomes did not form on the anthers of stamens where *AG* is normally expressed (Ito et al., 2007). This led to the idea that additional regulators may be redundantly supressing trichome initiation on these organs. To this end, a previously described dexamethasone inducible amiRNA against *PI* ($35S_{PRO}$:LhG4-GR/6xOp_{PRO}:PI-amiRNA) (Wuest et al., 2012) was crossed with the *AG* EtOH inducible amiRNA. Upon single activation of the PI-amiRNA no trichomes were noted on the carpel valves or anthers. However when *PI* and *AG* were simultaneously knocked down through EtOH and DEX treatments, trichomes were seen on the carpel valves but also on the abaxial surface of the anthers (Fig. 3.3 (J)). These experiments showed that other floral organ identity factors, the B function genes, are redundantly involved in the repression of trichome initiation in flowers. Because expression of the A class gene *AP1* is known to expand into the centre of the flower when *AG* is activated (Gustafson-Brown et al., 1994), its involvement in redundantly suppressing trichome formation in the flower was also analysed. To this end, the inducible AG-amiRNA was crossed into *ap1-1* null mutant plants and the number of trichomes was quantified. No increase in trichome numbers was seen on the carpel valves upon *AG* perturbation relative to an AG knockdown in a wild-type background, suggesting that *AP1* is not involved in the suppression of trichome initiation when *AG* is inactive.

3.1.5.4 *TRY* suppresses trichome initiation in parallel with *AG*

Finally, the number of trichomes per gynoecium was seen to be relatively low compared to other described mutants, such as $35S_{PRO}$:GL1 *try* plants, which are characterized by the formation of a large amount of trichomes on the carpel values (Schnittger et al., 1998).

It was hypothesised that there was possibly another pathway repressing the formation of trichomes on carpel valves. *TRY* has been shown to play an essential role in controlling trichome initiation, with mutations resulting in higher trichome density on leaves and sepals (as discussed in section 3.1.1). It was previously noted that the expression levels of *TRY* commence at roughly the same stage as *AG* in early flower development (Wellmer et al., 2006). As mentioned before, qPCR experiments showed that *TRY* levels are largely independent of *AG* function, suggesting that others factors promote its transcription in early flower development (Fig. 3.3 (C)). Lastly, knock down of the *AG* in the *try* background led to a dramatic increase in trichome numbers on carpel valves compared to the AG-amiRNA activated on its own (Fig. 3.3 (H-I). These results together with the qPCR experiments suggest that *TRY* supresses trichome formation in parallel with *AG*, and that there is at least one other pathway repressing trichome initiation on floral organs, as the AG-amiRNA phenotype is enhanced in the *try* mutant background and *try* is not transcriptionally controlled by *AG* (O' Maoileidigh et al., 2013).

This novel work on the homeotic genes, and how they at to directly repress the leaf developmental programs during flower organogenesis, lays the groundwork for this chapter. Using trichome initiation and distribution as a proxy for the leaf developmental programs, this thesis aims to uncover further the molecular mechanisms regulating how the leaf

developmental programs are actively repressed during flower development by the floral organ identity factors. How the flower has adopted this strategy, and actively repressed these programs through evolution, is a question which has remained unanswered for some time and this work aims to add to the growing body of knowledge of how this is carried out developmentally. This is done through the analysis of trichome initiation and distribution in flowers with the use of inducible amiRNAs, phytohormone treatments, inducible overexpression constructs, and analysis of genetic interactions from crosses of described mutants and available T-DNA lines.

3.2 Results

3.2.1 AG suppresses the formation of trichomes on carpel valves in parallel with TRY

Previous published work from the Wellmer laboratory showed that AG is essential to prevent the formation of single and branched trichomes on carpel valves (Ó'Maoiléidigh et al., 2013). This was done using an amiRNA against *AG* mRNA, whose expression is controlled by the ethanol-inducible $AlcA_{PRO}$/AlcR promoter system ($35S_{PRO}$:AlcR/$AlcA_{PRO}$:AG-amiRNA, hereafter referred to as: AlcA:AG-amiRNA). When these transgenic plants were treated under mock conditions flowers were indistinguishable from those of the wild type (Fig. 3.4 A). Conversely, when treated with EtOH vapour for 24 hours, *ag*-like phenotypes and the presence of simple and branched trichomes on carpel valves was observed (Fig. 3.4 B) (Ó'Maoiléidigh et al., 2013). Further to this, the introduction of a *try* mutant allele into the AlcA:AG-amiRNA background resulted in an enhanced trichome phenotype after EtOH treatment, with many more (including three-branched) trichomes forming on carpel valves (Fig. 3.4 C) (Ó'Maoiléidigh et al., 2013).

To confirm the results of these published experiments, the weak *ag-10* allele (Fig. 3.4 D) was crossed with *try-29760* (Fig. 3.4 E). The double mutant of this cross resulted in many single, branched, and stellate trichomes forming along the carpel valves, a phenotype never observed in either of the single mutants (Fig. 3.4 F). This results confirms that *AG* is required to suppress the formation of trichomes on carpel valves.

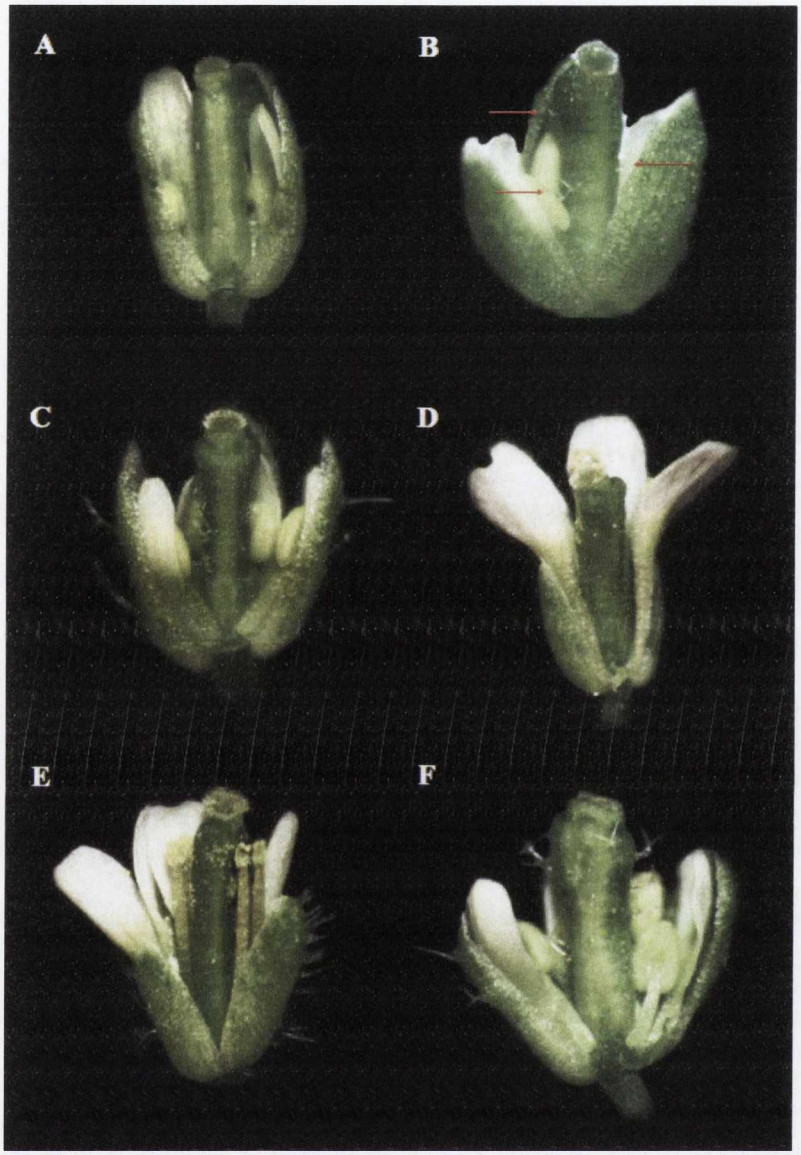

Figure 3.4: *AG* suppresses the formation of trichomes on carpel valves in parallel with *TRY*.

(A) A mock-treated AlcA:AG-amiRNA flower with no trichomes forming on carpel valves. (B) An EtOH-treated AlcA:AG-amiRNA flower with trichomes forming on carpel valves (red arrows). (C) A AlcA:AG-amiRNA *try-29760* flower treated with EtOH, with many more trichomes forming on carpel valves when compared to an *AG* knockdown in a wild-type background. (D) An *ag-10* flower. (E) A *try-29760* flower. (F) An *ag-10 try-29760* double-mutant flower with trichomes forming on carpel valves.

3.2.2 The known leaf trichome activation complex is required for ectopic trichome initiation on floral organs

The activator complex (MBW complex) is required for the initiation of trichomes on leaves and stems. To test if the same regulatory mechanisms are required for the formation of trichomes on floral organs after an *AG* knockdown, loss-of-function alleles of several of the main trichome regulators were crossed into the AlcA:AG-amiRNA background (Fig. 3.5) The following homozygous lines were isolated: AlcA:AG-amiRNA *gl1-20990*, AlcA:AG-amiRNA *gl2-1*, AlcA:AG-amiRNA *gl3-1 egl3-1,* and AlcA:AG-amiRNA *ttg1-1*. All of these lines bore no trichomes, except for the AlcA:AG-amiRNA *gl2-1* line, whose leaves have a reduced number of trichomes compared to the wild type (Koorneef et al., 1981).

AlcA:AG-amiRNA plants that were treated with EtOH formed simple and branched trichomes on the carpel valves (Fig. 3.5 B), whereas no trichomes formed on the mock-treated plants as previously described (Ó'Maoiléidigh et al., 2013). Next, AlcA:AG-amiRNA *gl1-20990*, AlcA:AG-amiRNA *gl3-1 egl3-1* and AlcA:AG-amiRNA *ttg1-1* plants were treated with EtOH and compared to AlcA:AG-amiRNA plants. No trichomes formed on the carpel valves of any of these lines, yet *ag*-like knockdown phenotypes were seen, indicating that the AG-amiRNA was active in these plants (Fig. 3.5 C-F).

In the AlcA:AG-amiRNA *gl2-1* double mutant some trichomes formed on carpel valves after EtOH treatment, but their number was smaller than that observed after an AG knockdown in a wild-type background (Fig. 3.5 D). This result is in agreement with the reduction of trichome numbers on leaves of *gl2-1* plants, which are not entirely glabrous (see above). These results show that AG has a role in inactivating the MBW complex either directly or indirectly to inhibit trichome formation on carpel valves.

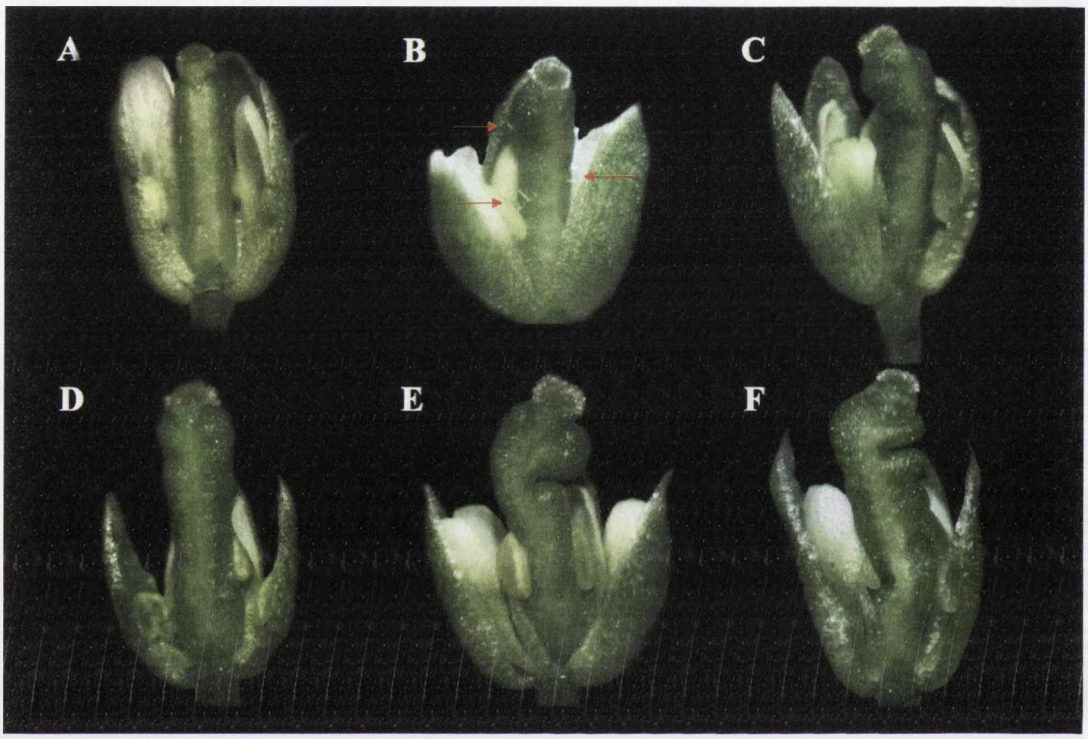

Figure 3.5: The leaf trichome activation complex is needed for trichomes to form on floral organs.

(A) A mock-treated flower of a $35S_{PRO}$:AlcR/$AlcA_{PRO}$:AG-amiRNA (AlcA:AG-amiRNA) plant. (B) Flower of an EtOH-treated AlcA:AG-amiRNA plant with trichomes forming on carpel valves and a slightly bent carpel. (C) Flower of an EtOH-treated AlcA:AG-amiRNA *gl1-20990* plant with no trichomes on any organs. (D) Flower of an AlcA:AG-amiRNA *gl2-1* plant with no trichomes on any organs. (E) Flower of an EtOH-treated AlcA:AG-amiRNA *gl3-1 egl3-1* plant. All organs are glabrous. (F) Flower of an EtOH-treated AlcA:AG-amiRNA *ttg1-1* plant with no trichomes on any organs. All flowers were photographed one week after EtOH treatment and at around the time of anthesis.

3.2.3 The *SHATTERPROOF* genes regulate trichome formation in flowers together with *AG*

The *SHP* genes (*SHP1* and *SHP2*) are paralogs (59% amino acid identity) of *AG* and are known to play redundant roles with *AG* during flower development (Pinyopich et al., 2003). We therefore investigated whether they also act redundantly with *AG* in the suppression of trichome initiation in flowers. To this end, the AlcA:AG-amiRNA transgene was crossed into the *shp1-1 shp2-1* double-mutant background. Homozygous lines were generated and treated with EtOH vapour or were mock-treated (Fig. 3.6 A-D). While mock-treated AlcA:AG-amiRNA *shp1-1 shp2-1* plants did not form trichomes on any floral organ type but sepals (Fig. 3.6 A-B), AlcA:AG-amiRNA *shp1-1 shp2-1* plants treated with EtOH vapour (Fig. 3.6 C) formed substantially more trichomes along carpel valves than plants in which *AG* had been knocked down in a wild-type background (Fig. 3.8 E (blue bar)). These trichomes also appeared to often have more branches (Fig. 3.6 D insert), suggesting that the *SHP* genes may somehow affect endoreduplication, which is known to lead to higher trichome branching (Pattanaik et al., 2014).

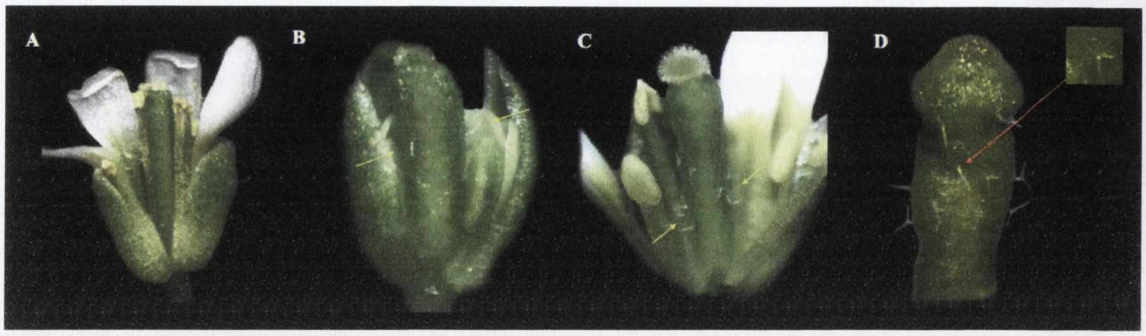

Figure 3.6: The *SHP* genes redundantly regulate trichome formation with *AG*.

(A) Flower of a mock-treated AlcA:AG-amiRNA *shp1-1 shp2-1* plant. (B) Flower of a EtOH-treated AlcA:AG-amiRNA plant with single and branched trichomes forming on carpel valves. (C) Flower of an EtOH-treated AlcA:AG-amiRNA *shp1-1 shp2-1* plant with a higher number of trichomes forming on carpel valves than in EtOH-treated AlcA:AG-amiRNA lines. (D) Gynoecium of an EtOH-treated AlcA:AG-amiRNA *shp1-1 shp2-1* flower with stellate trichomes forming on carpel valves (yellow arrows). All flowers were photographed at around the time of anthesis one week after mock or EtOH treatments.

The results from the experiments described above suggested that AG and the SHPs may work together in the suppression of trichome formation on carpel valves. To further test this idea we determined whether an inducible over-expression of a SHP2-GFP fusion protein could suppress trichome formation after an AG knockdown. To this end, we generated a line that expressed SHP2-GFP under control of the OP_{PRO}/GR-LhG4 dexamethasone-inducible promoter system (OP_{PRO}:SHP2-GFP) (Fig. 3.7 A). To test whether this line was functional, the transgene was crossed into the *ag-1* mutant background (Fig. 3.7 B). Upon dexamethasone treatment, the transgene was able to partially complement the *ag-1* mutant phenotype (Fig. 3.7 C-D). Also, in a wild-type background, it caused the transformation of petals into stamens, similar to what has been previously described for SHP2 mis-expression (Pinyopich et al., 2003) (Fig. 3.7 F-G). Thus, the transgene appeared to be fully functional.

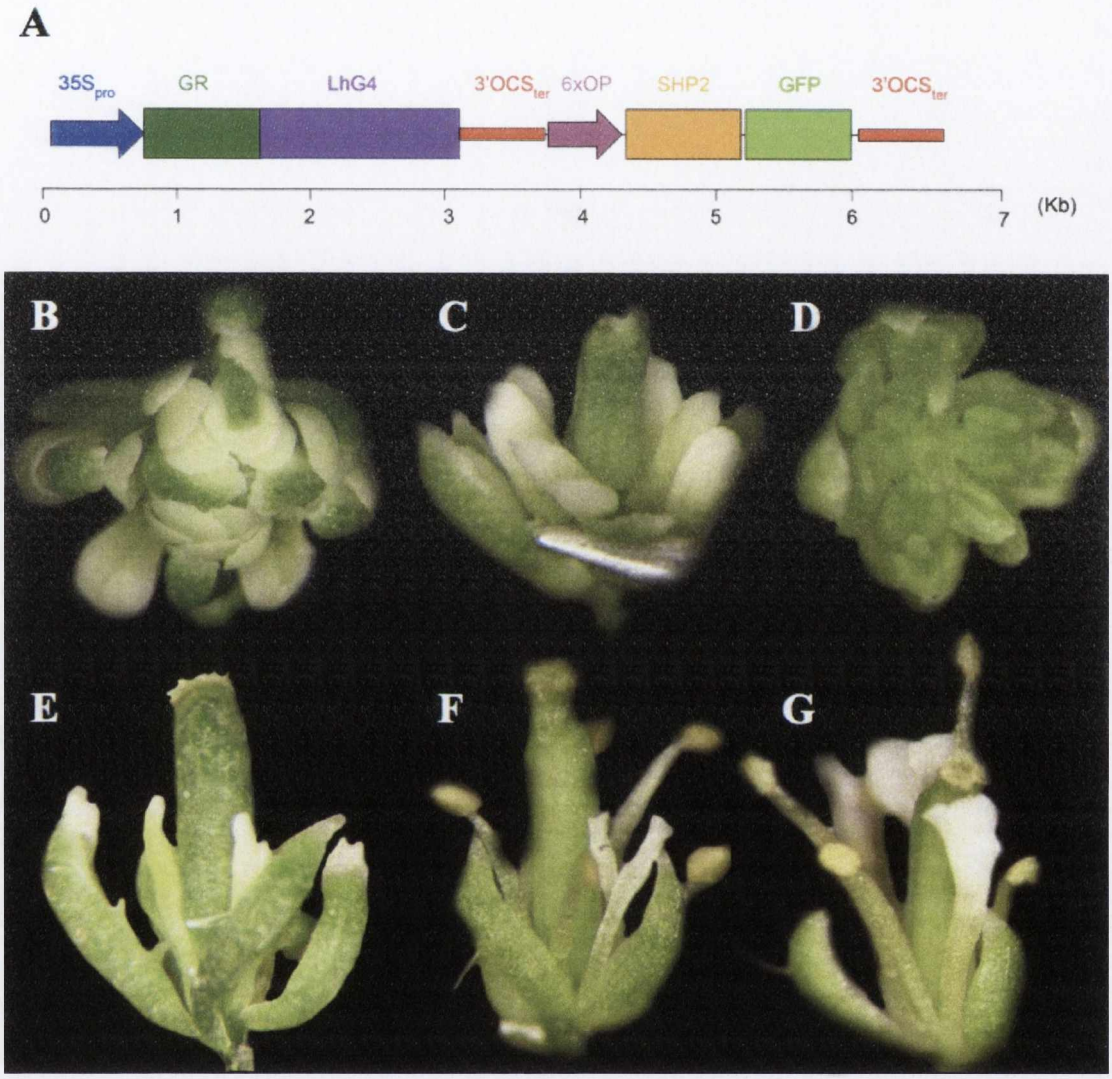

Figure 3.7: Over-expression of *SHP2* rescues the *ag* mutant phenotype.

(A) Schematic of the $35S_{PRO}$:LhG4-GR/$6XOP_{PRO}$:SHP2-GFP T-DNA (denoted: OP:SHP2-GFP). (B) An *ag-1* flower. Considered a null allele, *ag-1* results in recurring whorls of sepals and petals. (C-E) Flowers of *ag-1* OP:SHP2-GFP plants treated with 10 μM dexamethasone. Images were taken 14 d after the treatment. (C) Flower with partially restored carpel morphology. (D-E) Flowers with partially restored carpel and stamen morphology. (F-G) Flowers of a OP:SHP2-GFP (in wild-type L-*er*) plant treated with 10 μM dexamethasone. Images were taken 14 d after the treatment. Narrowing of petals and transformation towards stamens can be seen.

The OP_{PRO}:SHP2-GFP transgene was crossed into the AlcA:AG-amiRNA background, and a line doubly homozygous for both transgenes was isolated. The resulting OP:SHP2-GFP AlcA:AG-amiRNA line was then treated with EtOH vapour alone to specifically knock down *AG* function (Fig. 3.8 A and C), or with a combination of EtOH vapour and dexamethasone to simultaneously knock down *AG* and activate SHP2-GFP expression (Fig. 3.7 B and D). As expected, flowers of plants treated with EtOH alone formed a small number of trichomes per gynoecium (Fig. 3.8 E (Orange bar)), while gynoecia of plants treated with both EtOH and dexamethasone bore far fewer trichomes (Fig. 3.8 E (Red bar)). Thus, it appears that the over-expression of SHP2-GFP partially compensated for a loss of AG function in this line. Overall the results of the loss and gain-of-function experiments described above showed that the *SHP* genes contribute to the repression of trichome formation on carpel valves together with AG. Although I did not test this here specifically, it seems likely that this redundancy is due to AG and the SHP transcription factors targeting the same set of trichome regulatory genes.

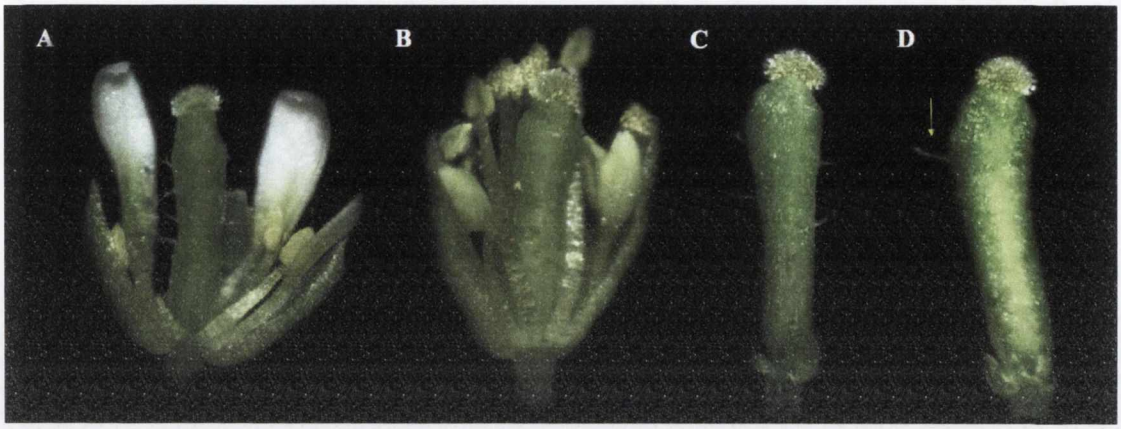

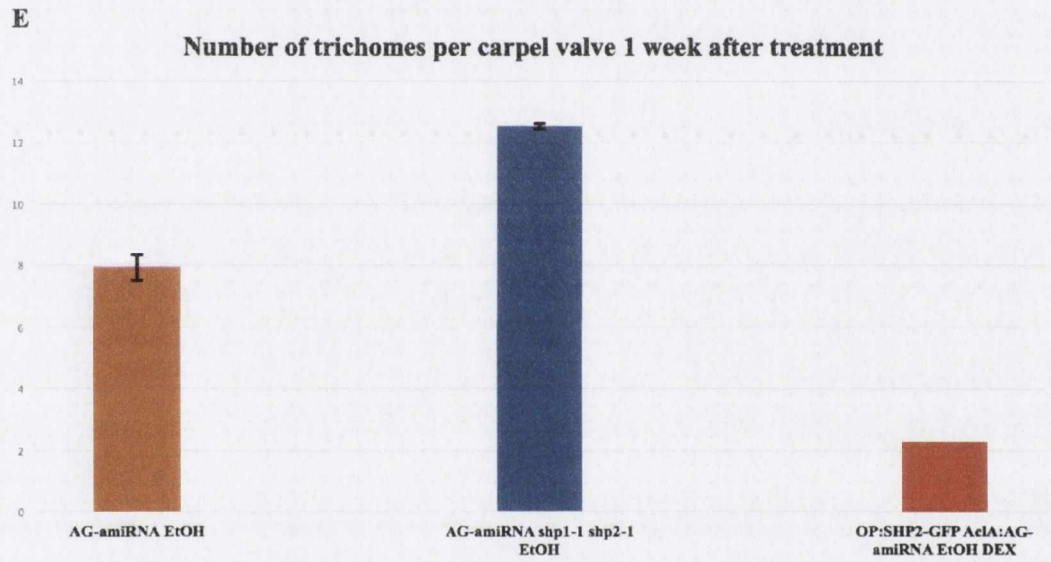

Figure 3.8: Over-expression of *SHP2* can partially repress trichome initiation caused by an *AG* knockdown.

(A) Flower of an OP:SHP2-GFP AlcA:AG-amiRNA plant at anthesis after treatment with EtOH. Trichomes are visible on carpel valves. (B) Flower of an OP:SHP2-GFP AlcA:AG-amiRNA plant treated with EtOH and dexamethasone. No trichomes are visible on carpel valves. The flower displays the carpel phenotype typically observed after an *AG* knockdown, and petals have started to transform into stamens. (C) A gynoecium of a OP:SHP2-GFP AlcA:AG-amiRNA plant treated with EtOH only. Trichomes are visible on carpel valves. (D) A gynoecium of a OP:SHP2-GFP AlcA:AG-amiRNA plant treated with EtOH and dexamethasone. One unbranched trichome is visible on a carpel valve. (E) Numbers of trichomes per gynoecium one week after treatment. AlcA:AG-amiRNA and AlcA:AG-amiRNA *shp1-1 shp2-1* were treated at the same time. Knockdown of *AG* in the *shp1-1 shp2-1* back-

ground resulted in more trichomes forming per carpel valve than after an *AG* knock down in a wild-type background. Activation of the AlcA:AG-amiRNA and OP:SHP2-GFP transgenes at the same time results in a reduction in trichome numbers compared to AlcA:AG-amiRNA. Number of plants analysed: AlcA:AG-amiRNA (n=19); AlcA:AG-amiRNA *shp1-1 shp2-1* (n=53); AlcA:AG-amiRNA OP:SHP2-GFP (n=36). Error bars indicate SE. Mock-treated plants (not shown) never bore any trichomes on carpel valves and resembled wild-type flowers.

3.2.4 The *SQUAMOSA PROMOTER BINDING PROTEIN-LIKE* genes redundantly regulate trichome initiation on carpels

As previously discussed (section 3.1.3), SPL9 and possibly other SPL family members regulate the suppression of trichomes on stems and pedicels of *Arabidopsis* by directly up-regulating the trichome repressor genes *TCL1* and *TRY* (Yu et al., 2010). However, whether the SPL transcription factors are also involved in regulating trichome initiation in flowers remained unknown. In fact, ectopic trichome formation has never been reported for any *spl* mutant combination or knockdown experiment described in the literature. To test whether the SPLs play a role in the suppression of trichome initiation in flowers, their genetic interaction with *AG* was investigated. To this end, a transgenic line, which overexpresses miR156 ($35S_{PRO}$:miR156) (Schwab et al., 2005), was crossed into the AlcA:AG-amiRNA background and subsequently, a line was isolated that harboured both transgenes. Once treated with EtOH there was a large increase in the number of trichomes forming on the carpel valves compared to the AlcA:AG-amiRNA line alone or to mock-treated control plants (Fig. 3.9 D). This result indicated that the miR156-targeted *SPL* genes contribute to the suppression of trichome formation on carpel valves in parallel with *AG*.

To test if the *SPL* genes were able to prevent trichome formation in the absence of *AG*, the AlcA:AG-amiRNA was crossed with a miR156 target mimicry transgene

(35S$_{PRO}$:MIM156) (Wang et al., 2008), which is known to block the effect of miR156, resulting in increased *SPL* activity (as discussed in section 3.1.3). Homozygous lines were isolated and treated with EtOH to knock down *AG* activity. This resulted in a reduction in trichome numbers on carpel valves relative to an *AG* knockdown in a wild-type background (Fig. 3.9 A, F-G). All lines also showed the *ag*-like phenotypes, indicating that the transgene was functional. To further validate these results the AlcA:AG-amiRNA was crossed with a miR156 insensitive version of *SLP9* (SPL9$_{PRO}$:GFP-rSPL9) and homozygous lines were isolated. When *AG* was knocked down, no trichomes initiated on carpel valves, yet *ag*-like phenotypes were evident (Fig. 3.9 H-I), indicating that the *AG* knockdown had been successful. Finally to test which *SPL* genes were regulating this process we introgressed the AlcA:AG-amiRNA transgene into an *spl9-4 spl15-1* double-mutant background. When these plants were treated with EtOH, an increase in the number of trichomes per carpel valve was observed relative to an *AG* knockdown in a wild-type background (Fig. 3.9 A-C). Overall these results show that the *SPL* genes suppress the formation of trichomes on carpel valves in parallel with *AG*.

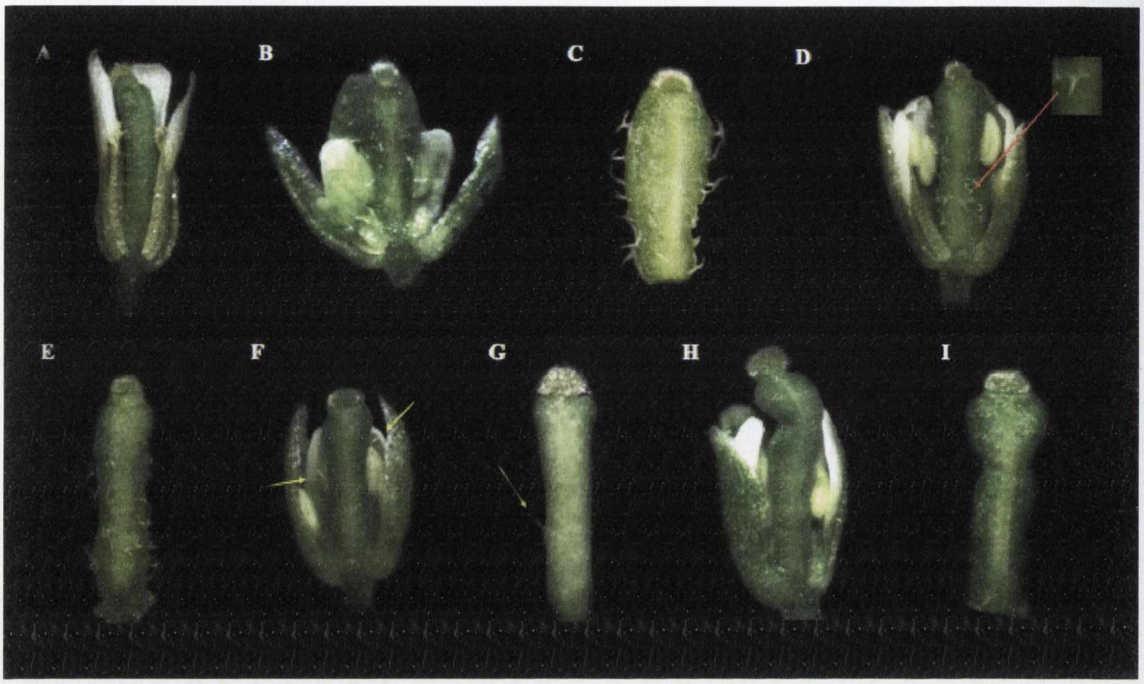

Figure 3.9: The *SPL* genes redundantly regulate trichome initiation on carpels with *AG*. (A) An AlcA:AG-amiRNA flower after EtOH treatment, with trichomes forming on carpel valves. (B) An AlcA:AG-amiRNA *spl9-1 spl15-1* flower after EtOH treatment, with numerous trichomes forming on carpel valves. (C) An AlcA:AG-amiRNA *spl9-1 spl15-1* gynoecium after EtOH treatment. (D) An AlcA:AG-amiRNA $35S_{PRO}$:miR156f flower after EtOH treatment, with numerous trichomes forming on carpel valves. Stellate trichomes also form (red arrow, inset). (E) An AlcA:AG-amiRNA $35S_{PRO}$:miR156f gynoecium after EtOH treatment. (F) An AlcA:AG-amiRNA $35S_{PRO}$:MIM156 flower after EtOH treatment, with a reduction in trichome numbers compared to EtOH-treated AlcA:AG-amiRNA plants alone. (G) A gynoecium of an EtOH-treated AlcA:AG-amiRNA $35S_{PRO}$:MIM156 flower with a single trichome. (H) A AlcA:AG-amiRNA $SPL9_{PRO}$:rSPL-GFP flower after EtOH treatment with no trichomes forming on carpel valves. (I) A dissected gynoecium of an AlcA:AG-amiRNA $SPL9_{PRO}$:rSPL-GFP flower after EtOH treatment with no trichomes forming on carpel valves. All images were taken one week after treatments.

3.2.5 *TRY* and *CPC* suppress trichome formation on floral organs

It has been previously shown that *AG* and *TRY* independently suppress the formation of trichomes on carpel valves (Ó'Maoiléidigh et al., 2013). To validate this observation and to

gain further insights into the interaction of these two genes, I carried out a number of experiments with *try* mutant alleles. *Try* mutants exhibit an increased trichome density and clustering of trichomes on rosette leaves (Fig. 3.10 A-C) when compared to the wild type. There is also an increase in trichome density and branching on the abaxial sides of *try* sepals compared to the wild type (Fig. 3.10 D-F). Trichomes do not form on any other floral organs. As previously described (Ó'Maoiléidigh et al., 2013), an amiRNA-mediated knockdown of *AG* in a *try-29760* resulted in an increase in trichome number and a substantial number of branched and stellate trichomes on carpel valves relative to an *AG* perturbation in a wild-type background (Fig. 3.10 G-H and Fig. 3.13 C-E). These results corroborate the previous findings that *TRY* represses trichome initiation on carpel valves in parallel with *AG* (Ó'Maoiléidigh et al., 2013).

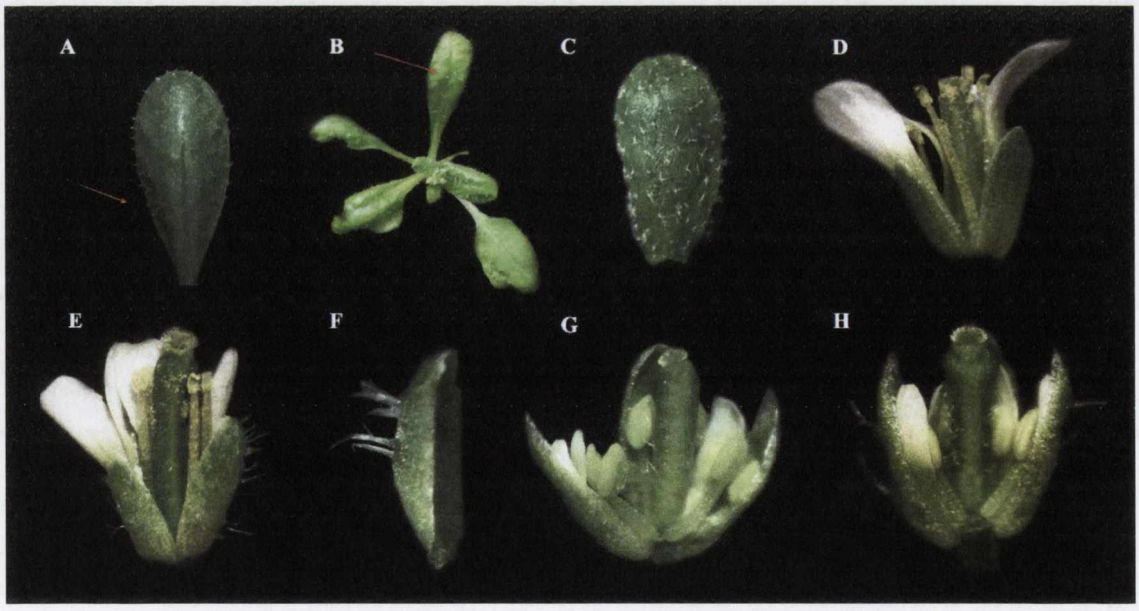

Figure 3.10: *TRY* represses trichome initiation in parallel with *AG*.

(A) A mature rosette leaf of a wild-type AlcA:AG-amiRNA plant with an even distribution of trichomes (red arrow). (B) An AlcA:AG-amiRNA *try-29760* plant with clustering of trichomes (red arrow). (C) Mature rosette leaf of an AlcA:AG-amiRNA *try-29760* plant with clustering of trichomes

compared to the wild type (not shown). (D) A wild-type flower. (E) A *try-29760* flower with increased trichome density on sepals, and branching of trichomes. (F) A dissected sepal of a *try-29760* plant with clustering of trichomes and branching visible. (G) An EtOH-treated AlcA:AG-amiRNA flower at anthesis one week after treatment. (H) An EtOH-treated AlcA:AG-amiRNA *try-29760* flower at anthesis one week after treatment. More trichomes are visible compared to EtOH-treated AlcA:AG-amiRNA flowers, with branching occurring more often. Stellate trichomes can also be seen (not shown).

Next, the role of another single repeat R3 MYB trichome repressor, CAPRICE (CPC), was investigated. In *cpc-1* mutant plants, an increase in trichome density on rosette and cauline leaves relative to the wild type is observed (Fig. 3.11 A-C). There is also an increase in simple and sometimes branched trichomes on the abaxial side of sepals compared to wild-type sepals (Fig. 3.11 D-F), but no trichomes form on any other floral organs. To assess the role of *CPC* in regulating trichome formation on flowers, the *cpc-1* mutanttion was introgressed into the AlcA:AG-amiRNA background. Upon EtOH treatment of the resulting plants, I observed an increase in the number of simple and branched trichomes forming on carpel valves relative to an *AG* knockdown in a wild-type background (Fig. 3.11 G-H and Fig. 3.13 F-H). This result shows that *CPC* contributes to the suppression of trichome formation on gynoecia.

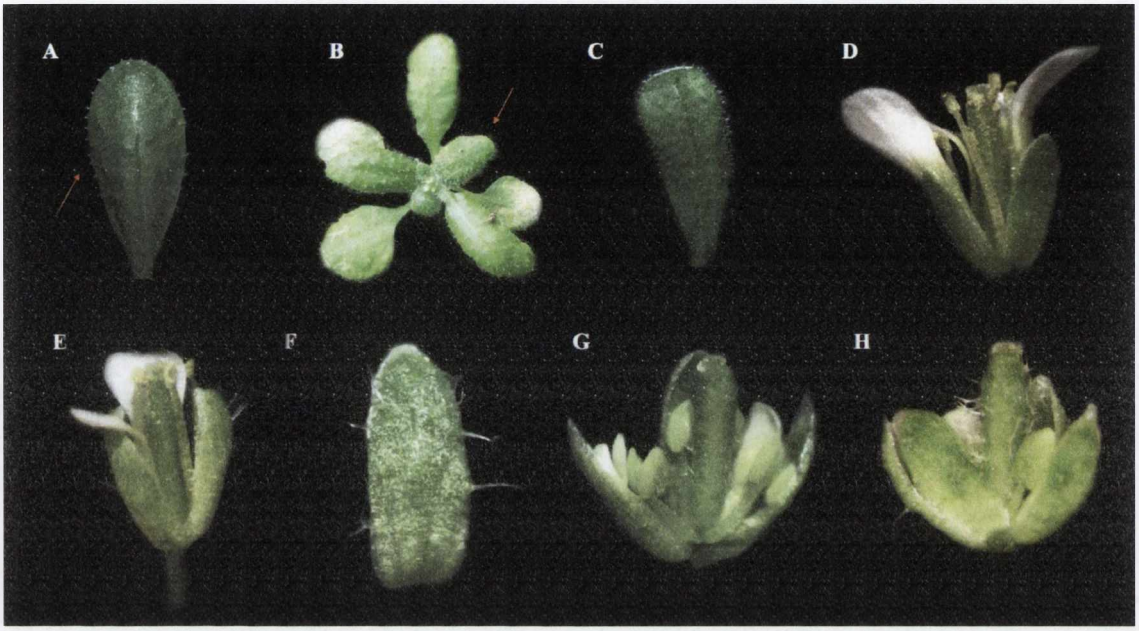

Figure 3.11: *CPC* represses trichome initiation together with *AG*.

(A) A mature rosette leaf of an AlcA:AG-amiRNA plant (in a wild-type background) with an even distribution of trichomes (red arrow) on rosette leaves. (B) An AlcA:AG-amiRNA *cpc-1* plant with a higher density of trichomes on leaves (red arrow). (C) Mature rosette leaf of an AlcA:AG-amiRNA *cpc-1* plant with a greater number of trichomes compared to wild-type (not shown). (D) A wild-type flower. (E) A *cpc-1* flower with an increased number of trichomes on sepals. Trichomes were mostly unbranched. (F) A dissected sepal of a *cpc-1* flower with an increased number of trichomes, which were mostly unbranched. (G) An AlcA:AG-amiRNA flower treated with EtOH, at the time of anthesis. Image was taken one week after the treatment. (H) An EtOH-treated AlcA:AG-amiRNA *cpc-1* flower at anthesis one week after treatment. More trichomes are visible compared to the AlcA:AG-amiRNA flower treated alone, with trichomes being mostly unbranched.

To investigate whether *TRY* and *CPC* play redundant roles in repressing trichomes on floral organs, the *cpc-1 try-29760* double mutant was introgressed into the AlcA:AG-amiRNA background. *Cpc-1 try-29760* double mutants are characterized by a substantial increase in trichome numbers, and clustering on rosette leaves, compared to either of the single mutants or the wild type (Fig. 3.12 A-C). There is also an increase in trichome density and branching on the abaxial side of sepals compared to either of the single mutants or the wild type (Fig.

3.12 D-F). Upon EtOH treatment of the *cpc-1 try-29760* AlcA:AG-amiRNA plants a 200% increase in the number of trichomes on carpel valves was observed relative to a AlcA:AG-amiRNA-mediated *AG* knockdown in a wild-type background, and most of these trichomes were two-branched or three-branched (Fig. 3.12 G-H and Fig. 3.13 I). Further to this, trichomes sometimes formed on the distal tip of the gynoecium likely from a region underneath the stigmatic papillae (Fig. 3.13 I).

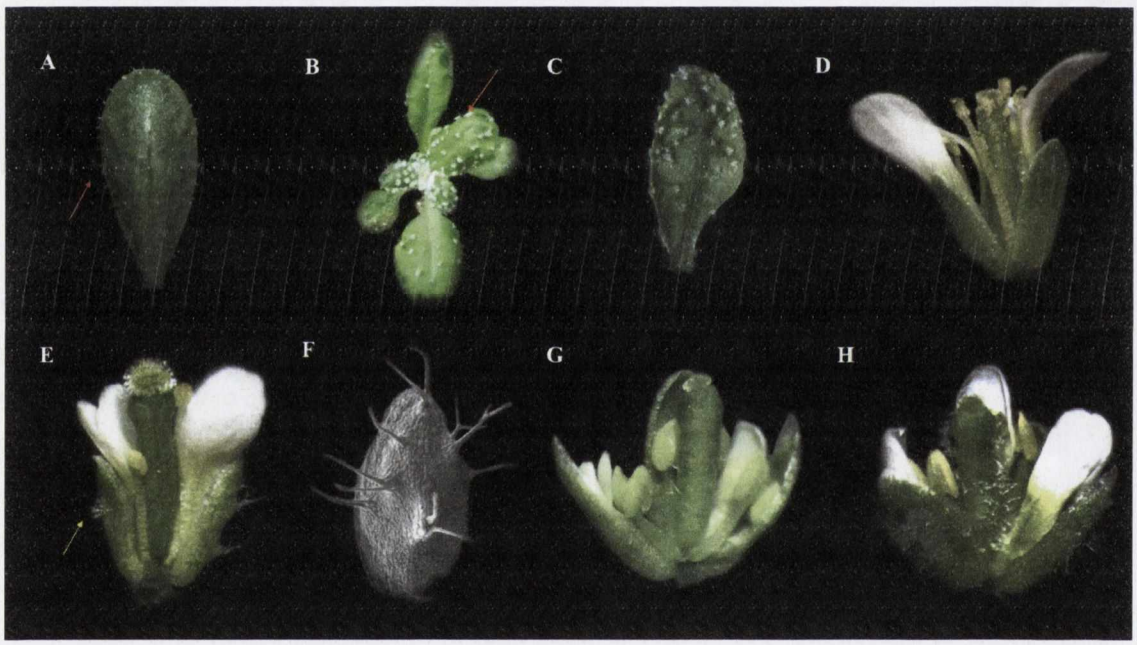

Figure 3.12: CPC and TRY together contribute to the suppression of floral trichomes.
(A) A mature rosette leaf of an AlcA:AG-amiRNA plant with even distribution of trichomes (red arrow). (B) An AlcA:AG-amiRNA *try-29760 cpc-1* plant with a higher density of trichomes which form clusters on leaves (red arrow). (C) Mature rosette leaf of an AlcA:AG-amiRNA *try-29760 cpc-1* plant with trichome clusters. (D) A wild-type flower. (E) A *try-29660 cpc-1* flower with trichome clusters on sepals (yellow arrow). (F) A dissected sepal of a *try-29760 cpc-1* flower with a greater density of trichomes, which unlike the wild type, form clusters. (G) An EtOH-treated AlcA:AG-amiRNA flower at anthesis one week after treatment. (H) An EtOH-treated AlcA:AG-amiRNA *try-29760 cpc-1* flower at anthesis one week after treatment. Many more trichomes are visible than in (G). Most trichomes are branched and sometimes stellate.

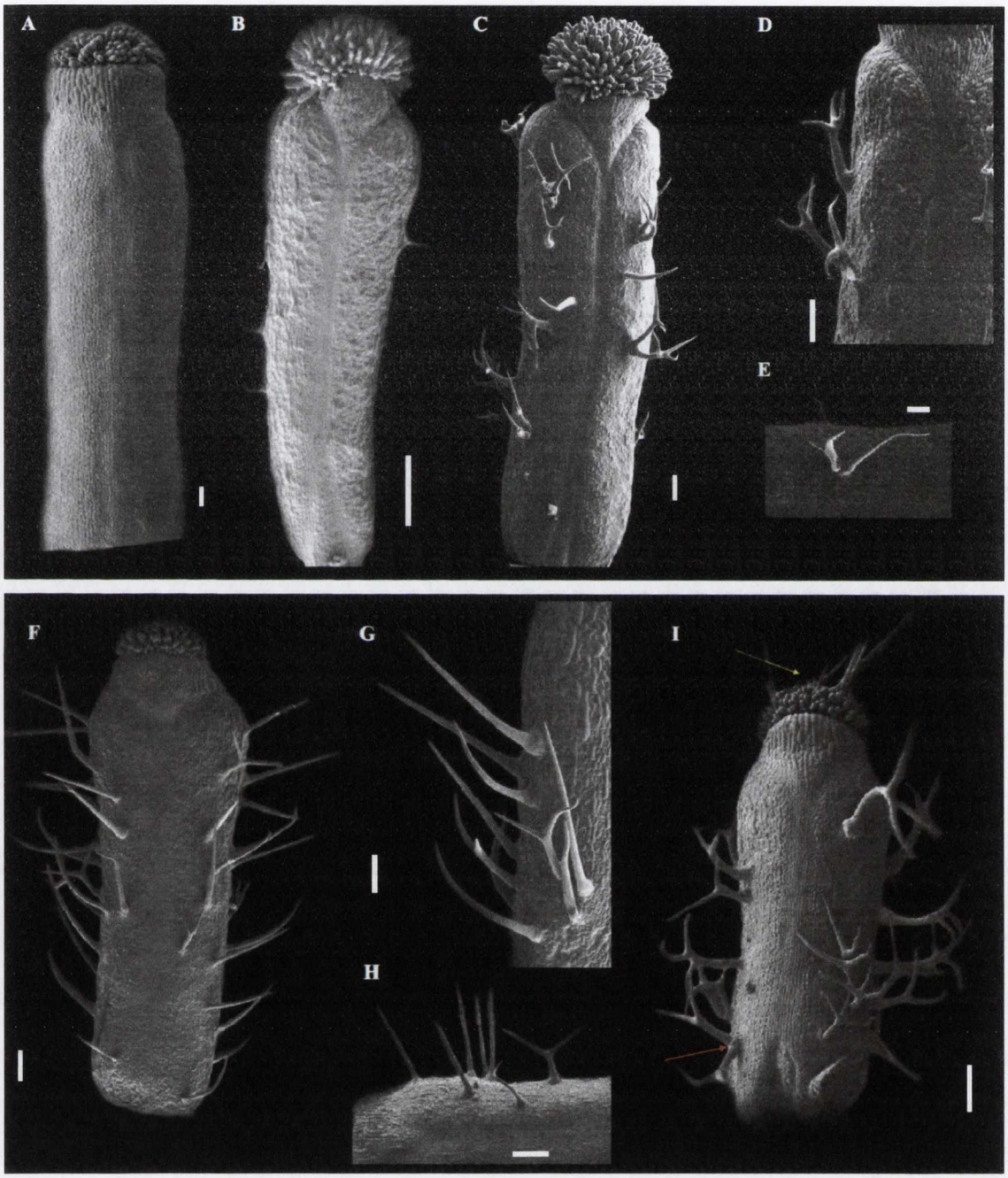

Figure 3.13: *TRY* and *CPC* repress trichome formation together with *AG*.

(A) A wild-type gynoecium at anthesis with no trichomes forming on the valves. (B) An AlcA:AG-amiRNA gynoecium at anthesis treated with EtOH. Trichomes form on carpel valve. (C-E) An AlcA:AG-amiRNA *try-29760*. Branched trichomes form in clusters along the carpel valves (C) Gynoe-

cium one week after EtOH treatment. More trichomes form compared to the AlcA:AG-amiRNA plants alone. (D) Stellate and branched trichomes occur in higher numbers compared to the AlcA:AG-amiRNA alone. (E) Two trichomes clustered together on the carpel valve, which is not seen in the wild type. (F-H) Gynoecium of AlcA:AG-amiRNA *cpc-1* plants. (F) A carpel at anthesis one week after EtOH treatment. (G) Close-up of a valve showing mostly unbranched trichomes. (H) Trichomes are mostly unbranched and do not initiate from the adjacent cells like in AlcA:AG-amiRNA *try-29760* plants. (I) A gynoecium of an EtOH-treated AlcA:AG-amiRNA *try-29760 cpc-1* flower one week after the treatment. The double mutant exhibited an additive effect on trichome number. Trichomes formed from adjacent points (red arrow) and sometimes from the tip of the gynoecium (yellow arrow). Scale bars: 100 μm.

In addition to trichomes forming on the tips of the gynoecia of EtOH-treated *cpc-1 try-29760* AlcA:AG-amiRNA plants, strikingly, trichomes were also observed on the adaxial surface (the inside) of carpel valves, a phenotype never observed in AlcA:AG-amiRNA *cpc-1* or AlcA:AG-amiRNA *try-29760* plants after an *AG* knockdown (Fig. 3.14 A-E). Thus, it appears that AG, TRY and CPC together suppress trichome formation not only on the abaxial but also on the adaxial side of carpel valves. Most of the adaxial trichomes were either two or three-branched (Fig. 3.15 A-B). In addition, trichomes also formed on the tips of anthers towards the adaxial side upon EtOH treatment of *cpc-1 try-29760* AlcA:AG-amiRNA plants (Fig. 3.16 D).

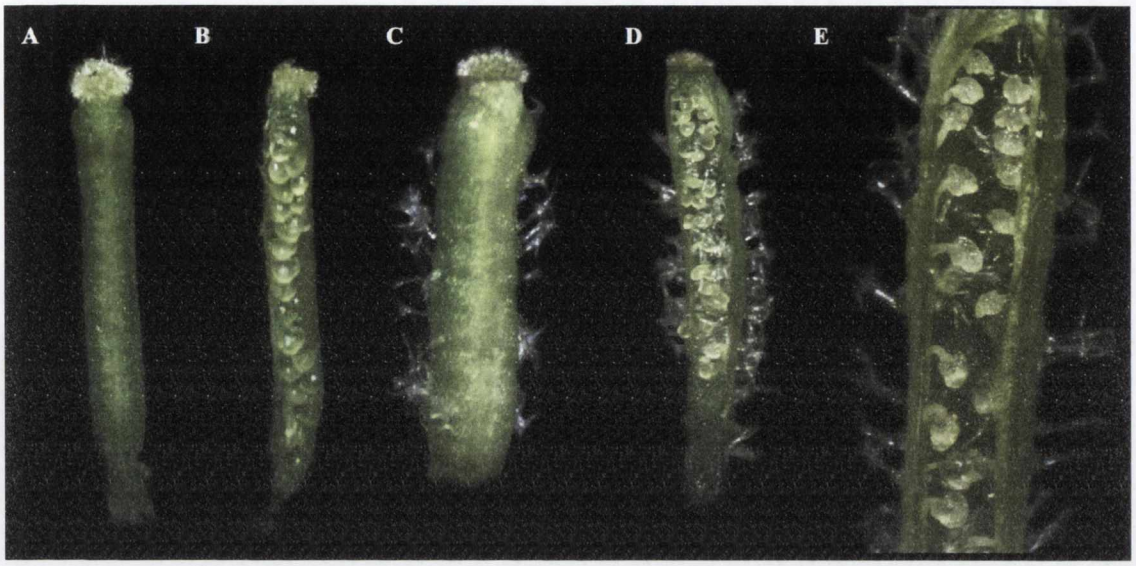

Figure 3.14: Trichomes form on the abaxial side of EtOH-treated AlcA:AG-amiRNA *try-29760 cpc-1* flowers.

(A) A gynoecium of an untreated AlcA:AG-amiRNA *try-29760 cpc-1* flower. (B) The adaxial surface of an untreated AlcA:AG-amiRNA *try-29760 cpc-1* gynoecium (C) Abaxial surface of a gynoecium of a EtOH-treated AlcA:AG-amiRNA *try-29760 cpc-1* flower with trichomes forming on carpel valves. (D-E) Adaxial side of a gynoecium of an EtOH-treated AlcA:AG-amiRNA *try-29760 cpc-1* flower with trichomes forming along the carpel valves.

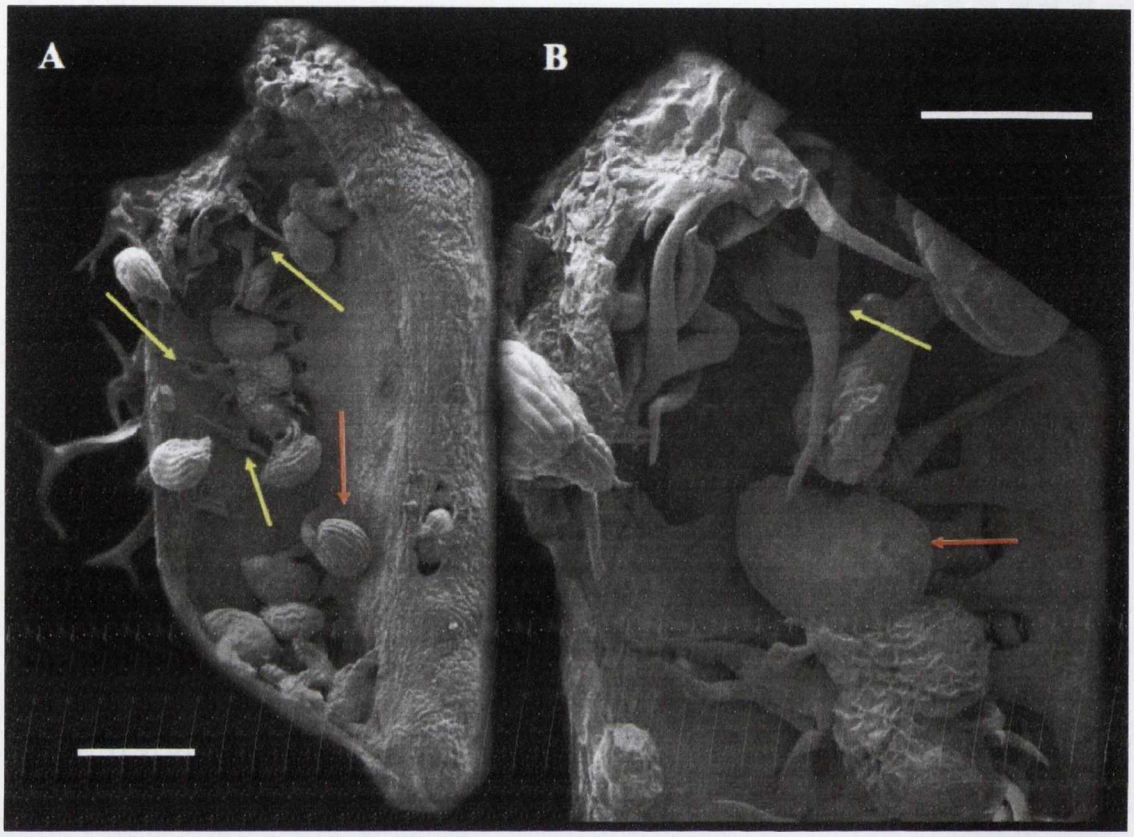

Figure 3.15: Trichomes form on the adaxial side of EtOH-treated AlcA:AG-amiRNA *try-29760 cpc-1* flowers.

(A-B) The adaxial side of an EtOH-treated AlcA:AG-amiRNA *try-29760 cpc-1* gynoecium with trichomes forming along the valves. (A) Trichomes can been seen forming on carpel valves (yellow arrows) next to ovules (red arrows). (B) Close-up of branched trichomes forming on carpel valves (yellow arrow) next to ovules (red arrow). Scale bars: 100 μm.

Previously it was shown that amiRNAs targeting the mRNAs of *AP3* and *PI* resulted in strong B function knock downs, causing the plants to phenocopy *ap3* and *pi* mutants (Wuest et al., 2012). These amiRNAs were put under the control of the dexamethasone-responsive OP_{PRO}/GR-LhG4 system (OP:AP3-amiRNA and OP:PI-amiRNA) (Wuest et al., 2012). When OP:PI-amiRNA was crossed with the AlcA:AG-amiRNA, and both amiRNAs induced at the same time, there was the formation of branched trichomes on the abaxial side of anthers on a

few flowers per plant (Ó'Maoiléidigh et al., 2013). This was also true for OP:AP3-amiRNA AlcA:AG-amiRNA flowers. Thus, the B and C function regulators appear to work together in the suppression of trichome formation in the third floral whorl.

To further assess *TRY*'s role in supressing floral trichome initiation, *try* was introgressed into an OP:AP3-amiRNA AlcA:AG-amiRNA background. When the resulting plants were simultaneously treated with dexamethasone and EtOH there was the formation of many more trichomes on the abaxial side of anthers, and the number of flowers that displayed this phenotype per plant increased (Fig. 3.16 A-C). The localization of these trichomes was different compared to the AlcA-AG-amiRNA *tyr-29760 cpc-1* trichomes, which only formed on the tips of anthers more towards the adaxial side, but never forming on the abaxial side (Fig. 3.16 D). These observations suggest that *CPC* and *TRY* control the localization of trichomes on the abaxial and adaxial side not only of carpels but also of stamens.

Overall these results show that *TRY* and *CPC* have roles in regulating the suppression of trichomes on sepals, anthers and carpel valves on their abaxial and adaxial sides, and that they control these processes in parallel with *AG* and *AP3/PI*.

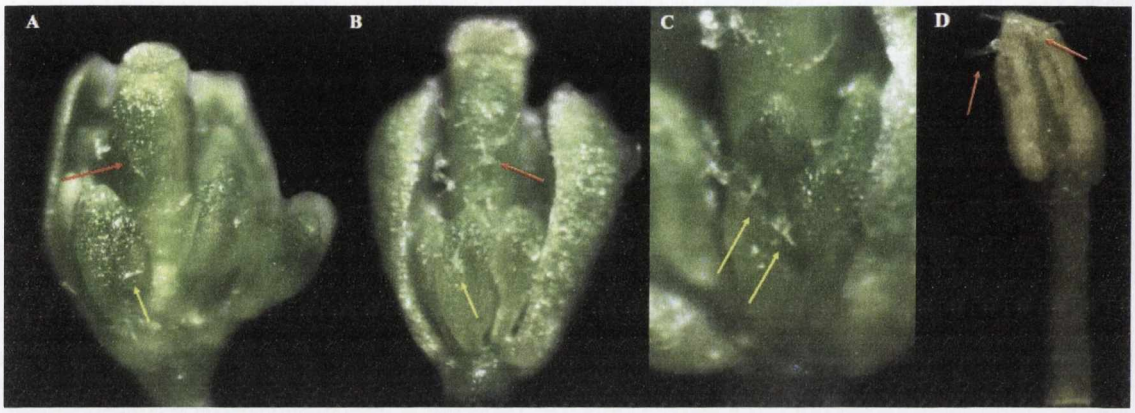

Figure 3.16: *AG*, *AP3*, *TRY*, and *CPC* redundantly repress trichome initiation on the abaxial side of anthers.

(A) An AlcA:AG-amiRNA OP:AP3-amiRNA flower with trichomes forming on the gynoecium (red arrow) and on the abaxial side of an anther (yellow arrow) after treatment with EtOH and dexamethasone. (B-C) Trichomes forming on carpel valves (red arrow) and the abaxial side of anthers (yellow arrow) of AlcA:AG-amiRNA OP:AP3-amiRNA *try-29760* flowers after EtOH and dexamethasone treatment. (C) Anther showing an increase in trichome density and stellate trichomes (yellow arrow). (D) An anther dissected from an EtOH-treated AlcA:AG-amiRNA *try-29760 cpc-1* flower with trichomes forming on the tip closer to the adaxial side.

3.2.6 *AG* acts as negative regulator of cytokinin signalling to repress trichome formation on flowers

Previous studies uncovered direct and indirect targets of AG during floral organ specification on a genome-wide scale (Ó'Maoiléidigh et al., 2013). Among the genes identified were many required for phytohormone responses and turnover. It is well known that several hormones, including gibberellins (GA), cytokinin (CK), and jasmonic acid (JA), promote trichome formation (Traw and Bergelson, 2003). To test whether any of these hormonal pathways contribute to the control of floral trichome formation, we exogenously treated inflorescences with solutions containing different hormones. To test if our hormone stocks were functionally

active, seedlings were grown on plates with 100 μM of either GA, CK, and JA. It is known that the number of trichomes on rosette leaves marginally increases in the presence of these hormones. In our experiments, this was indeed the case with GA_3, MeJA, and 6-Benzylaminopurine (BAP), a synthetic CK which had the strongest response compared to the control (Fig. 3.17 A). Thus, the hormone solutions we used for our work appeared to be active.

When we treated wild-type inflorescences with hormone solutions, we never observed the initiation of trichomes on the internal floral organs (not shown). We therefore repeated these experiments in a sensitized background. To this end, inflorescences of EtOH-treated AlcA:AG-amiRNA plants were treated with either GA_3, MeJA, or BAP containing solutions. In the presence of GA_3 and MeJA, a moderate increase in trichome numbers on carpel valves was observed relative to plants in which AG had been knocked down but that had not been treated with any hormone solution (Fig. 3.17 B). In contrast, there was a dramatic increase in the number of trichomes on carpel valves in plants that had been treated with BAP after an *AG* knockdown (Fig. 3.17 B and Fig. 3.18 A-C). I next tested whether this increase in trichome formation correlated with BAP concentration. Indeed, the number of trichomes on carpel valves increased with increasing concentrations of BAP (Fig. 3.17 C), with the most being produced when the inflorescences were treated with 2 mM BAP and EtOH vapour (Fig. 3.18 D). To confirm these results, the experiments were repeated with the *ag-10* mutant instead of the AlcA:AG-amiRNA line. In agreement with our initial observations suggesting that BAP has the strongest effect on floral trichome formation among the different hormones tested, only carpel valves of BAP-treated *ag-10* flowers formed trichomes in this experiment

(Fig. 3.18 E-H). These results imply that cytokinin is involved in the control of floral trichome initiation together with AG.

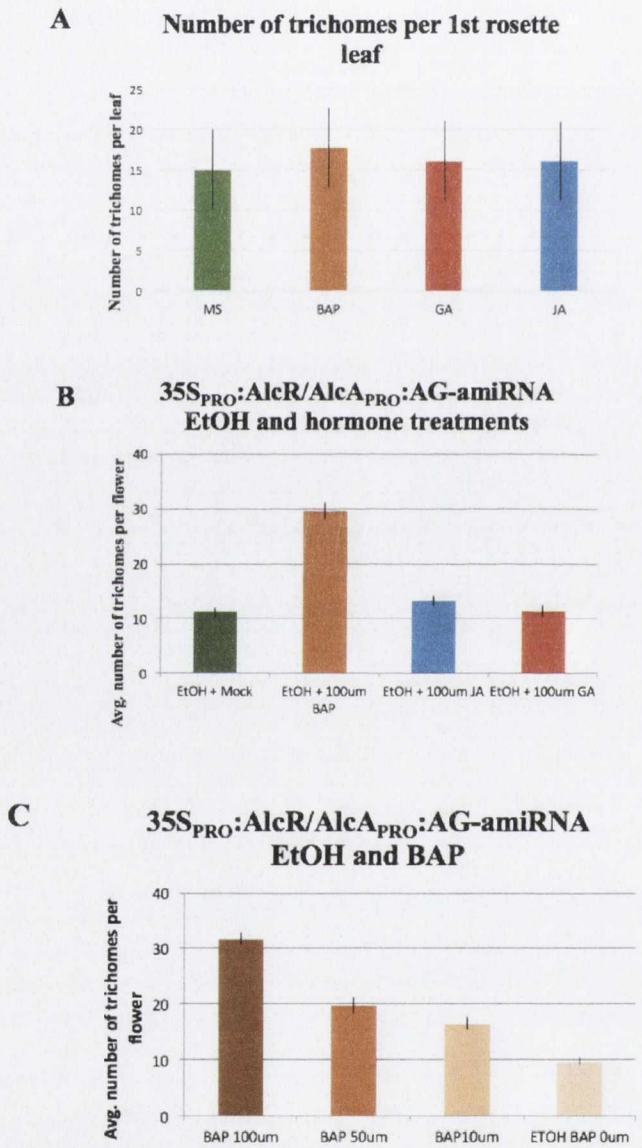

Figure 3.17: Loss of AG activity leads to increased phytohormone sensitivity and trichome formation on carpel valves.

(A) Number of trichomes per 1st rosette leaf on Murashige and Skroog (MS) plates with 100 µM of either BAP/JA/GA added. (B) Knock-down of *AG*, and treatment of inflorescences with different phy-

tohormones. Plants were treated with EtOH for 24 hours and either BAP/JA/GA at the same time. Counts were performed one week after the treatment. The number of trichomes forming on carpel valves were counted on flowers at the time of anthesis. (C) Knock-down of *AG* and treatment of inflorescences with varying concentrations of BAP. Counts were conducted one week after the treatment. The number of trichomes forming on the carpel valves were counted on flowers at anthesis. Error bars indicate SE. All experiments were independently repeated three times.

Figure 3.18: Loss of AG activity leads to cytokinin sensitivity and trichome formation on carpel valves.

(A) Flower of an AlcA:AG-amiRNA plant treated with 100 µM BAP. No trichomes formed on the carpel valves. (B) An EtOH-treated AlcA:AG-amiRNA flower with few trichomes forming on carpel valves (yellow arrows). (C) An EtOH-treated AlcA:AG-amiRNA flower treated with 100 µM BAP. Numerous trichomes formed on the carpel valves. (D) Gynoecium from an AlcA:AG-amiRNA flower, treated with EtOH vapor and 2 mM BAP, with a high number of trichomes forming on carpel valves. (E) An *ag-10* flower. (F) Gynoecium of an *ag-10* flower. (G) An *ag-10* flower treated with 100 µM BAP with trichomes forming on the carpel valves. (H) An *ag-10* flower treated with 1 mM of BAP with trichomes forming on the carpel valves. All images taken 1 week after treatment.

To further investigate the involvement of *AG* in suppressing cytokinin response in carpels, the AlcA:AG-amiRNA transgene was introgressed into mutants for the C2H2 zinc-finger transcription factors *ZFP8* and *GIS2*, which are known to be required for full cytokinin response in other floral organs (see section 3.1.4). In EtOH-treated AlcA:AG-amiRNA *gis2-1* plants, no trichomes were found on carpel vales but *ag*-like phenotypes were seen, indicating the amiRNA was functional (Fig. 3.19 A-B). In AlcA:AG-amiRNA *zfp8-1* plants treated with EtOH there was a reduction in the number of trichomes forming per carpel valve compared to the EtOH-treated AlcA:AG-amiRNA plants (Fig. 3.19 C-D). These observations suggest that *AG* acts partially upstream of *ZFP8* to prevent trichome formation and that *GIS2* is required for AG knockdown-dependent trichome formation on carpel valves.

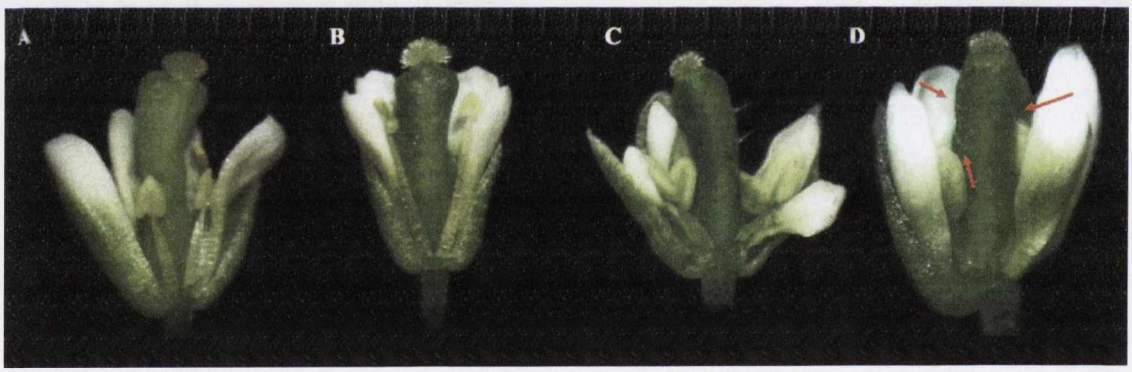

Figure 3.19: *GIS2* is required for trichome formation on carpels and *ZFP8* acts down-stream of *AG* to prevent trichome initiation.

(A-B) AlcA:AG-amiRNA *gis2-1* flowers, one week after EtOH treatment, with no trichomes forming on the carpel valves. (C-D) Flowers of AlcA:AG-amiRNA *zfp8-1* plants one week after EtOH treatment with a reduction in trichome numbers when compared to AlcA:AG-amiRNA-mediated *AG* knockdown alone.

3.2.7 *CPC* and *TRY* act as negative regulators of cytokinin signalling to prevent trichome formation in flowers

These previous results led us to investigate the interaction between *CPC*, *TRY*, and cytokinin. Firstly, AlcA:AG-amiRNA *cpc-1* plants were treated with BAP only. This resulted in a moderate increase in the number of trichomes on the abaxial sides of sepals, but not on carpel valves (Fig. 3.20 C). Next, these plants were treated with both EtOH vapour and BAP, which resulted in a dramatic increase compared to a treatment with EtOH alone (Fig. 3.20 D and Fig. 3.22 B). Equivalent experiments were then performed with a AlcA:AG-amiRNA *try-29760* lines. A treatment with BAP only resulted in the formation of a few trichomes on carpel valves in distinct clusters and an increase in trichomes on the abaxial side of sepals (Fig. 3.20 E). This line was then treated with both BAP and EtOH, which resulted in a dramatic increase in trichomes along the carpel valves (Fig. 3.20 F and Fig. 3.22 A).

Figure 3.20: The loss of *TRY* and *CPC* activity results in enhanced cytokinin sensitivity in wild-type and *AG* knockdown lines.

(A) An AlcA:AG-amiRNA flower treatment with 100 μM BAP with no visible trichomes forming on carpel valves. (B) An AlcA:AG-amiRNA flower after treatment with 100 μM BAP and EtOH vapor with trichomes forming on carpel valves. (C) An AlcA:AG-amiRNA *cpc-1* flower after treatment with 100 μM BAP with no visible trichomes. (D) An AlcA:AG-amiRNA *cpc-1* flower treated with 100 μM BAP and EtOH vapor with an increase in trichome number compared to AG knockdown alone. (E) An AlcA:AG-amiRNA *try-29760* flower treated with 100 μM BAP with trichomes forming on the carpel valves. (F) An AlcA:AG-amiRNA *try-29760* flower treated with 100 μM BAP and EtOH. Many trichomes can be seen forming on the carpel valves. (G) An AlcA:AG-amiRNA *try-29760 cpc-1* flower treated with 100 μM BAP k. Trichomes can be seen developing on carpel valves and on the tips of the gynoecium. (H) An AlcA:AG-amiRNA *try-29760 cpc-1* flower treated with 100 μM BAP and EtOH. Many trichomes can be seen forming on the carpel valves. All images were taken one week after treatment.

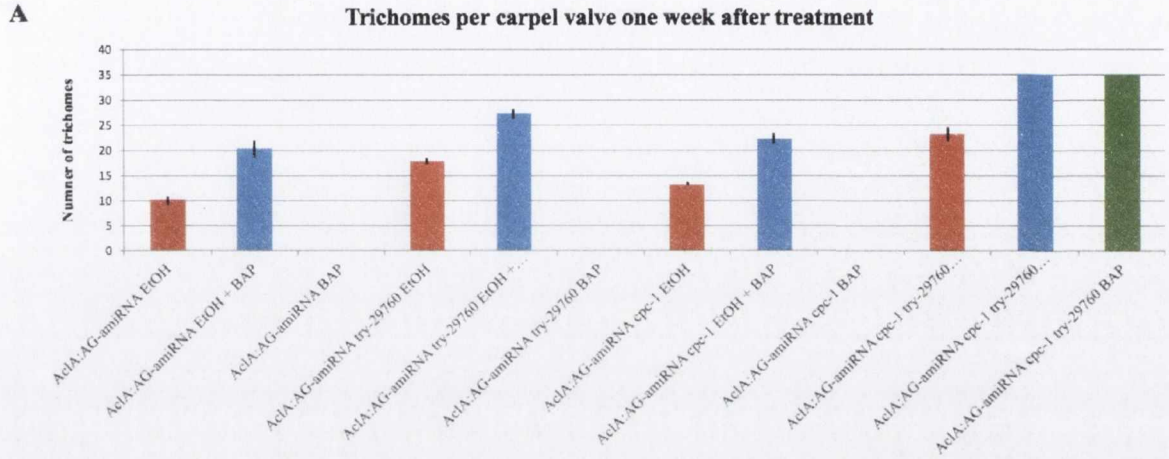

Figure 3.21: Number of gynoecial trichomes in flowers of different lines.

(A) The average number of trichomes counted per gynoecium. Genotypes and treatment conditions are indicated. Counts were performed in flowers at the time of anthesis one week after treatment with 100 µM BAP and EtOH vapor. Error bars indicate SE. Three biological replicates were conducted for each sample.

Finally, the triple mutant AlcA:AG-amiRNA *try-29760 cpc-1* was treated with BAP only. This resulted in trichomes forming along the carpel valves in distinct clusters, an increase in trichomes on the abaxial sides of sepals, and also many trichomes forming on the tips of the carpel (Fig. 2.23 A). This line was then treated with EtOH and BAP at the same time, which resulted in many trichomes forming along the carpel valves (Fig. 3.20 H). This treatment resulted in a number of trichomes on the carpel valves larger than in any other mutant combination tested here (Fig. 3.21 A). In this line trichomes were also observed on the tips of the gynoecium (Fig. 3.23 B), on the tips of anthers (Fig. 3.24 A-B), and also on the adaxial side of the carpel valves (Fig. 3.24 C) similar to EtOH-treated AlcA:AG-amiRNA *try-29760 cpc-1* plants (Fig. 3.15 A-B).

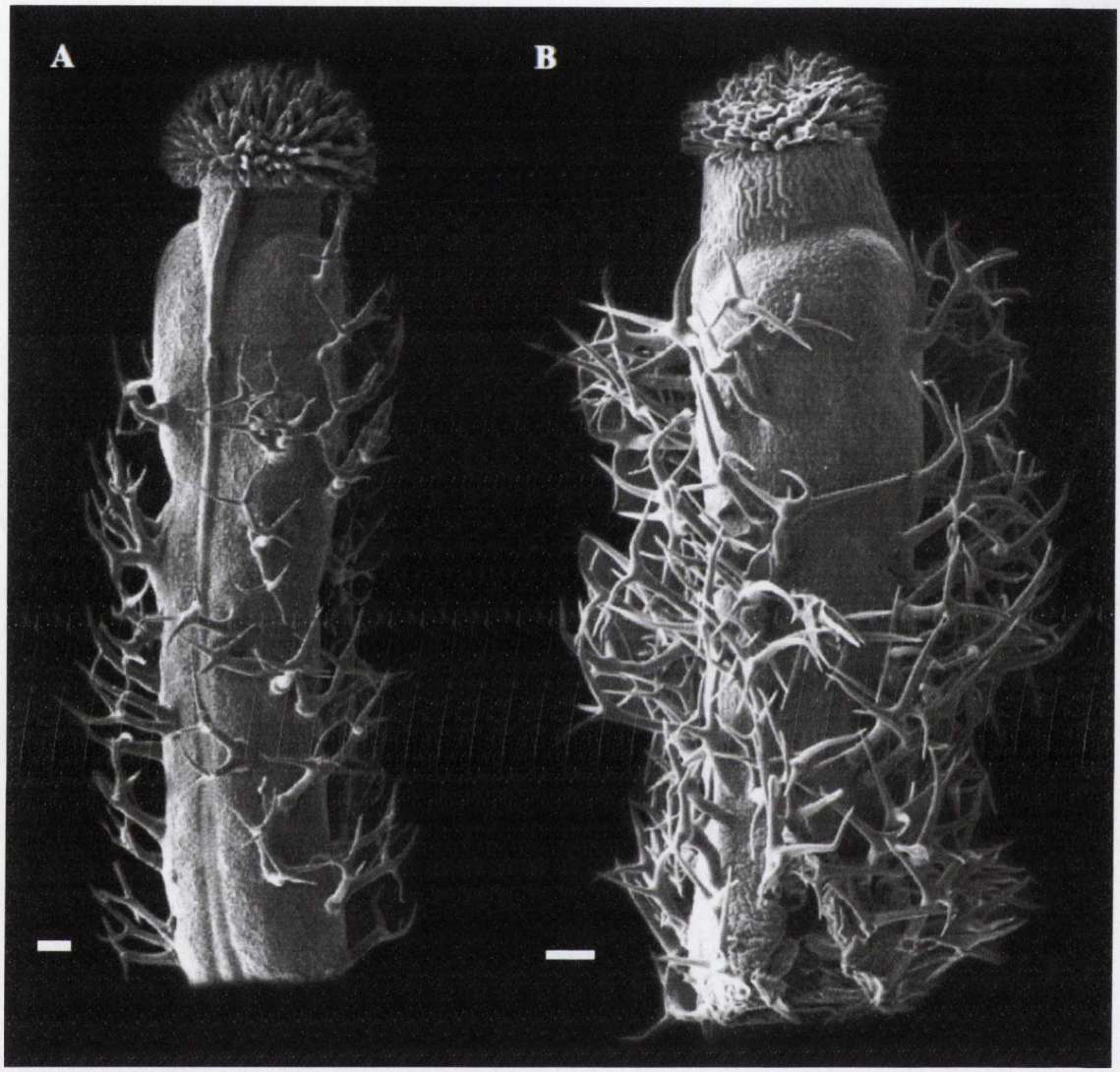

Figure 3.22: Interplay between *AG*, *TRY*, *CPC* and cytokinin.

(A) An AlcA:AG-amiRNA *try-29760* gynoecium one week after EtOH vapor and 100 µM BAP treatment. (B) A gynoecium of an AlcA:AG-amiRNA *try-29760 cpc-1* plant one week after treatment with EtOH vapor and 100 µM BAP. Scale bars in SEMs: 100 µm.

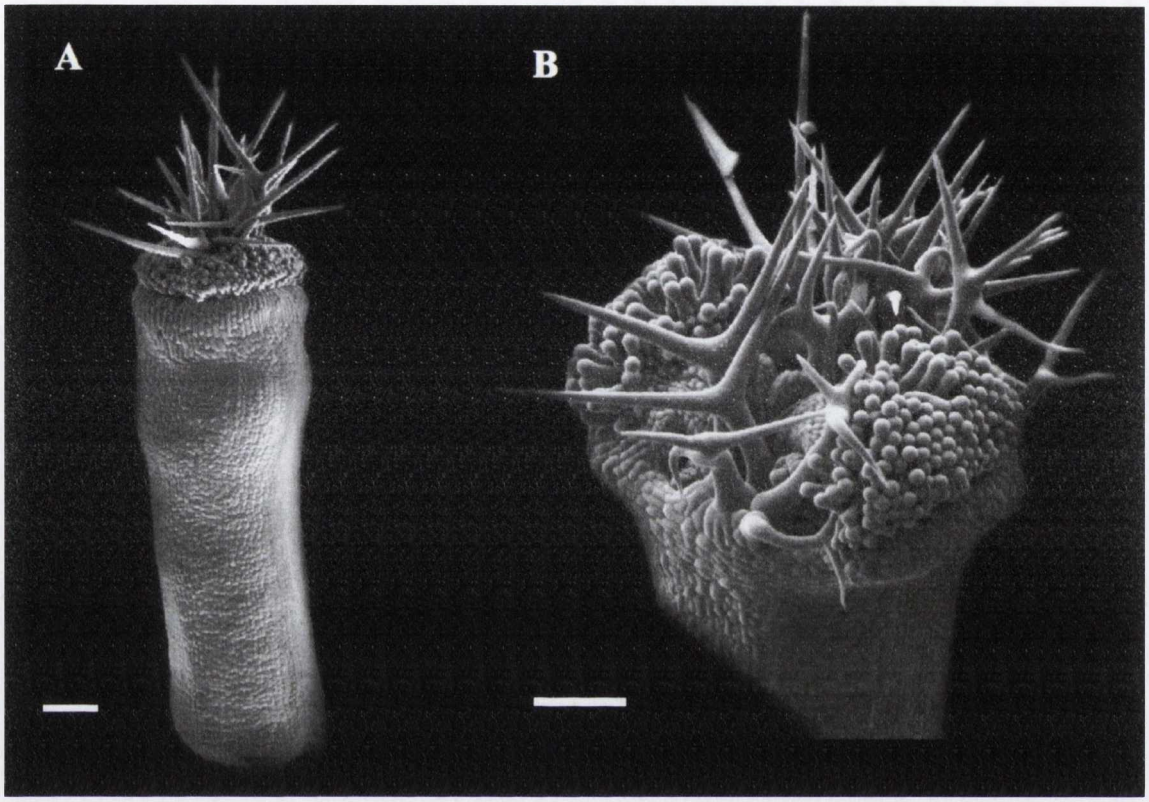

Figure 3.23: Trichomes form on the tips of carpels of BAP-treated *try cpc* flowers after an *AG* knockdown.

(A) A gynoecium of an AlcA:AG-amiRNA *try-29760 cpc-1* flower treated with 100 μM BAP. Trichomes can be seen initiating from the tips of the carpel. (B) A close-up of an AlcA:AG-*amiRNA try-29760 cpc-1* gynoecium treated with EtOH vapour and 100 μM BAP. Trichomes appear to initiate from underneath the stigmatic papillae. Images were taken one week after the treatment. Scale bars: 100 μm.

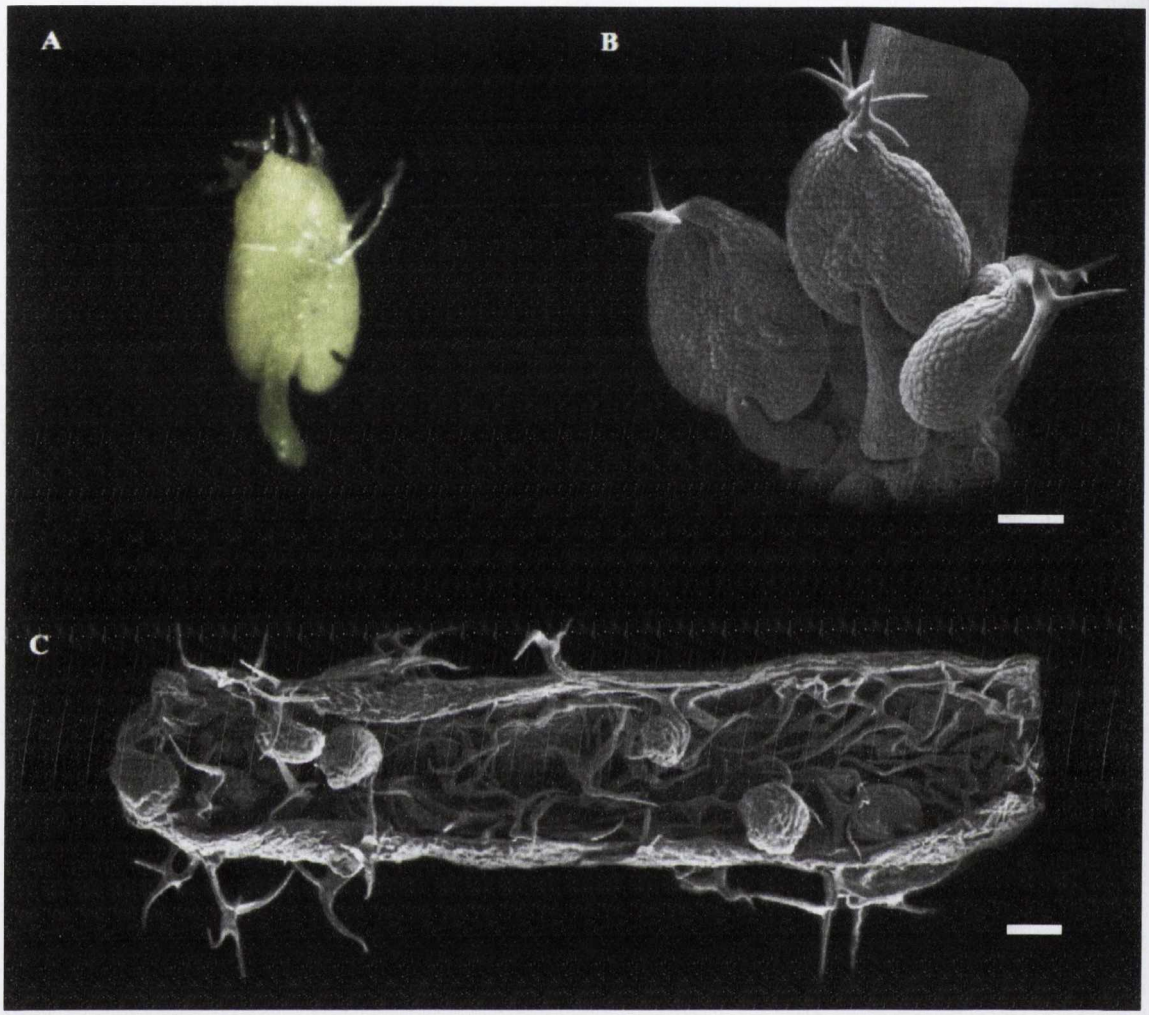

Figure 3.24: After BAP treatment, trichomes form on the tips and abaxial side of anthers, and the adaxial side of carpels, in both *try cpc* double mutants and *AG* knockdown lines.

(A-C) Floral organs from AlcA:AG-amiRNA *try-29760 cpc-1* plants treated with EtOH vapor and 100 μM BAP. (A) Trichomes forming on the tips and the abaxial side of anthers. (B) SEM of trichomes forming on the tips of anthers. (C) SEM of trichomes forming on the adaxial side (inside) of a carpel valve. Images were taken one week after the treatment. Scale bars: 100 μm.

To test whether *try* is the main regulator in the localization of the trichomes on the tips of the anthers and the carpels, the *try-29760* mutant was treated with BAP. This led to the formation

of trichomes on the tips of anthers more toward the adaxial side and also on the tips of the carpels (Fig. 3.25 A-C).

In conclusion, the results of the experiments outlined above demonstrate that *cpc* and *try* mutants are sensitive to BAP treatments, control the localization of trichome formation, and that a loss of *AG* activity further enhances their BAP sensitivity phenotype.

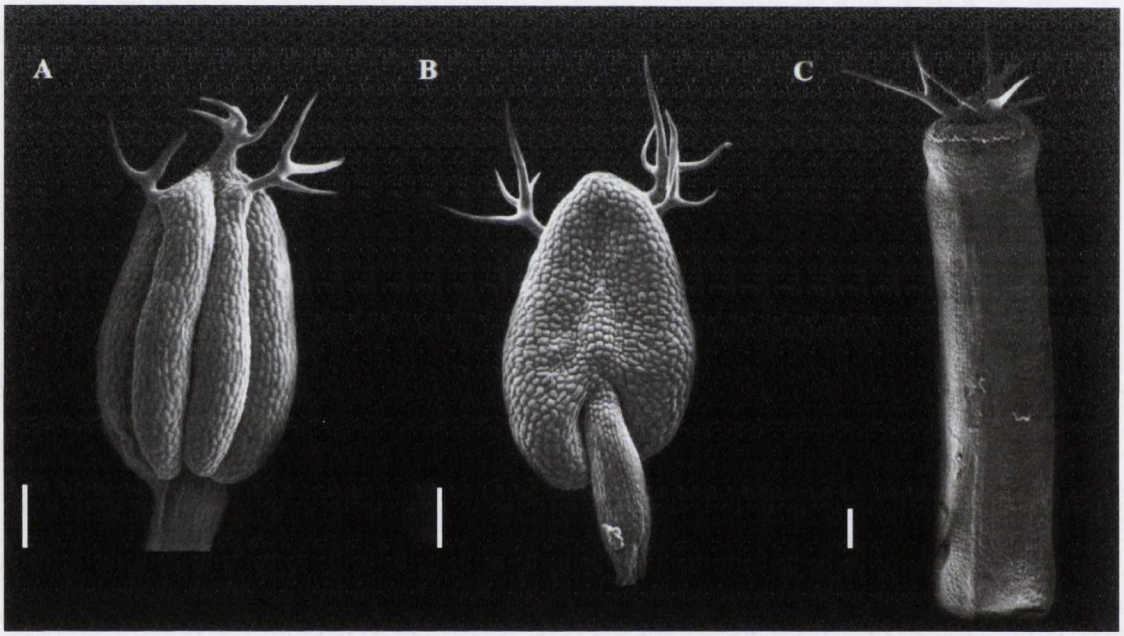

Figure 3.25: Trichomes form on the tips of floral organs in *try* after BAP treatment.
(A-C) SEMs of floral organs from *try-29760* mutant plants after treatment with 100 µM BAP. (A) Adaxial side of an anther with trichomes forming on the tips. (B) The abaxial side of an anther. (C) Trichomes forming on the distal tip of a gynoecium. Images were taken one week after the treatment. Scale bars: 100 µm.

3.2.8 *CPC* and *TRY* act antagonistically to pattern the gynoecium

While carrying out BAP treatments of the the different lines presented in this study, in addition to trichomes, medial outgrowths were observed to form along the replum of the carpel in BAP-treated AlcA:AG-amiRNA *try-29760* plants at later stages (Fig. 3.26 D).

Outgrowths similar to these have been reported when plants are continually sprayed with BAP, yet our AlcA:AG-amiRNA controls responded weakly to our controlled treatments with BAP (Fig. 3.26 A-C).

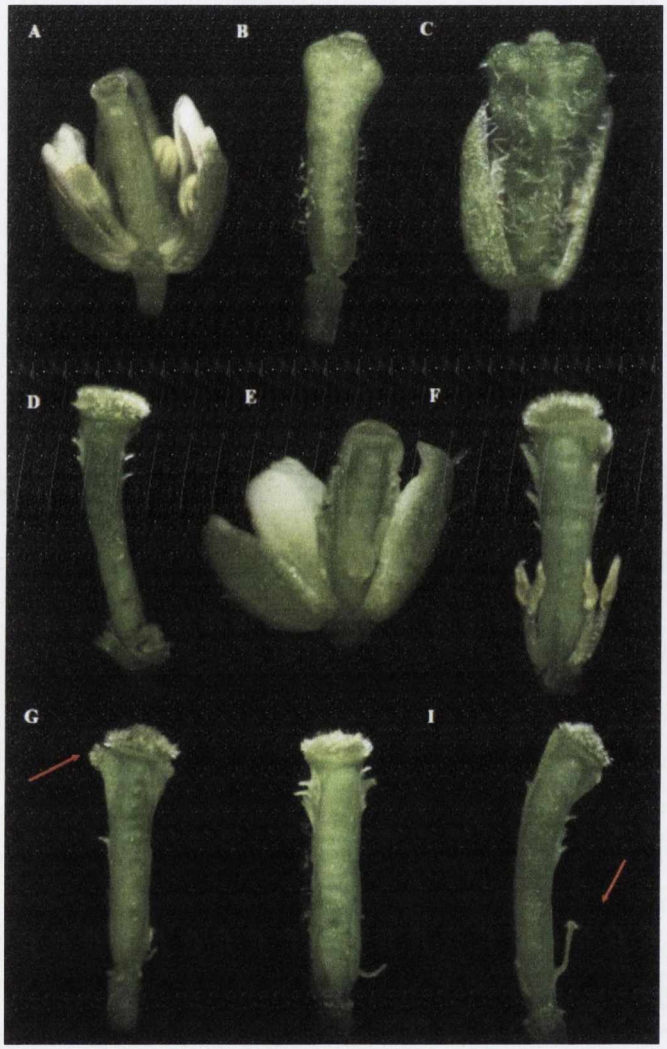

Figure 3.26: *TRY* and *AG* suppress cytokinin induced medial gyneoecial tissue outgrows. (A) An AlcA:AG-amiRNA flower treated with 100 μM BAP. Image was taken two weeks after the treatment. (B) An AlcA:AG-amiRNA gynoecium two weeks after treatment with EtOH vapor and 100 μM BAP. (C) An AlcA:AG-amiRNA gynoecium two weeks after treatment with EtOH and 2 mM BAP. (D) An AlcA:AG-amiRNA *try-29760* flower two weeks after treatment with 100 μM BAP. (E) An AlcA:AG-amiRNA *try-29760* flower two weeks after treatment with 100 μM BAP and EtOH va-

por. (F-I) An AlcA:AG-amiRNA *try-29760* flower two weeks after treatment with 2 mM BAP and EtOH vapor. (F) Outgrowths can be seen along the replum. (G) Ectopic stigmatic tissue can be seen growing from the style (red arrow). (H) Elongated outgrowths can be seen developing from the base of the gynoecium (red arrow). (I) Elongated outgrowths from the base of the gynoecium sometimes developed stigmatic tissue (red arrow).

No outgrowths, or minimal outgrowths, were seen when wild-type plants were treated with 100 μM BAP, but treated *try-29760* flowers resulted in regular outgrowths forming along the replum, suggesting that *try* is sensitive to BAP (Fig. 3.27 A-B). Further to this, when AlcA:AG-amiRNA *try-29760* flowers were treated with BAP (Fig. 3.27 C-F) gynoecia often formed outgrowths along the replum. The tips of these outgrowths were sometimes covered with stigmatic papillae (Fig. 3.27 D).

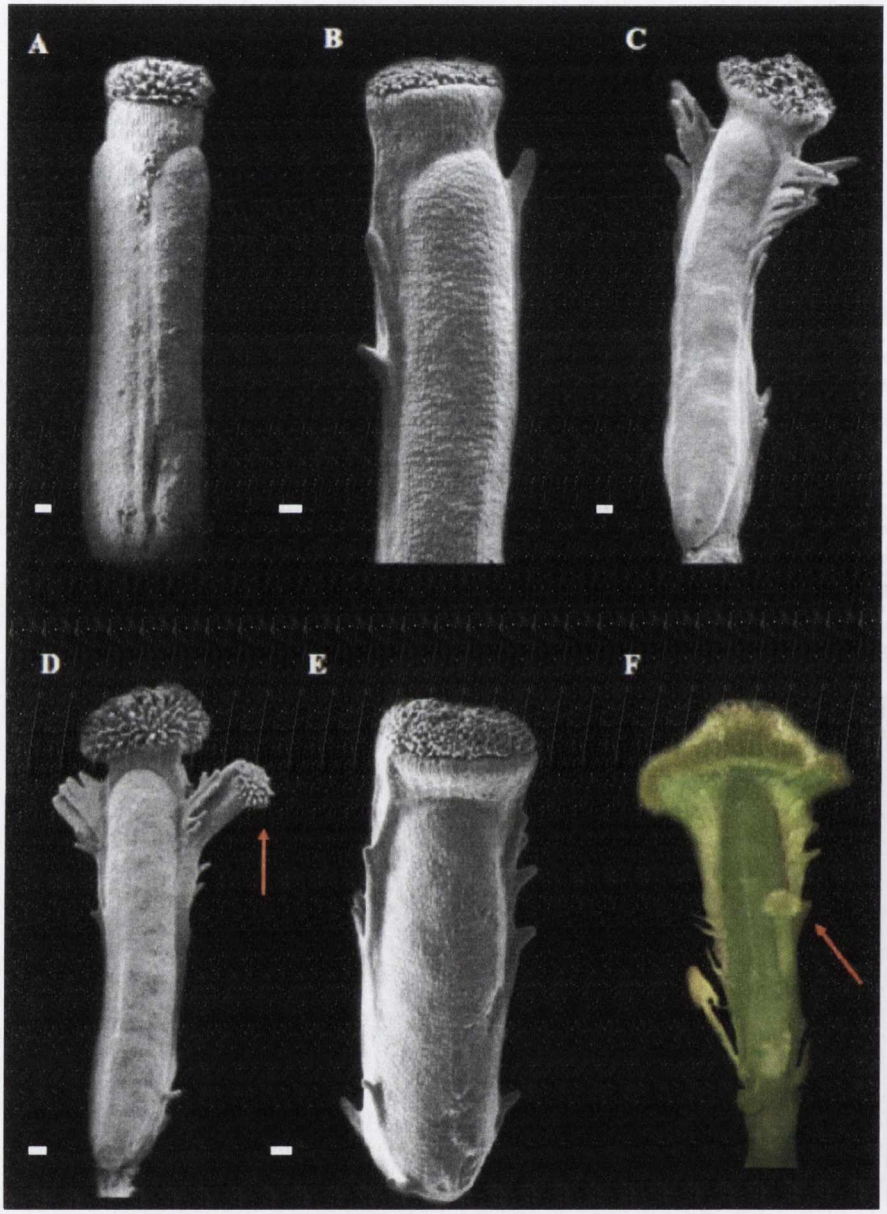

Figure 3.27: Genetic interaction between *AG* and *TRY*.

(A) A wild-type gynoecium after treatment with 100 μM BAP. (B) A *try-29760* gynoecium treated with 100 μM BAP with outgrowth from the replum. (C) An AlcA:AG-amiRNA *try-29760* gynoecium treated with 100 μM BAP. (D) An AlcA:AG-amiRNA *try-29760* carpel treated with 100 μM BAP with stigmatic tissue forming on the tip of an outgrowth (red arrow). (E-F) An AlcA:AG-amiRNA *try-29760* gynoecium treated with 100 μM BAP and EtOH. (E) A gynoecium with numerous outgrowths beginning to develop. (F) A gynoecium with many outgrowths along the replum (red arrow). Scale bars in SEMs: 100 μm.

To further investigate if other genes where involved in repressing these outgrowths, AlcA:AG-amiRNA *cpc-1* plants were treated with BAP. This resulted in no outgrowths forming from the replum but some flowers exhibited malformed styles (Fig. 3.28 A). Further to this result, when AlcA:AG-amiRNA *try-29760 cpc-1* plants were treated with BAP no outgrowths formed along the replum of carpels, but splitting of the stigma was sometimes seen (Fig. 3.28 D). These results suggest normal *CPC* function is required for the formation of the medial outgrowths.

To assess the role of *AG* in the formation of the gynoecial outgrowths, the lines were treated with BAP and EtOH to knockdown *AG*. In general, the severity of the outgrowths increased when AlcA:AG-amiRNA was activated in parallel with BAP treatment (Fig. 3.26 F-I and 3.27 E-F). Further to this, and in agreement with previous observations, AlcA:AG-amiRNA *cpc-1* and AlcA:AG-amiRNA *try-29760 cpc-1* plants did not respond to EtOH and BAP treatments even at higher (2 mM) BAP concentrations (Fig. 3.28 B, C, E, and F), while AlcA:AG-amiRNA plants began to respond and AlcA:AG-amiRNA *try-29760* plants were severely affected (Fig. 3.26 F-I).

Overall these results suggest that *CPC* is involved in suppressing the formation of medial tissues in response to exogenous BAP treatments, while the loss of *TRY* activity, especially in the absence of *AG* activity, causes more medial outgrowths to form in the presence of exogenous BAP treatment.

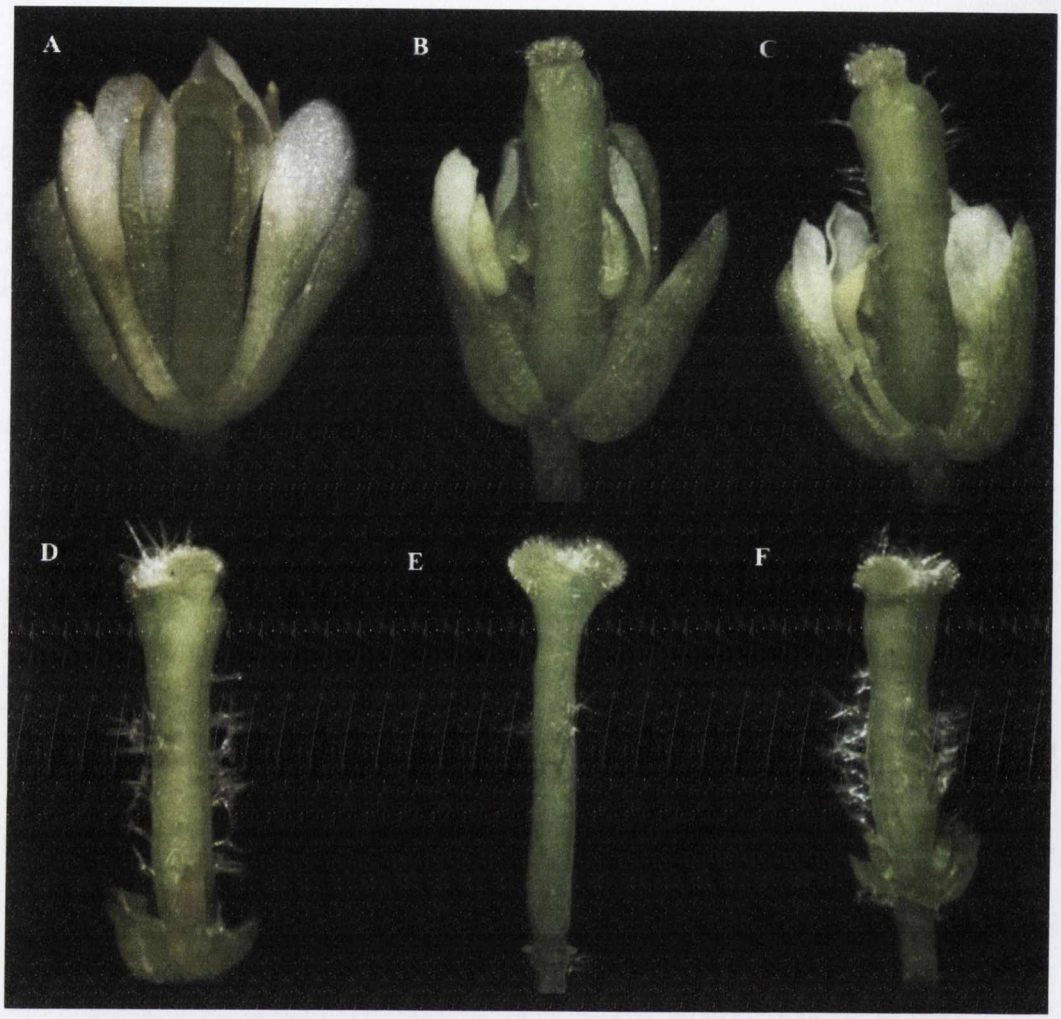

Figure 3.28: *CPC* is required for the formation of cytokinin-induced medial gynoecial tissue outgrowths.

(A) An AlcA:AG-amiRNA *cpc-1* flower treated with 100 μM BAP, with no outgrowths forming and minor malformation of the style. (B) An AlcA:AG-amiRNA *cpc-1* flower treated with 100 μM BAP and EtOH vapour, with no outgrowths forming but malformation of the style. (C) An AlcA:AG-amiRNA *cpc-1* flower treated with 2 mM BAP and EtOH vapour, with no outgrowths forming and elongation of the style. (D) An AlcA:AG-amiRNA *try-29760 cpc-1* gynoecium treated with 100 μM BAP, with slight malformation of the stigma and style, and no outgrowths forming on the carpel valves. (E) An AlcA:AG-amiRNA *try-29760 cpc-1* gynoecium treated with 100 μM BAP and EtOH vapour, with splitting of the stigma and malformation of the style, but no outgrowths forming on the carpel valves. (F) An AlcA:AG-amiRNA *try-29760 cpc-1* gynoecium treated with 2 mM BAP and

EtOH vapour, with splitting of the stigma but no outgrowths forming on the carpel valves. All photos were taken two weeks after treatments were performed.

3.2.9 *KANADI1* and *AG* suppress the formation of trichomes and control the growth of the gynoecium

The medial outgrowths seen when $AlcA_{PRO}$:AG-amiRNA *try-29760* plants are treated with EtOH and BAP looked very similar to the ones which form on *kanadi1* (*kan1*) mutant plants (Kerstetter et al., 2001). *KAN1* is known to be involved in specifying the abaxial identity of lateral organs and mutations in it result in medial outgrowths from the replum of carpels and ectopic ovules forming at the base of flowers (Fig. 3.29 A-D). Because of the similarity in phenotypes, we decided to test whether *AG* and *KAN1* work together in the control of trichome formation and gynoecial growth. To this end, we introgressed the $AlcA_{PRO}$:AG-amiRNA transgene into a *kan1-11* background. When we treated the resulting $AlcA_{PRO}$:AG-amiRNA *kan1-11* plants with EtOH we observed, on the abaxial side of the carpels, an increase in trichome number relative to mock-treated control plants and EtOH-treated $AlcA_{PRO}$:AG-amiRNA plants (Fig. 3.29 E-F). Further to this, there was a slight increase in the amount and frequency of medial outgrowths (Fig. 3.30 A). Next, $AlcA_{PRO}$:AG-amiRNA *kan1-11* plants were treated with BAP to test if the *kan1-11* background is sensitive to BAP. This resulted in an increase in the medial tissue protruding from the replum of the carpel valves (Fig. 3.30 B), as well as an increase in the number of ectopic ovules growing from the base of the carpel (Fig. 3.29 G-H), similar to *kan1-11* plants treated with BAP. Finally, $AlcA_{PRO}$:AG-amiRNA *kan1-11* plants were treated with a combination of EtOH and BAP, which caused a severe trichome and outgrowth phenotype (Fig. 3.30 C). In addition, multiple

ovules were seen to be growing from the base of the carpel (Fig. 3.29 I, J). These results suggest that *AG* and *KAN1* act together to suppress trichome formation and to specify the abaxial identity of medial carpel tissue.

Figure 3.29: *AG* interacts with *KAN1* to suppress trichome formation on carpel valves and medial outgrowths.

(A-D) Flowers and floral organs of *kan1-11*. (A) Medial outgrowths growing from the top of the replum (red arrow). (B) Ectopic ovules at the base of a gynoecium (red arrow). (C) Medial outgrowths growing from the bottom of the replum (red arrow). (D) Mature silique with multiple outgrowths from the replum. (E-F) Flowers of $AlcA_{PRO}$:AG-amiRNA *kan1-11* plants one week after treatment with EtOH vapor. (E) More trichomes form on carpel valves when compared to an *AG* knockdown in AlcA:AG-amiRNA plants. (F) Outgrowths are also enhanced compared to the *kan1-11* single mutant. (G-H) A *kan1-11* carpel treated with BAP, 1 week after treatment. (G) More enhanced outgrowths compared to untreated *kan1-11*. (H) More ectopic ovules growing form the base of the carpel compared to untreated. (I-J). An $AlcA_{PRO}$:AG-amiRNA *kan1-11* flower treated with EtOH and 100μM BAP, 1 week after treatment. (I) multiple outgrowths grow from the replum and trichomes from the carpel valves (red arrow). (J) Many ectopic ovules grow from the base of the carpel (red arrow).

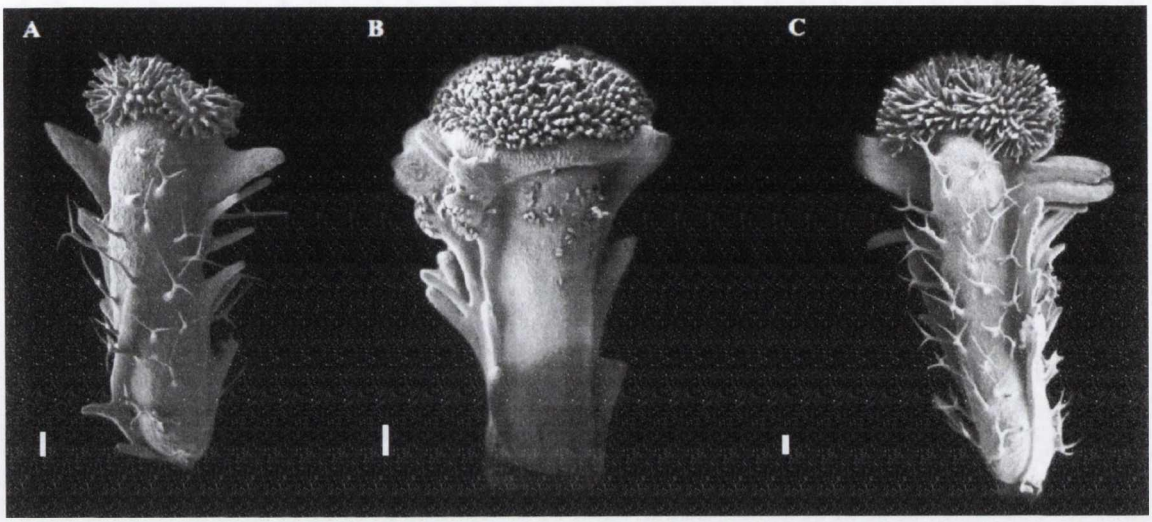

Figure 3.30: SEMs of *kan1* mutant flowers following perturbation of *AG*.

(A) Gynoecium of an $AlcA_{PRO}$:AG-amiRNA *kan1-11* flower with trichomes forming on carpel valves and many outgrowths forming from the carpel margin meristem. Image was taken one week after EtOH vapor treatment. (B) Gynoecium of an $AlcA_{PRO}$:AG-amiRNA *kan1-11* flower with enhanced outgrowths forming from the replum. Image was taken one week after treatment with 100 µM BAP (C) Gynoecium of an $AlcA_{PRO}$:AG-amiRNA *kan1-11* carpel with many trichomes forming on the carpel valves and severe outgrowths. Image was taken one week after treatment with 100 µM BAP and EtOH vapor. Scale bars: 100 µm.

3.3 Discussion

Although von Goethe had already proposed in the late 18th century that floral organs are derived from leaves, the question of how this transformation process actually occurs remained unanswered for many years. Genetic studies in the early 1990s uncovered a molecular framework for how flowers are organised, beginning to answer this question. The discovery of the floral homeotic mutants led to the formation of the ABC model of floral organ identity specification and early experiments showed that the inactivation of these genes led to the

conversion of floral organs to leaf-like structures. Later on came the discovery of the E class genes, known as the *SEP*s. The discovery of these genes led further to the idea that flowers are modified leaves, as when these genes were all knocked out, floral organs turned leaf-like. In addition, when E function genes were overexpressed with certain combinations of the ABC genes, leaves could be transformed into floral organs (Honma and Goto, 2001). All this early molecular work provided strong experimental support for Goethe's hypothesis. Genome-wide approaches such as ChIP-Seq and transcriptomics analyses have allowed for the study of direct and indirect targets of the floral organ identity genes and how their proteins regulate flower development (Kaufmann et al., 2010). However, one question which had still remained unanswered was, whether the floral organ identity genes not only upregulate other specific floral organ identity genes but also suppress the genes involved in leaf development?

As previously discussed, inducible perturbation of *AG* activity using the ethanol-inducible microRNA system resulted in the the transformation of carpel epidermis to more leaf-like morphology, which also resulted in the presence of branched trichomes, a hallmark of leaf development (O'Maoileidigh et al., 2013). In addition, knocking down *AP3* in combination with *AG* resulted in trichomes forming on anthers. This previous work showed that the homeotic genes are essential in repressing some of the leaf developmental programs in flowers and paved the way for the further experiments in this study. For ease of discussion, I will outline the results from this study and discuss them in the following sections.

3.3.1 *AG* suppresses trichome formation in flowers with the help of other MADS-domain transcription factors

Once the core regulatory network that controls trichome formation in leaves was shown to be similar in flowers, the floral regulators supressing trichome formation could then be investigated. *AG* and *AP3/PI* are known to be responsible for stamen development (O'Maoileidigh et al., 2015; Wuest et al., 2012) yet other interactions between these two genes have not been shown. This is interaction is similar between *AG* and the *SHP* genes with respect to the regulation of the carpel (Favaro et al., 2003). In this study the evidence suggests that *AP3/PI* and *SHP1/2* continually suppress the formation of trichomes on the surface of floral organs after they have been specified. These experiments add to the growing hypothesis that the MADS-domain transcription factors were the main drivers in the evolution to flowering plants (Sablowski, 2010).

3.3.2 The *SPL*s repress trichome formation in flowers in parallel with *AG*

Additional work conducted during this thesis showed that SPL transcription factors also play a central role in the suppression of floral trichome initiation. In fact, the results from experiments in which I increased or decreased SPL activity in flowers after an *AG* knockdown (Fig. 3.9) suggest that they act in a parallel with AG and other floral organ identity factors in this process. This result in particular provided insights into what happens with the leaf development program when floral organs develop from leaf-like structures.

The expression of many *SPL* genes is known to increase as the plant ages (Bartel and Bartel, 2003). This increase is a consequence of an age-dependent decrease in the expression

of miR156 miRNAs, which target many *SPL* family members (Wang et al., 2008). It has been shown that the gradual increase in *SPL* expression during plant development contributes to the redistribution of trichomes and that the underlying molecular mechanisms is the direct up-regulation of trichome repressor genes such as *TRY* by the SPL transcription factors (Yu et al., 2010). While trichomes are initially found exclusively on the adaxial side of rosette leaves, abaxial trichomes start to appear on later arising leaves (Telfer et al., 1997). In fact, cauline leaves, which form after the transition to the reproductive phase of development, exhibit trichome formation mainly on the abaxial side, with adaxial trichomes being confined to the tip region of the leaf. Notably, in sepals, this gradual shift towards abaxial trichome formation is complete because the adaxial side of sepals is fully glabrous. It has been shown convincingly that the SPL transcription factors also determine trichome distribution in this organ type (Yu et al., 2010). Thus, the SPL-dependent pathway for the control of trichome distribution appears to be active throughout most of plant development.

In fact, the results presented in this thesis suggest that this pathway remains active even in petals, stamens and carpels, which are naturally trichomeless. Thus, it appears that this aspect of the leaf development program remains very much active throughout floral organ development. Furthermore, these results suggests that, in the context of trichome initiation, the invention of the floral organ identity factors during evolution was mainly necessary for the suppression of abaxial trichomes on floral organs, which developed from a sepal-like precursor. This idea is supported by our observation that a perturbation of floral organ identity gene function primarily leads to the appearance of abaxial trichomes (e.g., Fig. 3.4 (B), 3.13 (B) and 3.16 (A)). In summary, the results presented here have provided some molecular insights into how the floral organ identity factors modify the underlying program for leaf

development to bring about floral organ morphogenesis. It would be of great interest to see whether other aspects of leaf development (e.g., the development of stomata, which are initiated on carpels but do not fully develop) are modified through similar mechanisms.

3.3.3 Regulation of cytokinin sensitivity is key to supressing trichome formation in flowers and the regulation of carpel patterning

Phytohormones are known to play many essential roles throughout plant development. In particular correct cytokinin synthesis and signalling is essential for controlling trichome initiation, meristem size, ovule development, and the correct patterning of the gynoecium (Pajoro et al., 2014). Here the results indicate that *AG*, *KAN* and some of the single repeat R3 MYBs are crucial in negatively regulating cytokinin responses in the control of trichome initiation. Most surprisingly was the involvement of *TRY* and *CPC* in regulating this response to patterning the carpel. These two genes have been intensely studied over the years but a role for them in floral patterning is completely novel. Further work will hopefully uncover by which direct mechanisms they control floral organ patterning. Interestingly these genes also have a role in the abaxial/adaxial regulation of trichomes. This control of spatial trichome identity is similar to the function of *KAN1* in specifying the abaxial identity of organs (Kerstetter et al., 2001). The hypothesis that these single repeat R3 MYBs and the *KAN* genes act in the same developmental pathway is a question which will be investigated next.

3.3.4 Floral trichomes as a possible new avenue for crop protection

Trichomes have evolved to act as a primary defence against chewing and sap-feeding insects (Olsson et al., 2009). For instance, glandular trichomes produce and store a range of poisonous, bitter or psychoactive metabolites to deter herbivores from feeding on the plants (Traw and Bergelson, 2003). In fact, this ability of plants to produce and store metabolites in a specific cell type on the outside of the plant where they are easily accessible is of considerable interest for industry (Schilmiller et al., 2008). Although floral organs are typically glabrous, trichomes do form on the abaxial side of sepals, protecting the floral buds and the subjacent inflorescence meristem from herbivorous insects that feed on them. Interestingly, several plant species, such as some soybean varieties or white mustard (*Sinapis alba*, a member of the *Brassicaceae*), do produce trichomes especially on seed pods to deter insect pests and to safeguard the development of their offspring (Lam and Pedigo, 2001).

Because fruits and their seeds are of pivotal importance for food supply, their protection from pests is a key concern in agriculture. The results obtained in this study have provided detailed insights into the mechanisms that suppress trichome formation on floral organs of *Arabidopsis*. They showed that this process is mediated by a complex interplay of distinct pathways (Fig. 3.31). These results can now be used to try to induce floral trichomes on agriculturally important plant species as a new strategy for crop protection. Of particular interest in the context would be oilseed rape (*Brassica napus*), a plant that is of considerable importance for oil and biofuel production, and is closely related to *Arabidopsis*. Also, because oilseed rape naturally produces only very few trichomes, an increase in trichome density through the type of genetic manipulations we conducted in *Arabidopsis* may lead to especialy large beneficial effects.

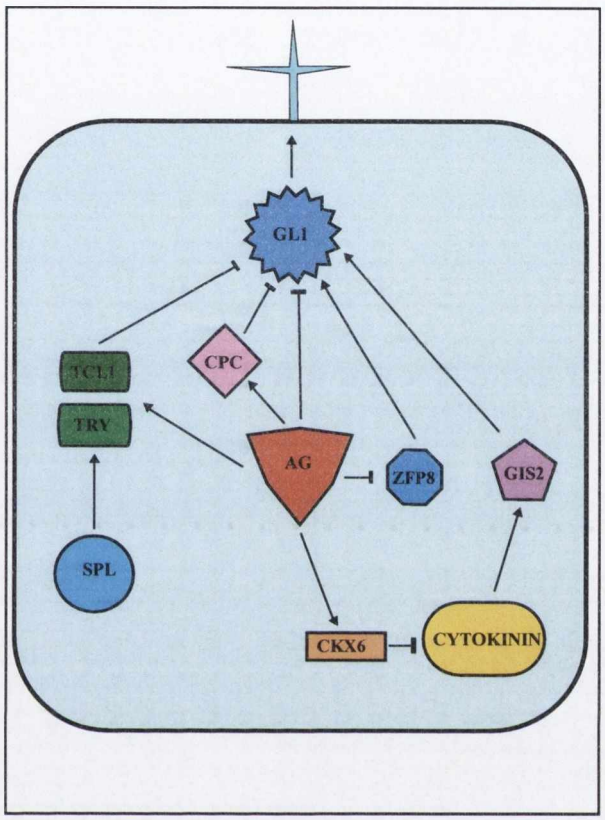

Figure 3.31: Current model for the control of trichome formation on floral organs.

AGAMOUS (AG) transcriptionally controls regulators of trichome initiation directly. It activates expression of repressors of trichome initiation (*TRICHOMELESS1* (*TCL1*), *CAPRICE* (*CPC*)), while suppressing the expression of known activators (*ZINC FINGER PROTEIN 8* (*ZFP8*), *GLABRA1* (*GL1*)). AG also up-regulates genes involved in the control of cytokinin levels in the flower (*CYTOKININ OXIDASE 6* (*CKX6*)), which affect (*GLABROUS INFLORESCENCE STEMS* (*GIS*) levels in turn. Parallel pathways also fine-tune the expression of a number of key genes, such as members of the *SQUAMOSA PROMOTER BINDING PROTEIN-LIKE* (*SPL*) gene family, directly regulating *TRIPTYCHON* (*TRY*) and *TCL1*. *AG*'s control is also central, along with other MADS-domain transcription factors (not shown), in regulating *GL1*, the levels of which are the penultimate deciding factor on whether or not the pavement cell specifies a trichome.

Chapter 4 - Investigating the gene regulatory network downstream of the zinc-finger transcription factor SUPERMAN

4.1 Introduction

As described in Chapter 1, a key event during early flower development is the patterning of floral meristems to establish spatially restricted domains of gene expression (reviewed in: O'Maoileidigh et al., 2014). This involves most notably the floral organ identity genes, which are expressed in overlapping domains. How the spatial expression of these master regulators is controlled is still not understood in its entirety but a large number of regulatory genes involved in this process have been identified in recent years. One of these genes is *SUPERMAN (SUP)*. *SUP* was originally discovered through an ethyl methane sulfonate (EMS) mutagenized population of *Arabidopsis* wild-type plants and initially named *FLO10* (*FLORAL MUTANT 10*) (Schultz et al., 1991; Bowman et al., 1992). *SUP* is thought to be a cadastral gene, maintaining the boundaries between stamens and carpels by regulating cell proliferation in the third and fourth whorl of the developing flower and also excluding expression of the B function genes, *AP3* and *PI*, from being expressed in the centre of the flower (Bowman et al., 1992; Sakai et al., 1995). In *sup* mutant flowers this boundary is shifted towards the centre of the flower, resulting in the formation of extra stamens, and depending on the allele, an increase or a decrease in the formation of carpel tissue (Fig. 4.2 B) (Bowman et al., 1992; Gaiser et al.,1995; Sakai et al., 1995).

Sup mutant flowers also exhibit indeterminacy defects, suggesting that SUP plays a role in regulating floral meristem determinacy (reviewed in Sun and Ito, 2010). However, the exact role that SUP plays in this process is not well understood. Based on the results of double-mutant analyses, it has been suggested that *SUP* regulates floral meristem determinacy in parallel with the C-class floral organ identity gene *AG* by repressing the stem cell regulator *WUS* in the centre of the floral meristem. However, there is still limited evidence supporting this conjecture (Prunet et al., 2008).

In situ hybridization experiments and SUP_{pro}:GUS (β-glucuronidase) fusion analyses showed that *SUP* is expressed in a very limited region around the third-fourth whorl boundary during early flower development, at roughly stage 3/4 (Fig. 4.1 A-B) (Ito et al., 2003; Sakai et al., 1995; Sakai et al., 2000). Originally it was thought that SUP positively regulates the expression of *AP3* and *PI* in the third whorl while repressing them in the fourth whorl (Schultz et al., 1991), but it was later shown that *AP3* and *PI* expression actually commences shortly before that of *SUP*. It was concluded that they probably form a regulatory feedback loop between each other as *AP3* and *PI* were shown to be needed for *SUP* expression (Bowman et al., 1995; Sakai et al., 1995). Furthermore, *SUP* was recently shown to be directly regulated by AP3 and PI: the results of ChIP-seq experiments revealed that AP3 and PI bind to the *SUP* promoter and *SUP* expression was reduced after an inducible knockdown of *AP3* function (Wuest et al., 2012).

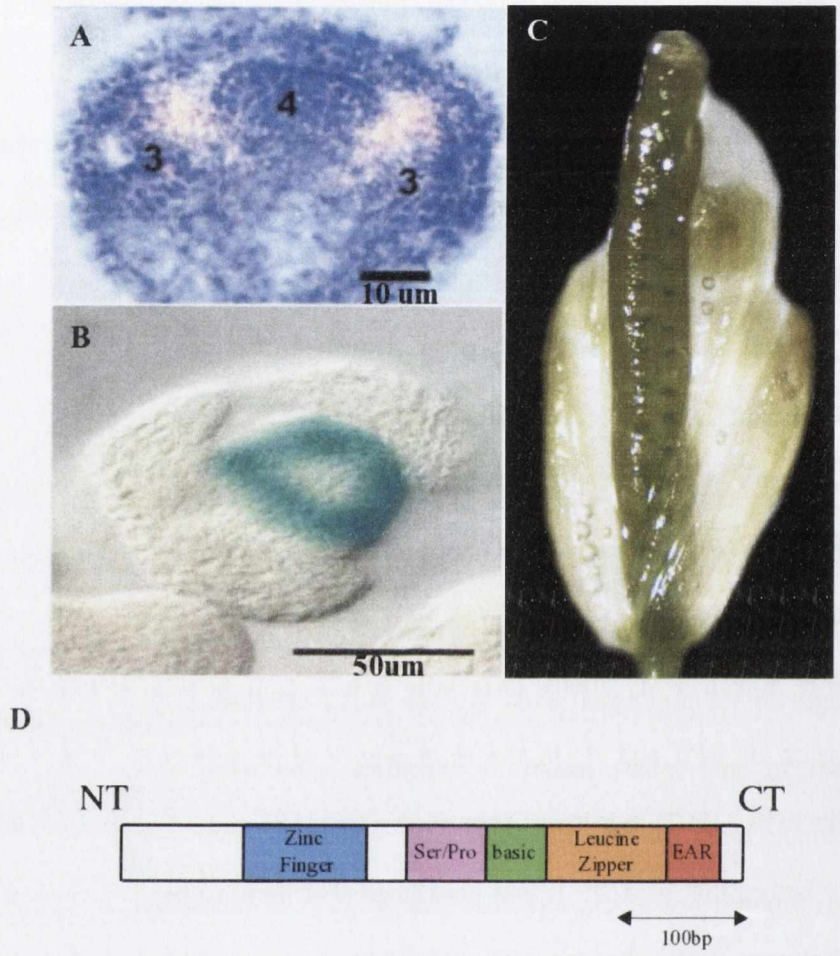

Figure 4.1: *SUP* expression pattern during flower development and schematic representation of the *SUP* locus.

(A) *SUP* expression starts at roughly stage 3 at the boundary between whorls 3 and 4. The stamen and carpel primordia produce a ring-like pattern around the carpel primordia. (B) Z-stack of Arabidopsis inflorescence expressing fluorescent reporters for *AP3* (green), *SUP* (red) and *CLV3* (blue). (C) At later stages of development *SUP* is expressed in the developing ovules. A flower at stage 15/16 of SUP_{pro}:GUS with staining in the ovules seen through the carpel. (D) The structure of the *SUP* locus. The transcribed region of *SUP* is roughly 600 bp and contains a zinc-finger domain, a Serine/Proline-rich domain, a basic domain followed by a leucine zipper-like domain with a C-terminal EAR-like repression motif. Figure adapted from Sakai et al. (2000) and Prunet and Meyerowitz (2016).

Further to its expression early in flower development, *SUP* was found to be also expressed in ovules at roughly stage 12/13 (Fig. 4.1 C) (Gaiser et al., 1995). *SUP* is now known to be involved in controlling the growth of the integuments during the development of the ovules at later floral stages (Villanueva et al., 1999). *SUP* is partially involved in this process by repressing, directly or indirectly, the spatial pattern of *INNER NO OUTER* (*INO*) expression, which is necessary for polarity determination in the central part of the ovule (Villanueva et al., 1999). Research on *SUP*'s involvement in regulating ovule development has not progressed much since these original experiments and is beyond the scope of this thesis.

The *SUP* gene was cloned in the mid 1990s and consists of a single exon, approximately 600 bp long (Sakai et al., 1995). It encodes a protein which contains a zinc-finger domain, a serine/proline-rich domain, a basic domain, a leucine zipper-like domain as well as a C-terminal ethylene-responsive element binding factor-associated amphiphilic repression (EAR)-like domain (Fig. 4.1 D) (Bowman et al., 1995; Isernia et al., 2003; Ito et al., 2003). The presence especially of the latter domain led to the hypothesis that *SUP* was a transcriptional repressor. In fact, SUP has since been shown to bind DNA through its zinc-finger domain *in vitro* (Dathan et al., 2002) and to be an active repressor (Hiratsu et al., 2002; Hiratsu et al., 2004; Ito et al., 2003). Ectopic expression of *SUP* lacking its repressor domain results in a phenotype similar to the *sup* mutant, with supernumerary stamens and extra carpel tissue in the centre of the flower, indicating that the repressive activity of *SUP* is essential for normal flower development (Hiratsu et al., 2004).

The supernumerary organ mutant phenotype of *SUP* has led to the idea that it regulates cell proliferation in the developing flower. *SUP* is thought to do this by repressing

the transcription of genes that are involved in the promotion of cell division between the third and fourth whorl (Hiratsu et al., 2002). Experiments have shown that constitutive over-expression of *SUP* from the 35S Cauliflower Mosaic Virus promoter in tobacco (*Nicotiana tabacum*) and *Arabidopsis* results in dwarfism, which is attributed to an effect on cell proliferation, differentiation, and expansion (Bereterbide et al., 2001; Hiratsu et al., 2002). This was also the case in petunia (*Petunia hybrida*), as the over-expression of the *SUP* homologue *PhSUP1* resulted in a size reduction of petals, leaves, and inflorescence stems, which was a consequence of a decrease in cell number (Nakagawa et al., 2014). Furthermore, ectopic expression of *SUP* in the flower using the flower-specific *AP1* promoter resulted in fewer floral organs as well as a reduction in organ size, consistent with the effect of *SUP* on cell proliferation (Yun et al., 2002). It was also suggested that in tobacco and *Arabidopsis* *SUP*'s role as a regulator of cell division may be through regulating hormonal changes in the flower (Nibau et al., 2011). There is ample anecdotal evidence that *SUP* does indeed regulate cell proliferation, but to what end it does, and how, is still largely unclear.

Recently, another zinc-finger transcription factor, JAGGED (JAG), which is closely related to SUP, has been shown to directly suppress the expression of the genes *KIP RELATED PROTEIN 2* (*KIP2*) and *KIP4*, which are both involved in regulating the transition of DNA synthesis phase (S-Phase) of the cell cycle (Schiessl et al., 2014). This work shows that the Cys_2His_2-type zinc finger transcription factors can regulate genes involved cell cycle control. This leads to the possibility that *SUP* could mediate its biological effects through regulating the cell cycle.

The position of *SUP* in the genetic network governing early flower development has been partially resolved, but its downstream targets and the exact biological processes it regulates are still unknown. The work described in this chapter aimed to uncover the downstream targets of *SUP* through the use of perturbation experiments and genome-wide localization studies. Furthermore, it also tried to address the link between *SUP* and the regulation of cell proliferation in the flower through the mediation of cytokinin synthesis or signalling.

4.2 Results

4.2.1 Phenotypic variation between mutant alleles of *SUP*

In order to gain a more in depth understanding of the function of *SUP*, a detailed characterization of the available mutant alleles was carried out. The *SUP* gene consists of a 5' untranslated region (UTR), followed by a coding region consisting of 615 bp and a 3' UTR. The *sup-5* allele, isolated through EMS mutagenesis, is thought to be the null allele (Fig. 4.1 C-F) and comprises of a deletion beginning before the transcriptional start site and encompassing the first 568 nucleotides of the coding region (Supplementary Fig.1.1) (Gaiser et al., 1995). When compared to the wild type (Fig. 4.1 A-B), *sup-5* flowers exhibit a dramatic increase in stamen number (Fig. 4.1 G). They also have an increase in carpel tissue with mosaic stamenoid carpels sometimes appearing in the centre of the flower. Due to the disruption of carpel tissue, fertilization is affected, and *sup-5* mutant plants are normally kept in a segregating population as the homozygous line produces very few seeds. *Sup-5* mutant plants also show prolonged growth and the inflorescence meristem produces flowers for an extended period of time when compared to the wild type.

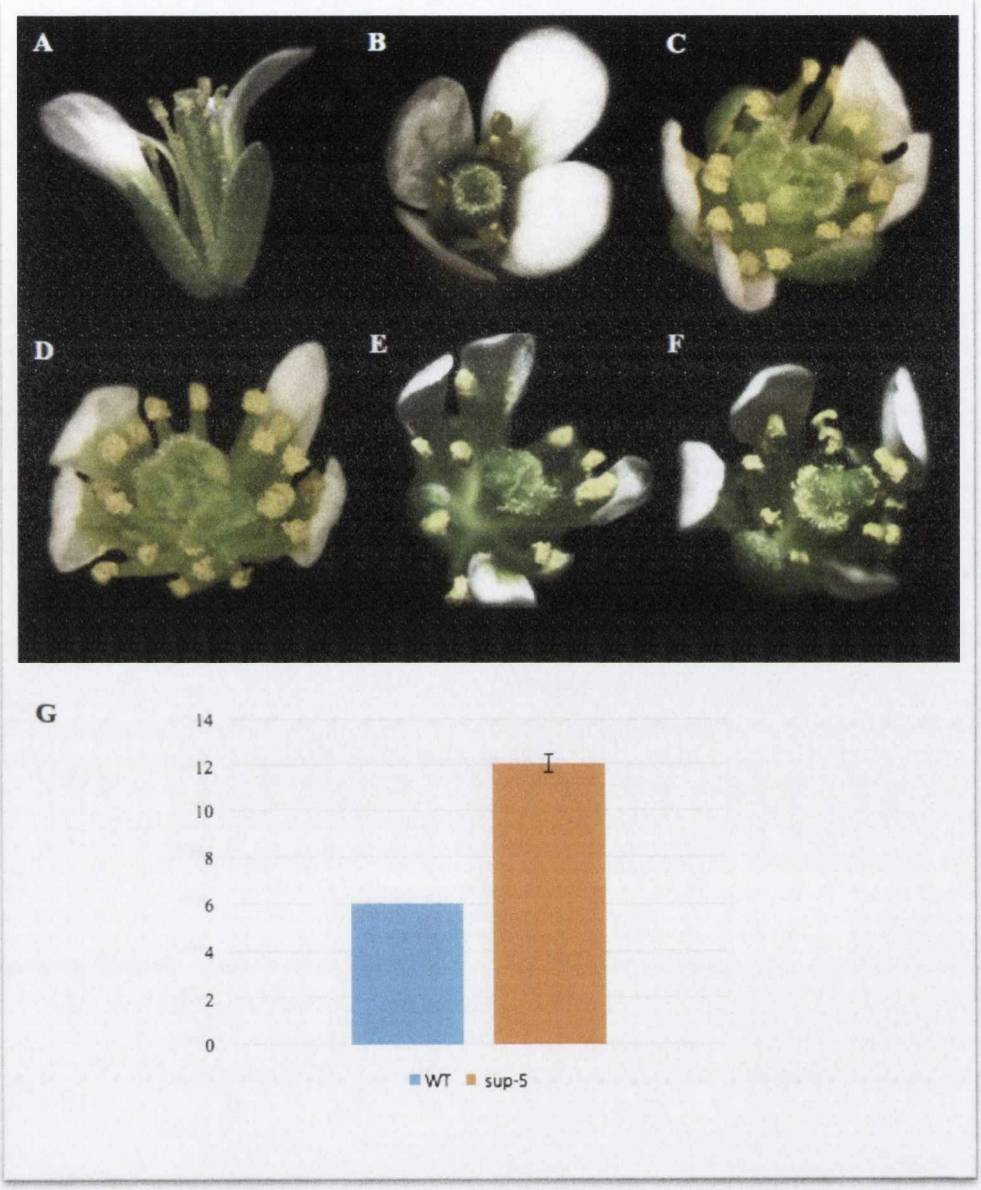

Figure 4.2: Mutations in *SUP* result in supernumerary stamens and extra carpel tissue.

(A-B) Wild-type flowers. (C-F) *sup-5* mutant flowers. (C-D) Flowers with supernumerary stamens and extra carpels forming in the centre of the flower. (E-F) Flowers with extra stamens and disrupted gynoecia. (G) Number of stamens per flower in wild-type and *sup-5* mutant plants. Error bars indicate SE.

The *sup-2* allele varies from the *sup-5* allele by the reduction or complete loss of carpel tissue (Fig. 4.2 A-C). This allele was isolated through EMS mutagenesis and has a nonsense mutation (TGG to TAG) 65 nucleotides downstream from the transcriptional start site, which creates a premature stop codon resulting in an N-terminal 22 amino acid truncated protein (Supplementary Fig.1.1) (Bowman et al., 1992 Sakai et al., 1995). The *sup-3* allele is more similar to *sup-2* than to *sup-5* in so much that it also has a loss of carpel tissue (Fig. 4.2 D-F). This mutant allele was isolated through EMS mutagenesis and has a missense mutation (GGT to GAT), which results in an altered amino acid in the conserved zinc-finger domain (G63 > D) (Supplementary Fig.1.1) (Bowman et al., 1992; Sakai et al., 1995).

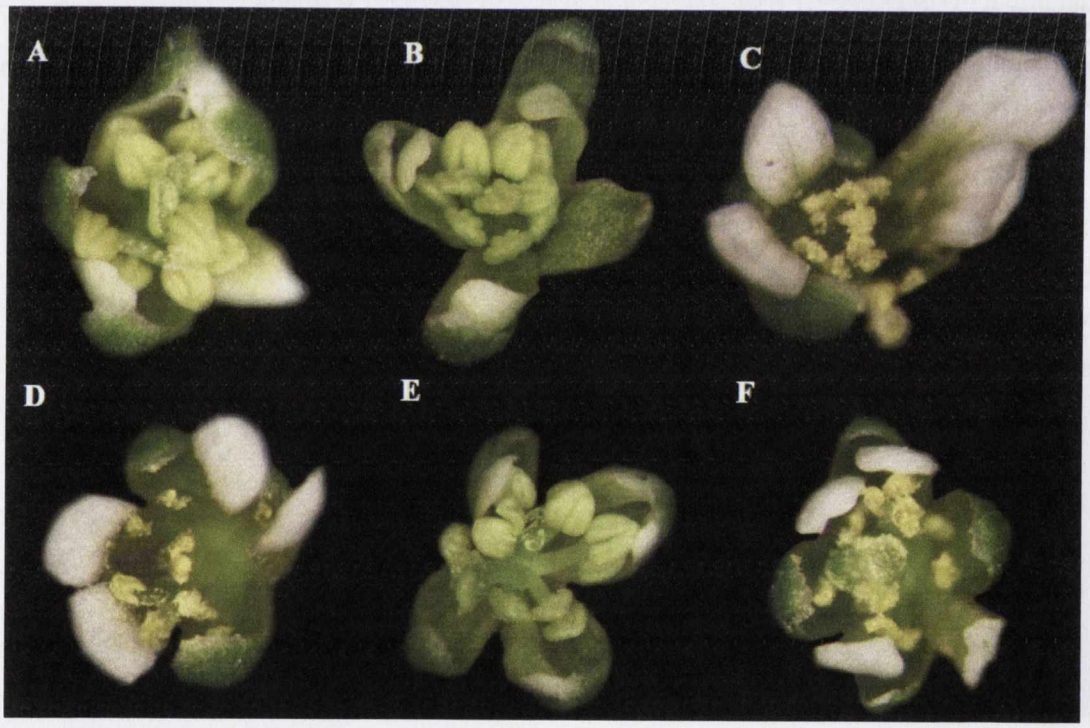

Figure 4.3: Defects of *sup* mutant flowers are allele-dependent.

(A-C) Flowers of *sup-2* mutants with little (or no) carpel tissue or mosaic stamenoid carpels in the centre of the flower. Flowers also have supernumerary stamens. (D-E) *sup-3* flowers with

supernumerary stamens and no carpel tissue. (F) *sup-3* mutant flower with extra stamens and a disrupted gynoecium.

In conclusion, *SUP*'s mutant phenotype always results in an increase in stamen number relative to the wild type as well as to impaired gynoecium development. However, depending on the mutant allele, there is either an increase in carpel tissue or a reduction (up to a complete loss) of the gynoecium. As flowers of the *sup-5* allele have the most severe phenotype, and the majority of the gene is deleted, this allele is thought to be the closest to a null allele and was used in the remainder of the study unless stated otherwise. The *sup-5* allele was crossed into the $35S_{PRO}$:AP1-GR *ap1-1 cal-1* floral induction system (Wellmer et al., 2006) by Dr. Andrea Raganelli. The resulting line is henceforth denoted as *sup-5* FIS.

4.2.2 Generation of an amiRNA targeting *SUP*

To allow a specific knockdown of *SUP* gene activity, three amiRNAs targeting the *SUP* coding region were designed using the software *WMD3* and expressed in wild-type plants under control of the constitutive Cauliflower Mosaic Virus (CaMV) 35S promoter (as described in section 2.6) (Supplementary table 2). For the resulting $35S_{PRO}$:SUP-amiRNA1 construct (Fig. 2.3 A), 32 independently transformed lines were analyzed in the T1 and T2 generations, and no discernible *sup* phenotypes were observed. Wild-type plants were then transformed with the $35S_{PRO}$:SUP-amiRNA2 construct (Fig. 2.3 A). Nineteen independently transformed lines were analyzed in the first and second generation, and as for the amiRNA1 construct described above, no discernible *sup* phenotypes were observed. Finally, the $35S_{PRO}$:SUP-amiRN3 construct was transformed into wild-type plants (Fig. 2.3 A). All of the

eight independent transgenic lines obtained showed a *sup* mutant phenotype. Two lines were relatively weak in phenotype; one was intermediate; four were strong, and one line was classified as very strong. The latter line will be henceforth referred to as SUPamiRNA3-4 (Fig. 4.3 E-I).

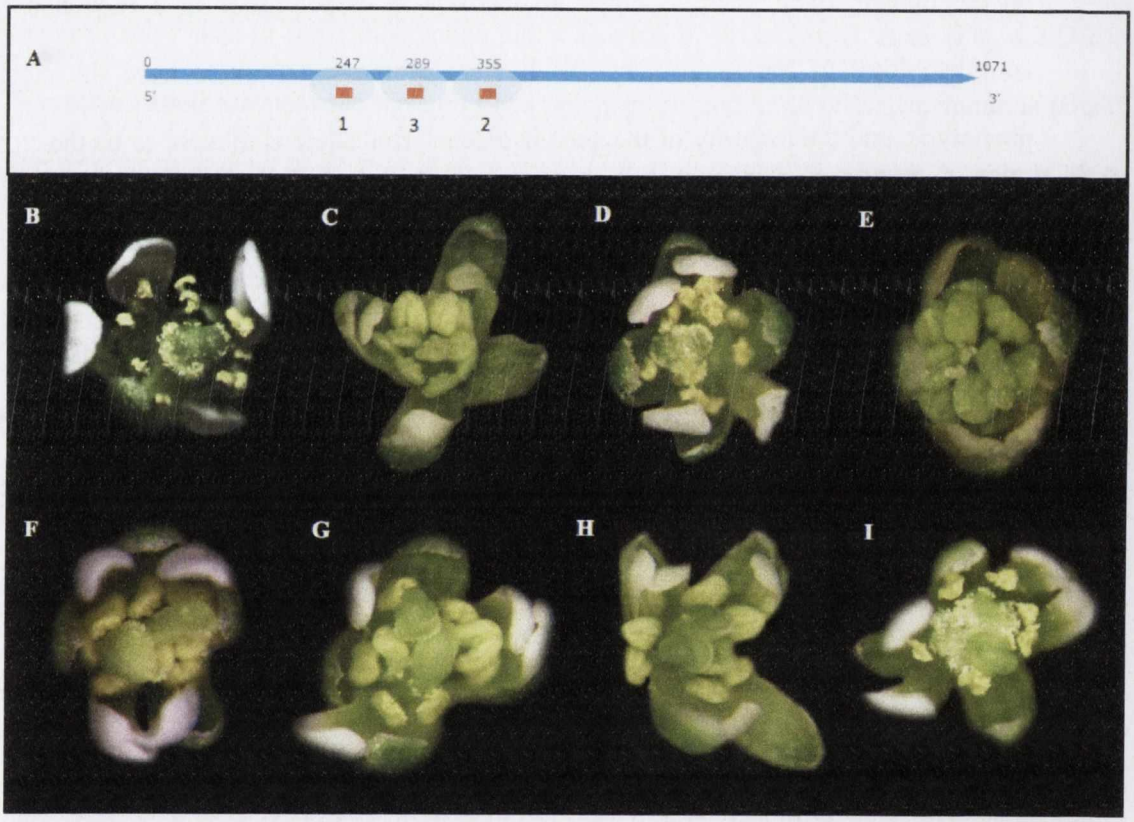

Figure 4.4: Isolation of a functional artificial microRNA against *SUP*.

(A) Schematic of binding sites for the different amiRNAs generated against *SUP*. (B) A *sup-5* mutant flower. (C) A *sup-2* mutant flower. (D) A *sup-3* mutant flower. (E-I) Phenotypes of flowers (line SUPamiRNA3-4) constitutively expressing SUP-amiRNA3. (E) Flower with supernumerary stamens and no carpel tissue. (F-G) Flowers with extra stamens and a split gynoecium. (H-I) Flowers with an increase in stamen number and carpel tissue.

Due to line SUP-amiRNA3-4 having the strongest phenotype, a homozygous line was isolated for further characterization. This line had a strong increase in stamen number when compared to wild-type plants (Fig. 4.5 A). Gynoecium development was also affected with carpel tissue being either mosaic or reduced in the majority of flowers (Fig. 4.5 B).

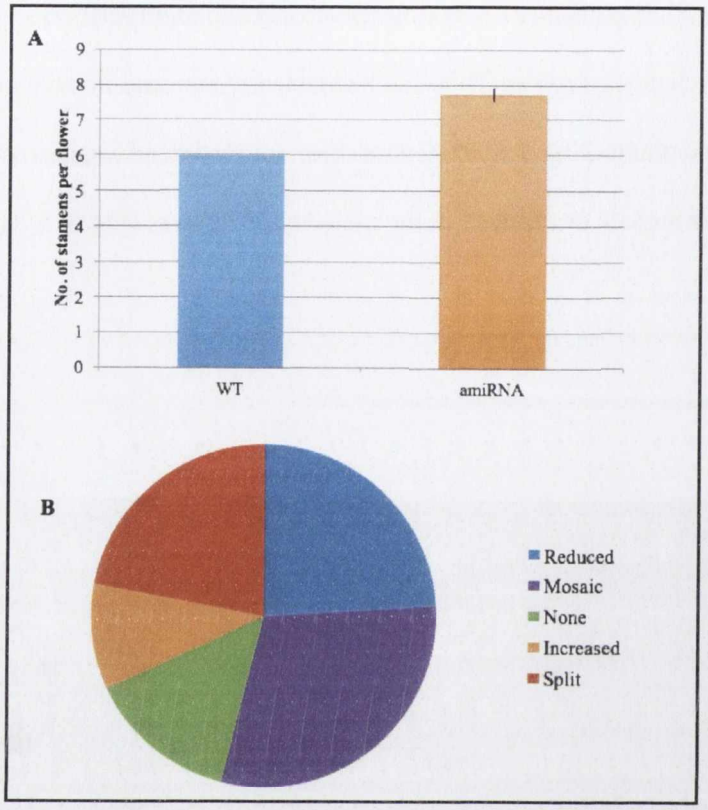

Figure 4.5: Characterization of 35S:$_{PRO}$SUP-amiRNA3-4 plants.

(A) Number of stamens per flower in 35S:$_{PRO}$SUP-amiRNA3-4 (amiRNA) and wild-type (WT) plants. An increase in stamen number was observed in the former lines when compared to the wild typ. (B) Estimated frequencies of carpel morphology defects observed in 35S:$_{PRO}$SUP-amiRNA3 mutant flowers. Note the occurrence of a wide range of phenotypes. 'Split' refers to gynoecia that were split open. Flowers were analysed at the time of anthesis. Error bars in (A) indicate SE.

4.2.3 Generation of an inducible amiRNA against *SUP*

As the constitutive expression of the SUP-amiRNA3 resulted in flowers resembling *sup* mutants, this sequence (Supplementary table 2) was cloned under control of the 35S$_{PRO}$:LhG4-GR/6XOP$_{PRO}$ dexamethasone-inducible promoter system (Fig. 4.6 A). The aim of this line is for an inducible knockdown of *SUP* to be used in the floral induction. Wild-type plants were transformed with the 35S$_{PRO}$:LhG4-GR/6XOP$_{PRO}$:SUP-amiRNA3 construct (henceforth

OP_{PRO}:SUPamiRNA3) and 110 independent lines were analyzed in the T1 generation with the help of an undergraduate student (Mr. Aistis Balciunas). Of these 110 lines, 10 showed strong *sup*-like phenotypes (Fig. 4.6 B-C) two weeks after treatment of inflorescences with a solution containing 10 μM dexamethasone. Of these lines, line 1 (OP_{PRO}:SUPamiRNA3-1) displayed the strongest phenotypic response to dexamethasone treatment, hence this line was selected for further characterization.

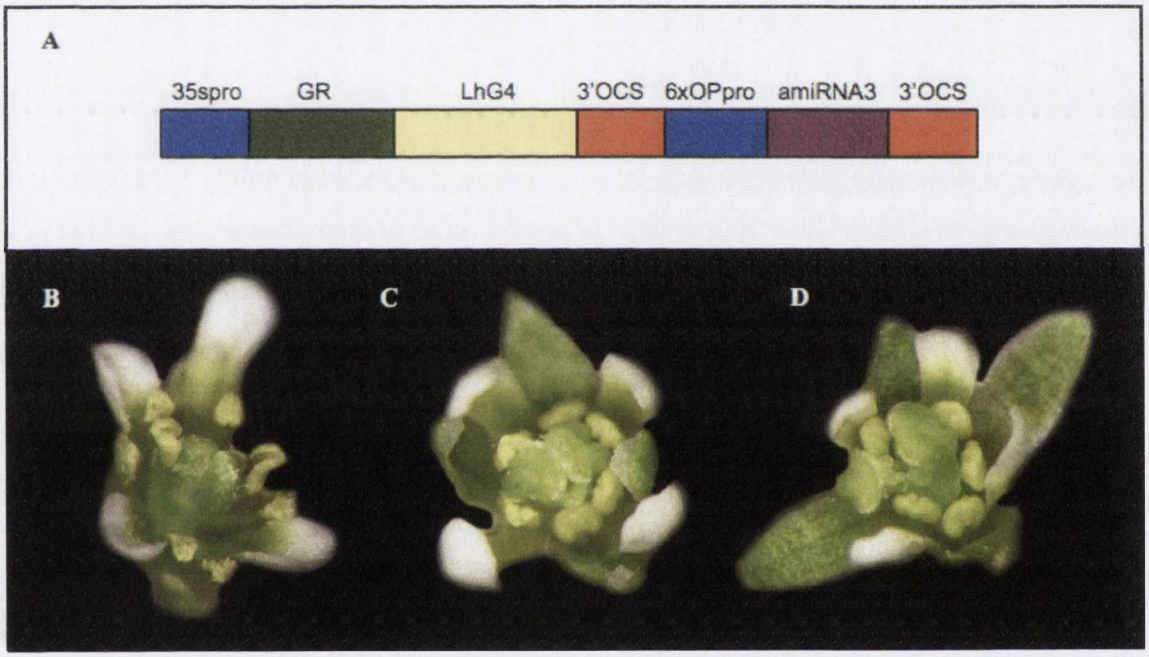

Figure 4.6: Generation of an inducible amiRNA against *SUP*.

(A) Schematic of the $35S_{PRO}$:LhG4-GR/OP_{PRO}:SUP-amiRNA3 (OP_{PRO}:SUP-amiRNA3) construct. (B-D) Flowers of OP_{PRO}:SUP-amiRNA3-1 plants 2 weeks after treatment with 10 μM dexamethasone. (B) Flower with extra stamens and a disrupted gynoecium. (C) Flower with a split gynoecium. (D) Flower with a disrupted gynoecium and mosaic stamenoid carpels.

Sup mutant phenotypes began to appear in OP_{PRO}:SUP-amiRNA3-1 transgenic plants 10-14 d after the initial dexamethasone treatment. The strongest floral phenotypes observed resembled

those seen in the $35S_{PRO}$:SUPamiRNA3 line (Fig. 4.3 E-I), suggesting that the inducible knockdown system was functional. Different floral phenotypes were observed depending on which developmental stage any given flower was at when treated with dexamethasone (Fig. 4.6 A-J). After 10 d, the first flowers to show abnormal phenotypes would have been at a late developmental stage when the *SUP* mRNA was targeted by the amiRNA. Later flowers, after the first few with phenotypes, would have been in earlier stages of development. Flowers at 10 to 12 d after the treatment had an increase in stamen number compared to mock-treated wild-type plants (Fig. 4.6 A-E). There was also an increase in carpel tissue with the gynoecium also being split in the majority of flowers (Fig. 4.6 A-E). Mosaic stamenoid carpels were also seen in the 4th whorl. Furthermore, flowers arising later had an increase in stamen number and began to show a reduction in carpel tissue (Fig. 4.6 F-G). After roughly 15 d the flowers analyzed would have been at an early developmental stage when the dexamethasone treatment took place, and these showed an increase in stamen number and a complete loss of carpel tissue (Fig. 4.6 H-J), with the inner most whorl occupied by stamens or stamenoid carpels. Finally, restoration of wild-type flowers after roughly 16 d indicated that *SUP* activity can be perturbed in a temporary manner.

In conclusion, the knockdown of *SUP* mRNA using the dexamethasone-inducible promoter system, driving the expression of an amiRNA against *SUP*, results in strong *sup*-like mutant phenotypes. These phenotypes showed an increase in stamen number which is described in *sup* mutants and depending on the stage of knockdown either an increase or loss of carpel tissue. This line will now be crossed into the floral induction system (FIS) for stage-specific knockdown experiments.

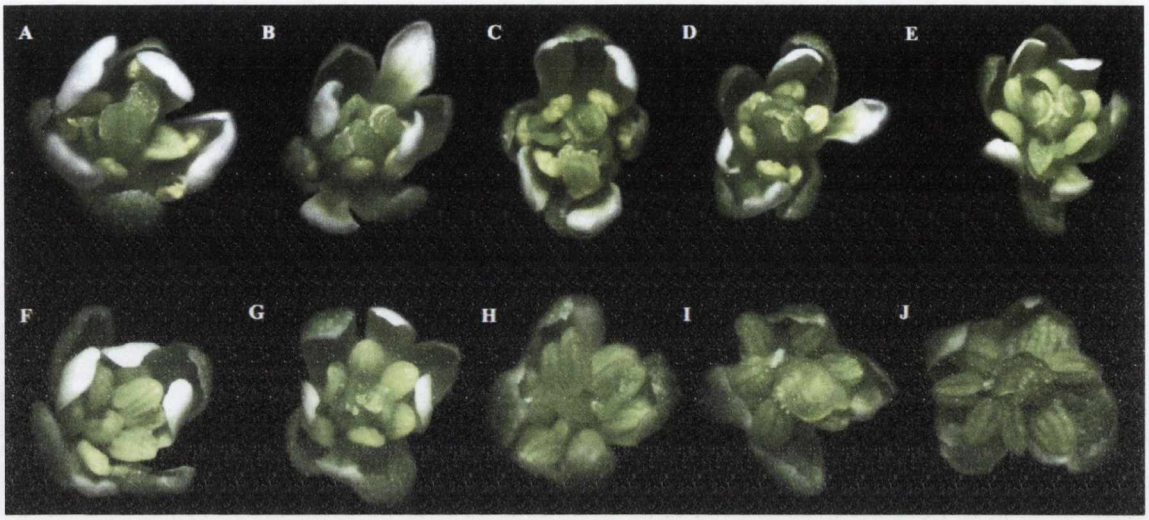

Figure 4.7: Defects observed in flowers of OP_{PRO}:SUP-amiRNA3 plants.

(A-J) Flowers of OP_{PRO}:SUP-amiRNA3 plants 10 d after treatment with a solution containing 10 μM dexamethasone. (A-E) Flowers with an increase in stamen number and an increase in carpel tissue after 10-12 d. (C) Flowers sometimes formed mosaic stamenoid carpels in the centre of the flower. (E) A carpel with extra supernumerary stamens and a split gynoecium. (F-H) Flowers 13-15 d after treatment. (F-G) Flowers with supernumerary stamens and loss of carpel tissue. (H-J) Flowers with supernumerary stamens and mosaic carpel stamens in the centre of the flower. Flowers were analysed at the time of anthesis over four successive days until normal flower morphology was restored.

4.2.4 Generation of a stable knockout of *SUPERMAN* using CRISPR/Cas9 technology

A functional CRISPR/Cas9 system in *Arabidopsis* has been developed (section 1.6), which effectively produces disruptions in target regions of the genome complementary to the selected guide sequence. This occurs *via* infrequent nucleotide insertions or deletions, which are the result of non-homologous end joining of double strand breaks induced by Cas9 (Hyun et al., 2015). I decided to target the *SUP* locus in order to obtain a full *SUP* knockout, in order to verify whether or not the *sup* mutant alleles available truly reflect a full ablation of its

activity. To this end, 2 separate guide sequences (Supplementary table 3) were generated against the *SUP* coding sequence (see section 2.7 for cloning of CRISPR constructs) and cloned into a plasmid downstream of the *U6 snRNA* promoter, derived from *Arabidopsis* genomic DNA. Cas9 expression is driven by the *INCURVATA2* promoter, which is highly active in cells that divide, such as meristematic cells. Activation of this transgene should create somatic mutations, which will then be passed onto the following generation. Plants have been transformed with this construct, and due to only the recent availability of these tools, they are yet to be analysed.

4.2.5 Genes acting downstream of SUP

To understand which genes and processes are effected upon *SUP* perturbation, microarray analysis was carried out on *sup-5* FIS plants vs. pooled heterozygous and wild-type FIS plants.

This work was carried out in part by myself and Dr. Andrea Raganelli for the 0, 2.5, and 5 d time-points after induction. The labelling of the samples with fluorescent dyes and co-hybridization to the custom Agilent microarrays was carried out by Ms. Kamila Kwasniewska, and all computational analysis was carried out by Dr. Patrick Ryan in the Wellmer laboratory.

Firstly, as *SUP* peak expression is at roughly 3.5 d, another microarray was carried out on plants collected at this stage of their development after induction of flowering with dexamethasone. To validate the quality of the RNA collected to be used for hybridization qRT-PCRs were carried out to check for the levels of *SUP* being expressed in the samples.

Across all four biological replicates *SUP* levels were all below 0.03% compared to the wild type (Fig. 4.7 A). Once the microarray was carried out a global overview of differentially expressed genes was visualized by generating MA-plots for the different replicates. These plots illustrate the mean processed signal intensity (x-axis) against the $\log_2$-transformed ratios of the mean fold change values (y-axis) (Fig. 4 B-E).

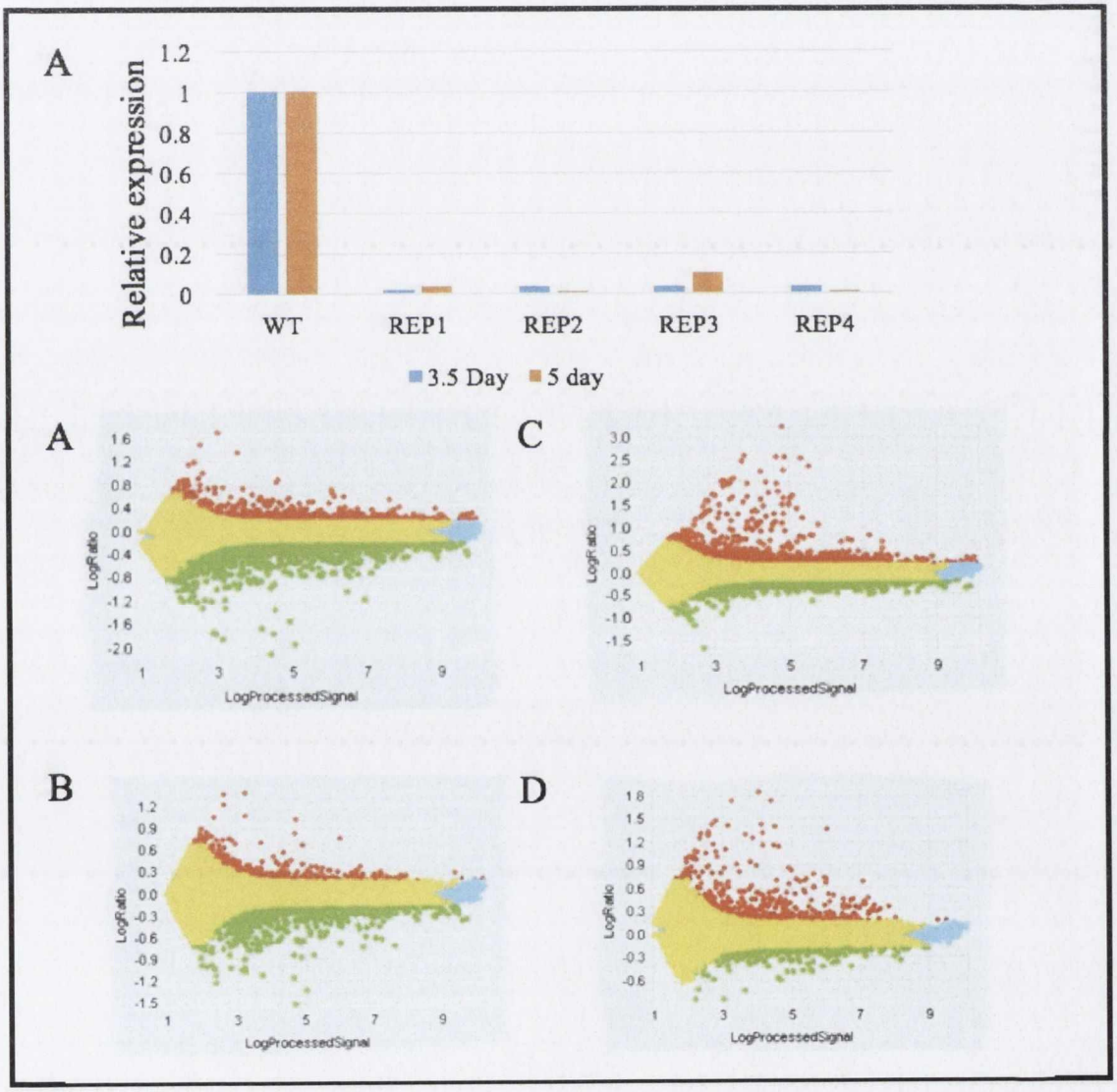

Figure 4.8: Microarray data from the comparison of the transcriptomes of *sup-5* FIS vs. pooled wild-type and *sup-5* heterozygous FIS for the repeated 5 day time point.

(A) Measurements of *SUP* mRNA levels at 3.5 and 5 day time-points. FIS *sup-5* homozygous plants are compared to wild-type and heterozygous plants (B-E) MA-plots with the mean expression values (x-axis) plotted against log_2-transformed fold-change expression ratios (y-axis), visually representing differentially expressed genes for the four replicates of the repeated 5 day time point. Yellow dots indicate no differential expression; blue dots behind the yellow bots indicate reference genes used to normalize the data; red dots indicate genes that are significantly up-regulated; green dots indicate genes that are significantly down-regulated in the mutant relative to the wild type.

After statistical analysis of the dataset was carried out by Dr. Patrick Ryan and a stringent unadjusted *P*-value cut-off of 0.01 was applied, 138 genes were seen to be differentially expressed at the 0 d time-point; 149 at 2.5 d; 147 at 3.5 d, and 129 at the 5 d time-point (Fig. 4.8 A). Overall there were 30 more genes up-regulated than down-regulated at the 2.5 day time point which is consistent with the idea of SUP being primarily a repressor. However, more genes were downregulated across all the other time points analysed, suggesting that SUP might also function as an activator. As expected, the levels of *SUP* mRNA were drastically reduced in comparison to the wild type over the 2.5 d, 3.5 d, and 5 d time-points.

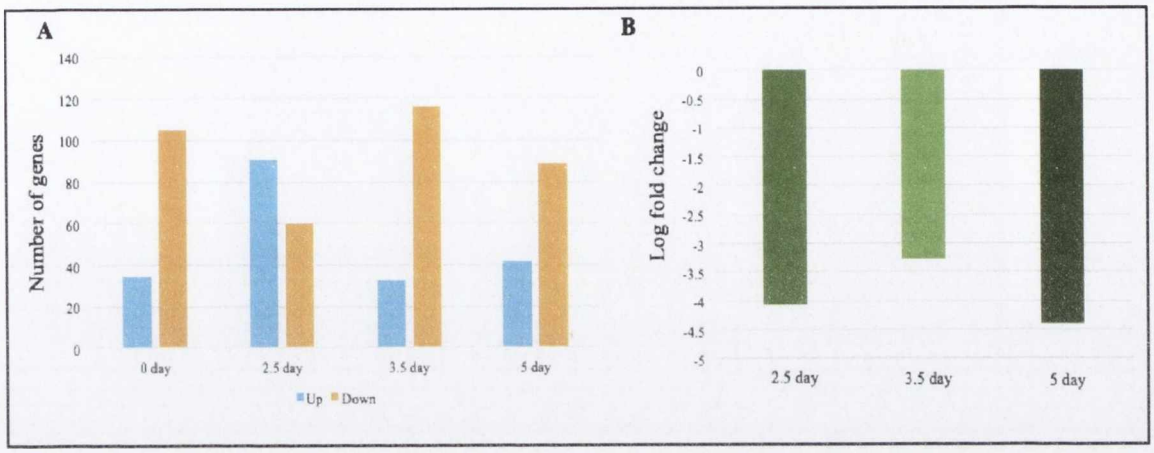

Figure 4.9: Genes differentially expressed in *sup-5* mutant flowers.

(A) Number of differentially expressed genes identified in the 0, 2.5, 3.5, and 5 d time-points by microarray analysis. (B) Transcript levels of *SUP* across the 2.5, 3.5, and 5 d time-points. Data shown are log_2-transformed fold-change expression ratios.

Across the varying time-points there was significant differential expression of multiple genes known to be involved in flower development (Table 4.1). Of considerable interest were genes involved in stamen development, such as *DORNROESCHEN-LIKE* (*DRNL*) (Chandler et al., 2008) and the floral organ identity gene *PISTILLATA* (*PI*) (Bowman et al., 1989). Genes involved in carpel development such as *SHATTERPROOF1* and *-2* (*SHP1*/*SHP2*) (Liljegren et al., 2000) and *HECATE1* and *-2* (Gremski et al., 2007) were also present, as well as genes involved in boundary formation, such as *CRABS CLAW* (*CRC*) (Alvarez and Smyth, 1999), *JAGGED LATERAL ORGANS* (*JLO*) (Borghi et al., 2007) and members of the LBD (LOB-domain containing) family (Shuai et al., 2002). *VERDANDI* (*VDD*), a gene involved in ovule formation (Matias-Hernandez et al., 2010), was also differentially expressed, and several genes known to be involved in the regulation of the floral meristem, cell fate, and cell growth, such as *CLAVATA3* (*CLV3*) (Clark et al., 1995), *KNUCKLES* (*KNU*) (Payne et al, 2004), and

members of the *WRKY* (Eulgem et al., 2000) and *WUSCHEL RELATED HOMEOBOX* (*WOX*) gene families (Haecker et al., 2000).

Table 4.1: Selected genes identified as differentially expressed in early stage *sup-5* flowers.

Table of candidate genes which might be directly or indirectly regulated by *SUP*. Table shows genes differentially expressed across 0, 2.5, 3.5, and 5 d time-points. Data shown are log_2-transformed fold-change expression ratios with an unadjusted *P*-value of <0.01.

Gene name	Log2 expression	Day	Gene name	Log2 expression	Day
ERF38	-0.777993656	5 day	NAT8	0.706719502	3.5 Day
AGO3	0.563202304	0 Day	PI	0.356634108	2.5 Day
AGO3	-0.348605943	2.5 Day	RTFL13	0.597216663	5 day
AGO3	-0.618150929	3.5 Day	RTFL7	-0.544936092	5 day
AGO5	0.569349524	3.5 Day	SAP	-0.732086619	2.5 Day
AGO9	-0.658827189	3.5 Day	SAP	-0.711884528	5 day
AGO9	-0.872170963	5 day	SHP1	-1.114404803	5 day
ARR21	-0.296825595	1 Day	SHP2	-0.911978822	5 day
ARR6	-0.601874527	3.5 Day	SPL3	-0.275171912	4 Day
AtMYB116	-0.461179341	2.5 Day	SUP	-4.074988009	2.5 Day
AtMYB50	-0.564706314	5 day	SUP	-3.259505218	3.5 Day
CLV3	0.477601166	2.5 Day	SUP	-4.404306482	5 day
CRC	-0.639260193	5 day	TBL19	0.439504044	2.5 Day
DRNL	0.59286944	3.5 Day	TEL1	0.660296042	3.5 Day
DRNL	1.523125668	5 day	TEL1	1.133688644	5 day
ERF9	0.532947655	3.5 Day	TGA9	-0.928144324	3.5 Day
FMA	-0.59921989	2 Day	TT16	0.726080759	2.5 Day
GA2OX1	0.766550784	5 day	ULT1	-0.297610101	2.5 Day
HDG7	-0.791068387	2.5 Day	URO	1.536418427	2.5 Day
HEC1	-2.876214935	5 day	URO	1.061412283	3.5 Day
HEC2	-2.388784905	5 day	URO	1.772210225	5 day
JAZ5	-1.012973946	3.5 Day	VDD	-0.509842545	5 day
JAZ6	-0.840292897	3 Day	WOX12	-1.332955835	2.5 Day
JAZ7	0.438940619	2.5 Day	WOX12	-1.406880008	3.5 Day
JLO	0.378787108	2.5 Day	WOX12	-3.056515085	5 day
JLO	0.747120438	5 day	WOX6	-0.671575308	2.5 Day
KNU	-1.372487347	5 day	WOX6	-1.968488724	5 day
LBD19	0.79161813	3.5 Day	WOX9	-0.676807402	5 day
LBD19	0.828331334	5 day	WRKY10	-0.791995683	2.5 Day
LBD31	0.646397368	2.5 Day	WRKY10	-1.253209616	5 day
LBD31	0.707334783	3.5 Day	WRKY40	-0.750902318	3.5 Day
LBD31	1.570572396	5 day	WRKY6	-0.585597375	2.5 Day
LBD42	-0.570059976	2.5 Day	WRKY6	-0.87290084	5 day
MYB50	-0.537368614	3.5 Day	ZFP3	-0.510401089	5 day

As *SUP* is normally expressed at roughly 3 d there should be a higher number of differentially expressed genes at later time-points compared to earlier ones analysed, but this was not the case for the 5 d time-point. Upon analysis of MA-plots for the 5 d time-point the spread of

differentially expressed genes was abnormal in some cases (Fig. 4.9 B). There was also some variation between the different replicates when compared to the samples collected for the 3.5 d time-point (Fig. 4.9 A). To this end, this 5-day time-point was repeated with four biological replicates and the RNA was validated to having low transcript levels of SUP (Fig. 4.7 A).

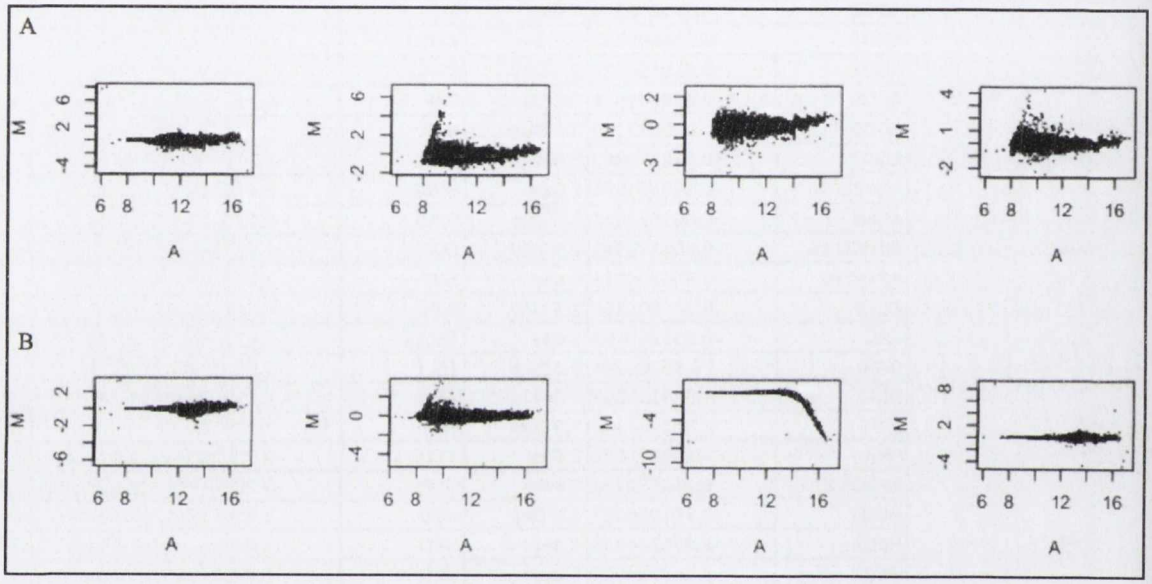

Figure 4.10 MA-plots of microarray data.

Mean expression values (x-axis) are plotted against $\log_2$-transformed fold-change expression ratios (y-axis). (A) Plots for replicates 1 through 4 (from left to right) showing differentially expressed genes identified in the 3.5 day time-point. (B) Plots for replicates 1 through 4 (from left to right) showing differentially expressed genes identified in the 5 day time-point carried out by Dr. Raganelli.

The data for this microarray experiment has yet to be analysed in detail. However, based upon the previous microarrays experiments, the expression of some of the candidate genes thought to be regulated by *SUP* was tested by qRT-PCR. The expression levels of *CLV3*, *DRNL*, and *WUSCHEL* (*WUS*) were found to be upregulated in *sup-5* flowers relative to the wild type (Fig. 4.10 A). Furthermore, genes involved in cytokinin response, such as *ARABIDOPSIS*

RESPONSE REGULATORS5 (*ARR5*) and *CYTOKININ OXIDASE6* (*CKX6*) were upregulated compared to the wild type, and these results will be further discussed below (section 4.2.3).

In conclusion, the results from the microarray experiments suggest that *SUP* regulates the expression of various genes involved in flower development. Candidate genes from these experiments include transcription factors, genes with known functions in boundary control, stamen development, and cell cycle control. These results are consistent with the *SUP*s hypothesized role and allow for further exploration of the exact functions and process controlled by *SUP*.

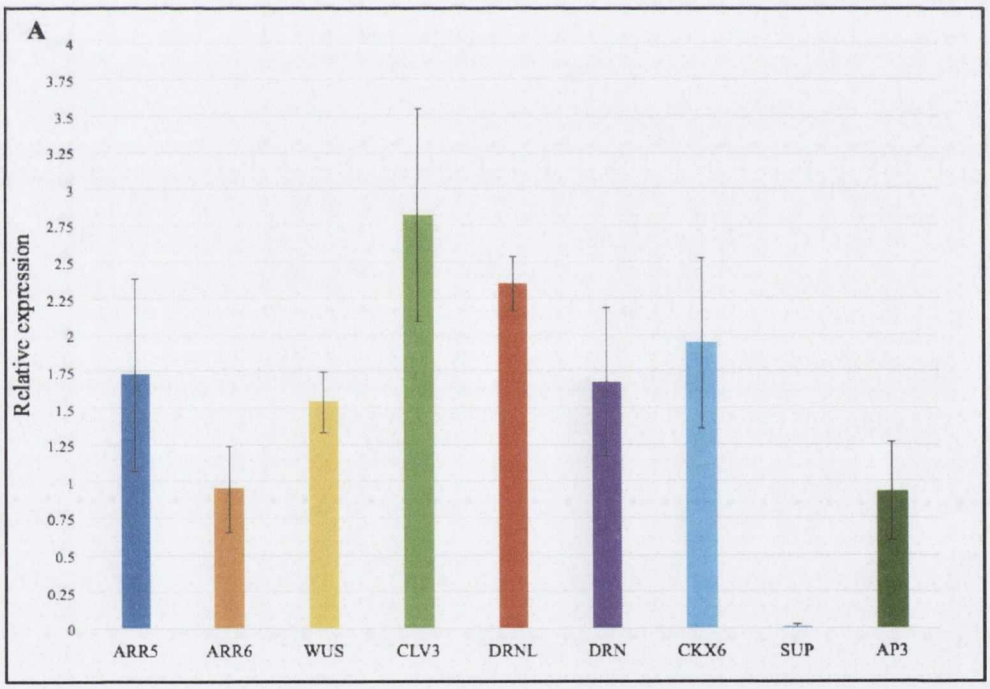

Figure 4.11: Confirmation of results from microarray experiments.

(A) Relative expression (*sup-5* vs. wild type) of candidate genes identified in the microarray experiments was determined by qRT-PCR in early stage floral buds 5 d after induction of flower development. Bars indicate averages of four biological replicates. Error bars indicate SE.

4.2.6 Mutations in *DORNROESCHEN* and *DORNROESCHEN-LIKE* partially rescue the *sup* mutant phenotype

DRN and its paralog *DRNL* encode functionally redundant AP2-type transcription factors, are known to be involved in embryo patterning, and are regulated by auxin (Chandler et al., 2007). They also contribute to cytokinin-independent shoot regeneration (Banno et al., 2001). *DRN* and *DRNL* are also expressed in the floral meristem, in stamen founder cells, and are responsible for stamen emergence (Nag et al.; 2007; Seeliger et al., 2016). Mutant flowers of *drn-1* and *drnl-1* have minor defects in organogenesis, with lower numbers of stamens and petals. Furthermore, fusions of stamens also occurs at low frequencies (Nag et al., 2007; Chandler et al., 2007).

As *DRNL* was found to be differentially expressed in the microarray experiments (Table 4.1), and has a known role in stamen organogenesis, seeds for its paralog, *DRN* were ordered and crossed into the *sup-5* mutant background. A line homozygous for *sup-5* and *drnl-1* was isolated and their floral phenotypes were characterized. *Drnl-1* mutant flowers have slightly lower numbers of petals and stamens than the wild type (Nag et al., 2007) (Fig. 4.11 A). *Sup-5* on the other hand exhibits a drastic increase in stamen number and an increase in carpel tissue when compared to the wild type (Fig. 4.11 B). *Drnl-1 sup-5* double-mutant plants resulted in near wild-type number of stamens forming (Fig. 4.11 C-H). Further to this there was also a reduction in carpel tissue compared to the *sup-5* mutant plants, although the gynoecium architecture was still abnormal in most flowers.

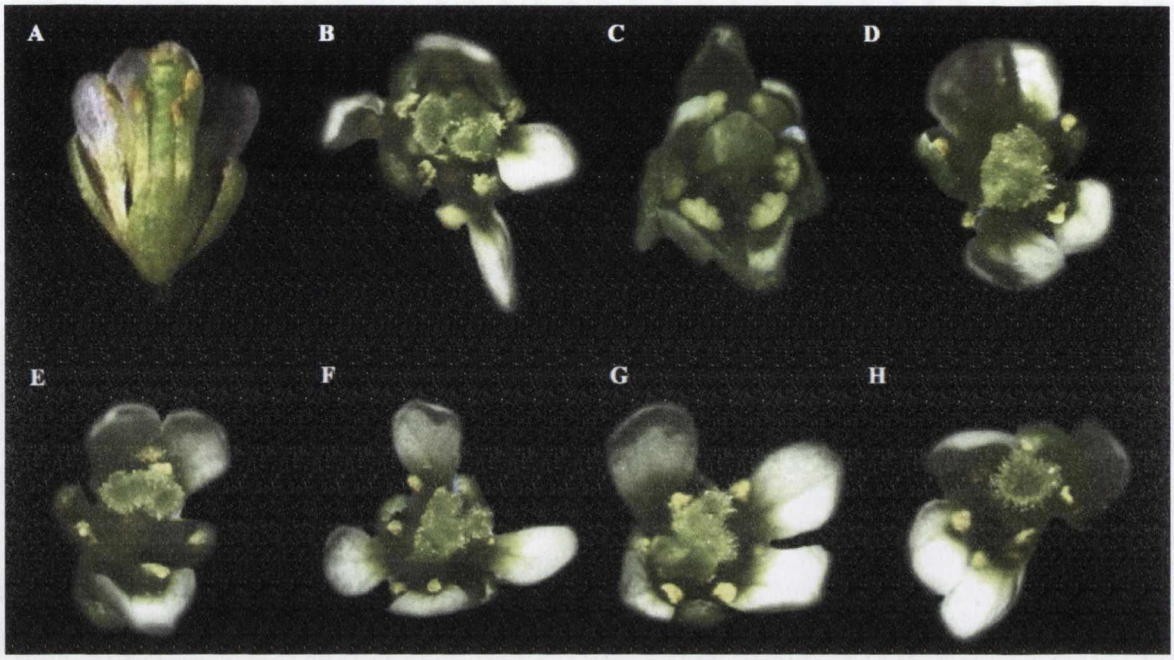

Figure 4.12: Loss of *DRNL* causes partial rescue of the *sup-5* mutant phenotype.

(A) A flower of a *drnl-1* mutant plant with 4 stamens (Nag et al., 2007) (B) A *sup-5* mutant flower with extra stamens and extra carpel tissue. (C-H) Flowers of *drnl-1 sup-5* mutant plants with wild-type numbers of stamens. Carpel tissue is somewhat reduced compared to *sup-5* but still disrupted.

As *DRN* is known to be functionally redundant to *DRNL,* the *drn-1* allele was crossed into *sup-5* and a homozygous line for both mutations was isolated. *drnl-1* also has a similar floral phenotype similar to *drn-1,* with a slight reduction in petals and stamen numbers (Fig. 4.12 A) (Nag et al. 2007). Upon examining flowers of the double mutant (Fig. 4.12), stamen number was again reduced compared to *sup-5* alone, approaching wild-type levels (Fig. 4.13). However, carpels were still abnormal compared to wild-type.

In conclusion, loss of *DRN* and *DRNL* activity leads to a partial rescue of the *sup* mutant phenotype. It can be hypothesised based on this genetic interaction that the supernumerary stamen phenotype in *sup* mutant flowers is a coincidence of an increase in *DRN* or *DRNL*

expression levels. Whether *SUP*, *DRN* and *DRNL* are in the same pathway regulating flower formation is still unknown. With *DRNL* being differentially expressed in the microarray data it is clear it is downstream of *SUP* but ChIP experiments in the future will be able to tell if this is a direct interaction.

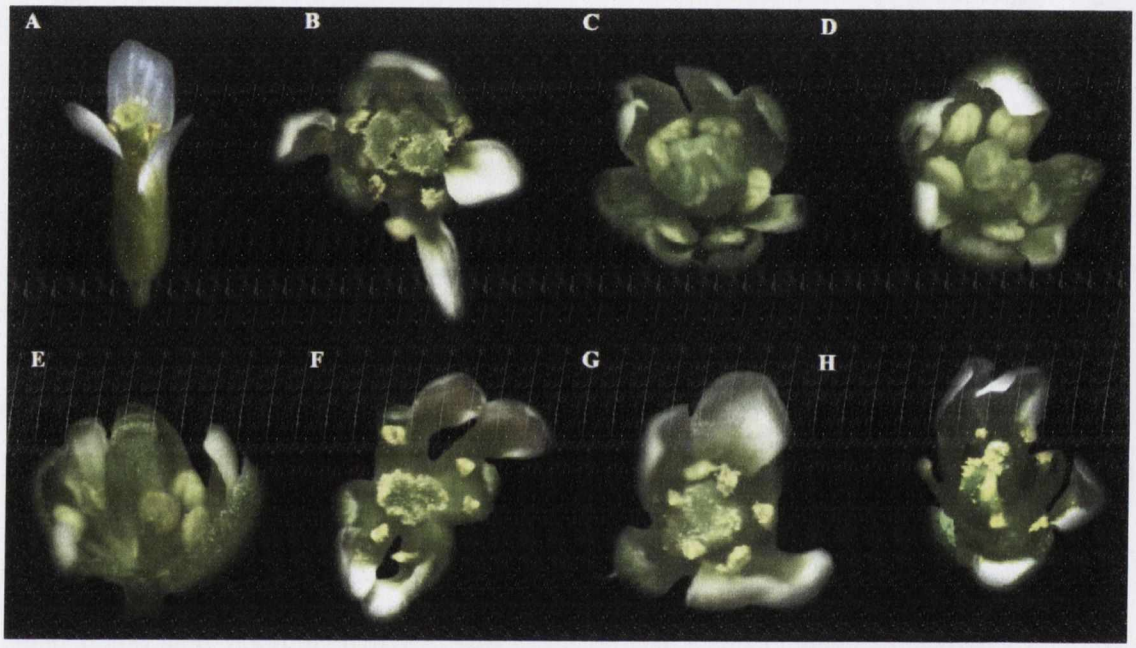

Figure 4.13: Loss of *DRN* causes partial rescue of the *sup-5* mutant phenotype.

(A) A *drn-1* mutant flower with abnormal organ numbers (Chandler et al., 2007). (B) A *sup-5* mutant flower with an increase in stamen number and an abnormal gynoecium. (C-H) *Drn-1 sup-5* mutant flowers. Overall flowers have a reduction in stamen number when compared to *sup-5* flowers alone. Carpel development is unaffected and still disrupted in the vast majority of flowers, similar to in *sup-5* mutant flowers.

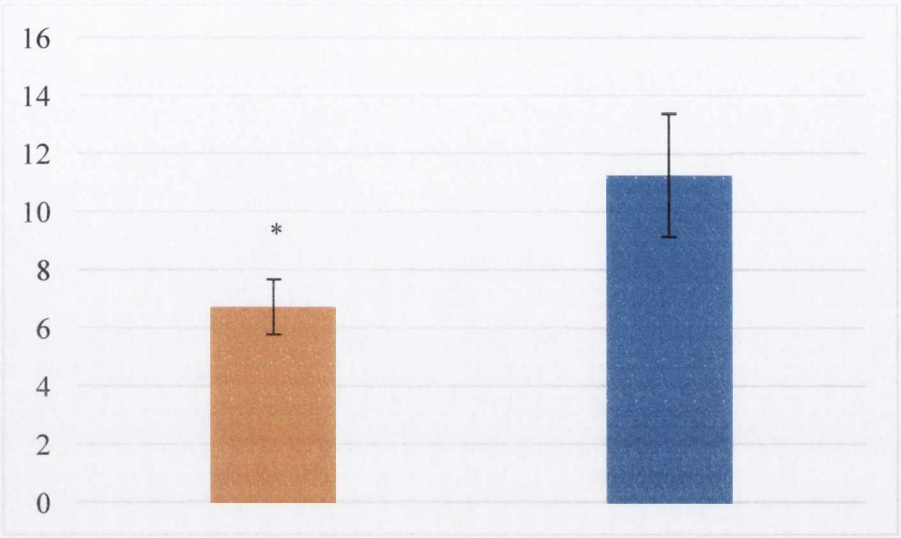

Figure 4.14: Loss of *DRN* rescues the supernumerary stamen phenotype of *sup-5*.

(A) The mutation in *sup*-5 leads to an average of 11 stamens per flower (blue bar). Mutations in *drn* in the *sup-5* mutant background result in restoration of stamen number comparable to the wild type (orange bar). *sup-5* n=50; *drn-1 sup-5* n= 100. Error bars indicate SE. An asterisk indicates statistical significance (*P*-value < 10^{-5}; two-tailed t-test).

4.2.7 Genes directly regulated by SUP

To identify genes directly bound to SUP a construct containing a Green Fluorescent Protein reporter gene (mGFP5) was translationally fused to the C-terminus of the genomic locus of SUP (Fig. 4.14 A). Further to this, *SUP*'s 3'UTR was cloned downstream of GFP, as this part of *SUP*'s sequence has been shown to be essential for its correct expression (Ito et al., 2003). The resulting construct was transformed into a population of segregating *sup-5* plants. Twenty-seven independent transformants were obtained. Of these transformants none harboured the *sup-5* mutation. Following this a homozygous mutant population of *sup-5* was transformed. Twelve independent transformants were selected through resistance to BASTA. Of the twelve lines selected one showed a partial rescue of the *sup-5* mutant phenotype. This

line was then genotyped for the presence of the GFP coding sequence. A homozygous line was obtained through analysis of segregation patterns of the T-DNA by BASTA resistance. In the homozygous rescue line, stamen numbers were returned to near wild-type levels (Fig. 4.14 C-E). Further to this, carpel development was mostly normal and this resulted in many seeds being able to be produced from each flower compared to *sup-5* mutant plants, which only produce small quantities of seeds. Confocal imagining by a collaborator (Dr. N. Prunet, Meyerowitz group, California Institute of Technology) of this line revealed no discernable GFP signal (not shown). This could be due to the nature of the mGFP5 reporter used, which is not as bright as more modern GFP variants (e.g., VENUS). The SUP_{PRO}:SUP-GFP-3'UTR *sup-5* line was then crossed into the $AP1_{PRO}$:AP-GR *ap1-1 cal-1* floral induction system as described in section 2.13.5. After plants that were homozygous for each transgene were obtained, treatment of the inflorescence with DEX resulted in activation of the AP1-GR transgene, resulting in the commencement of flowering (not shown). Upon analysis of the flowers a partial rescue of the *sup-5* mutant phenotype was evident similar to in the SUP_{PRO}:SUP-GFP-3'UTR *sup-5* mutant plants (not shown). This suggests that this line is functional and can now be used for chromatin immunoprecipitation (ChIP) experiments to find direct targets of the *SUP*.

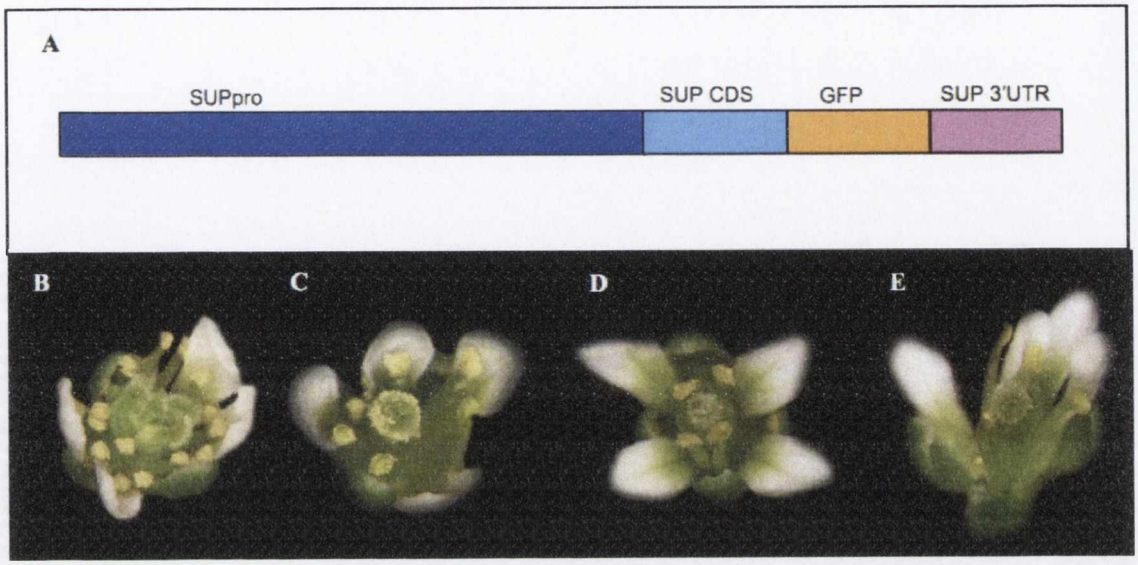

Figure 4.15: Generation of a SUP_{PRO}:SUP-GFP-3'UTR rescue construct.

(A) A schematic of the T-DNA insertion carrying the SUP_{PRO}:SUP-GFP-3'UTR transgene not to scale. (B) *sup-5* mutant plant with an increase in stamen number and carpel tissue. (C-D) SUP_{PRO}:SUP-GFP *sup-5* mutant plants. Flowers showing wild-type levels of stamens and restored gynoecium structure. UTR, untranslated region; CDS, Coding sequence; GFP, Green Fluorescent protein.

4.2.8 Generation of inducible SUP-GFP overexpression lines

To complement the *SUP* perturbation experiments, I sought to monitor gene expression also after an over-expression of SUP, which should result in the opposite responses for SUP target genes. SUP over-expression has been characterized by the conversion of petals to sepals, and the suppression of stamen development. Further to this, constitutive expression causes severe dwarfism in plants (Hiratsu et al., 2002; Yun et al., 2002). To allow the specific over-expression of SUP, SUP was translationally fused of GFP at its C-terminus, and the resulting fusion protein was expressed under the control of the $35S_{PRO}$:AlcR/$AlcA_{PRO}$ EtOH-inducible promoter system (Fig. 4.15 A). The initial design and cloning of this construct was carried out by Dr. Raganelli. A heterozygous population of *sup-5* plants, and wild-type plants, were

transformed. Of these, 13 lines in the wild-type background were selected, and 4 in *sup-5/+*. These lines were taken to the next generation and subjected to 24 hours of EtOH vapour treatment. From analysis of the wild-type plants harbouring the transgenes, no overexpression phenotypes were observed (not shown). In the four *sup-5/+* mutant lines one line (number 4.3) showed a strong partial rescue of the *sup-5* phenotype (Fig. 4.15 B-E). This result indicated that the over-expression construct is functional. With the addition of a GFP-tag fused at the C-terminus of the SUP coding sequence this line was also crossed into the $AP1_{PRO}$:AP-GR *ap1-1 cal-1* floral induction system and will be used for genome-wide binding studies.

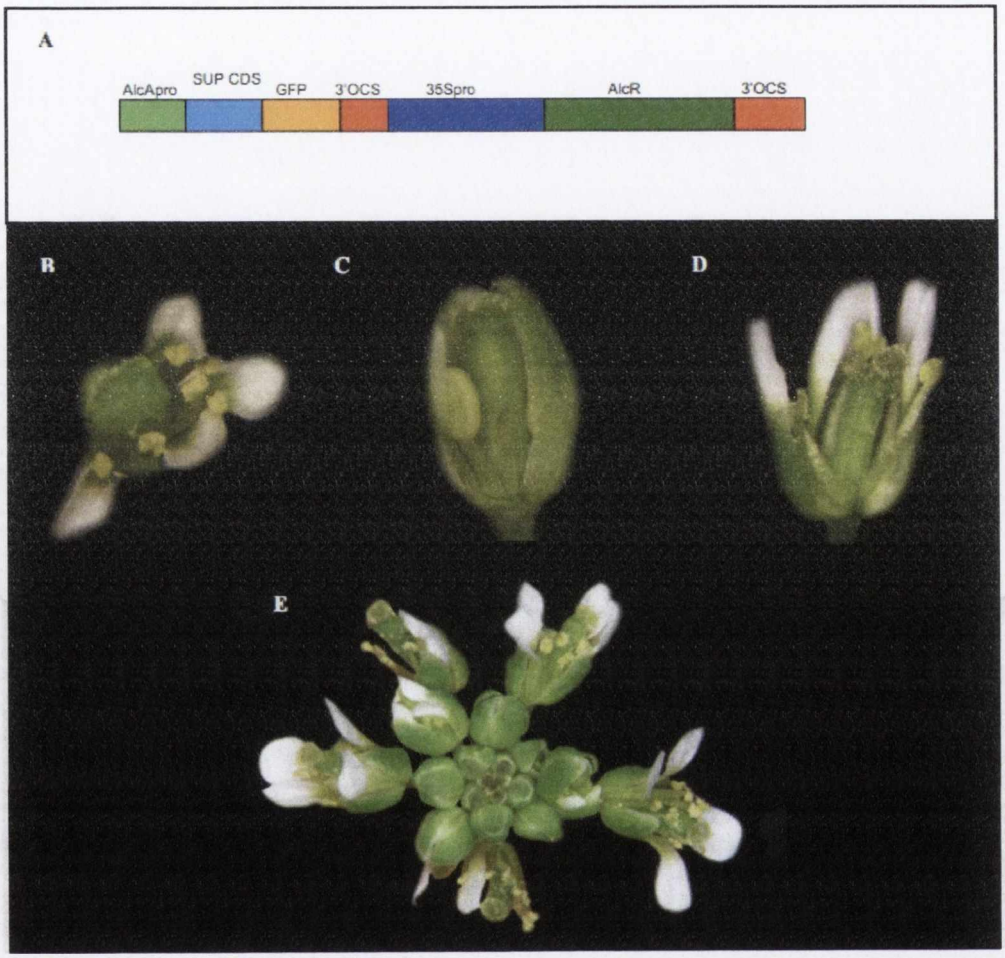

Figure 4.16: Generation of an inducible *SUP* over-expression line.

(A) Schematic of the T-DNA insertion carrying the $35S_{PRO}$:AlcR/$AlcA_{PRO}$:SUP-GFP ($AlcA_{PRO}$:SUP-GFP) construct. (B-D) Flowers of an $AlcA_{PRO}$:SUP-GFP *sup-5* plant 2 weeks after a 24 hour exposure to EtOH vapour. (B) Flower with wild-type stamen number. (C) Flower with normal carpel architecture. (D) Flower with wild-type number of stamens and restored carpel architecture. (E) Inflorescence with rescued flowers. CDS, Coding sequence; GFP, Green Fluorescent Protein; 3`OCS, octopine synthase terminator sequence.

Research conducted in our laboratory has shown that the $35S_{PRO}$:AlcR/$AlcA_{PRO}$ EtOH-inducible promoter system can produce many experimental artefacts and unreliable data due to the mis-expression of large numbers of stress-related genes, which can mask enrichment of

other differentially expressed genes in post-experimental analysis (O'Maoileidigh et al., 2015). To circumvent this potential problem, the same SUP-GFP fusion protein used for the ethanol-inducible over-expression construct was expressed under the $35S_{PRO}$:LhG4-GR/$6xOP_{PRO}$ dexamethasone-inducible promoter system (Fig. 4.16 A). Wild-type plants were transformed with the corresponding construct, resulting in the isolation of 8 independent T1 lines that carried the transgene (as confirmed through PCR-based genotyping). Once a homozygous line was isolated through segregation analysis by BASTA selection, *sup-5* was crossed into line 11.6.2, which was homozygous for the transgene. A line homozygous for the transgene was then selected in *sup-5*/+ mutant background through BASTA selection and PCR-based genotyping for the *sup-5* allele. Upon dexamethasone treatment plants which were wild-type or heterozygous for the *sup-5* deletion, were not phenotypically different from mock and untreated plants. However, flowers of plants homozygous for the *sup-5* deletion, which reached anthesis roughly 2 weeks after the initial treatment, had rescued stamen numbers and exhibited a partial rescue of the gynoecium phenotype typically observed in *sup-5* (Fig. 4.16 B-G). These results indicated that the overexpression construct was functional. To allow for genome-wide binding studies for SUP in the future, the transgene was also crossed into the dihydroxytestosterone-responsive $AP1_{PRO}$:AP-AR *ap1-1 cal1-1* floral induction system. This will ensure that the induction of flower development and the induction of SUP-GFP expression can be done independently from one another.

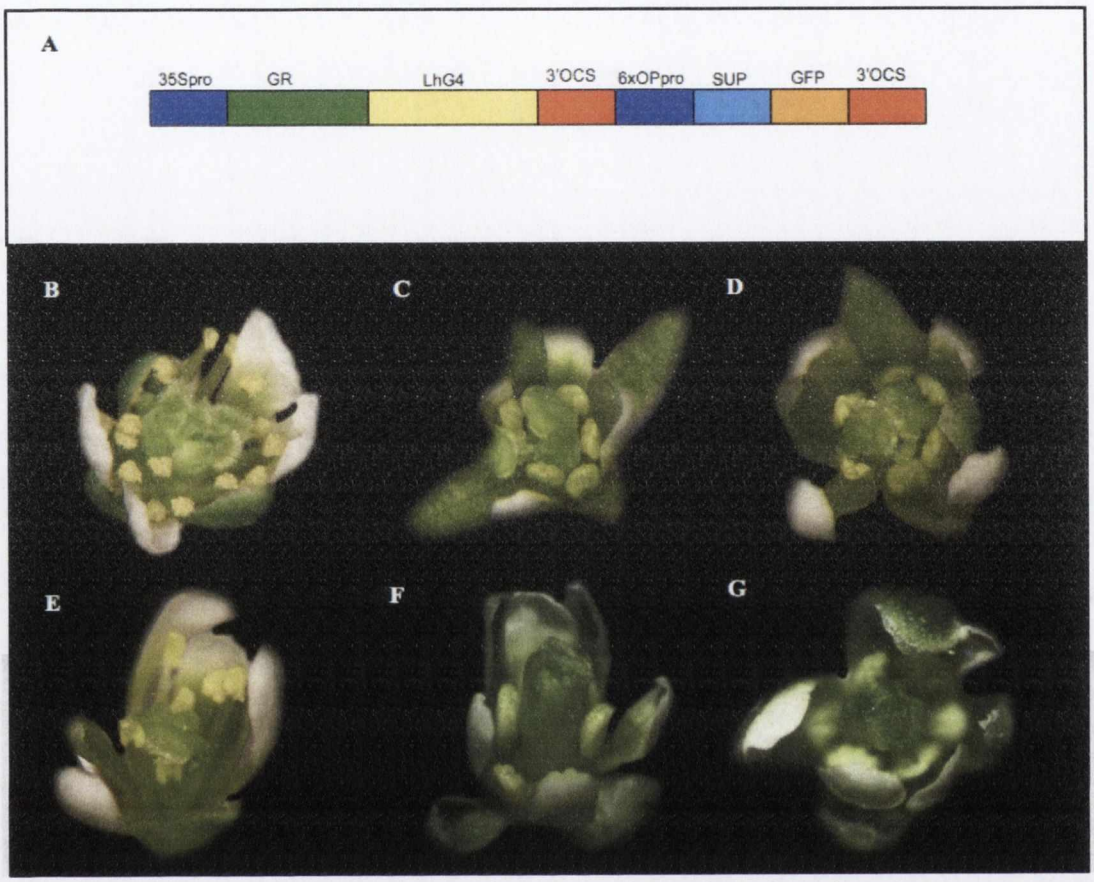

Figure 4.17: Generation of a dexamethasone-inducible *SUP* over-expression line.

(A) Schematic of the T-DNA insertion carrying the $35S_{PRO}$:LhG4-GR/6xOP_{PRO}:SUP-GFP (OP_{PRO}:SUP-GFP) construct. (B) *Sup-5* mutant flower with extra stamens and extra carpel tissue relative to the wild type. (C-G) Flowers of OP_{PRO}:SUP-GFP *sup-5* plants treated with 10 µM dexamethasone. Pictures were taken 2 weeks after the treatment. (C-E) Flowers showing a rescue of the supernumerary stamen number phenotype of sup-5 mutant flowers. (F-G) Flowers showing partial rescue of the carpel defects typically observed in *sup-5* mutant flowers. GFP, Green Fluorescent Protein; 3`OCS, octopine synthase terminator sequence.

4.2.9 Generation of a construct for the overexpression of a dominant negative version of SUP

As previously mentioned in section 4.1, SUP has been shown to act as a transcriptional repressor and this function was demonstrated to be carried out through the activity of its EAR-motif, located in the C-terminus of the protein (Hiratsu et al., 2002). Hiratsu et al. showed that this repressor domain is essential for normal SUP function by overexpressing a version of SUP with its repressor domain deleted (from nucleotide 175 to 204), $35S_{PRO}$:SUPΔRD. Overexpression was shown to result in the development of *sup*-like mutant flowers, as the endogenous SUP protein's function was inhibited by the relative abundance of SUPΔRD protein, reducing its repressive effects (Hiratsu et al., 2002). To this end, the generation of a mutated version of *SUP*, under the control of the $35S_{PRO}$:AlcR/$AlcA_{PRO}$ EtOH-inducible system, was thought to be an ideal control for the normal *SUP* overexpression construct previously generated (Fig. 4.15 A). The initial design and cloning of this construct was carried out by Dr. Raganelli. The coding region, from the 1st amino acid to the 174th, was cloned and the mGFP5 reporter gene was fused downstream of the SUPΔRD sequence. The construct was then cloned into the $35S_{PRO}$:AlcR/$AlcA_{PRO}$ promoter system (Fig. 4.17 A). Wild-type plants were transformed and 23 independent transformants were obtained. One line in the second generation showed the phenotypic response described by Hirastu et al. (2002) 2 weeks after 24 hours of EtOH treatment (Fig. 4.17 B-C). Flowers exhibited *sup*-like mutant phenotypes, such as extra stamens and extra carpel tissue in the fourth whorl. This phenotype indicated that the overexpression construct was functional. Once a homozygous line was obtained for the transgene, through segregation analysis, this was then crossed to the

AP1$_{PRO}$:AP1-GR *ap1-1 cal1-1* floral induction system, which will be used for genome-wide DNA binding studies complementary to the AlcA$_{PRO}$:SUP-GFP line.

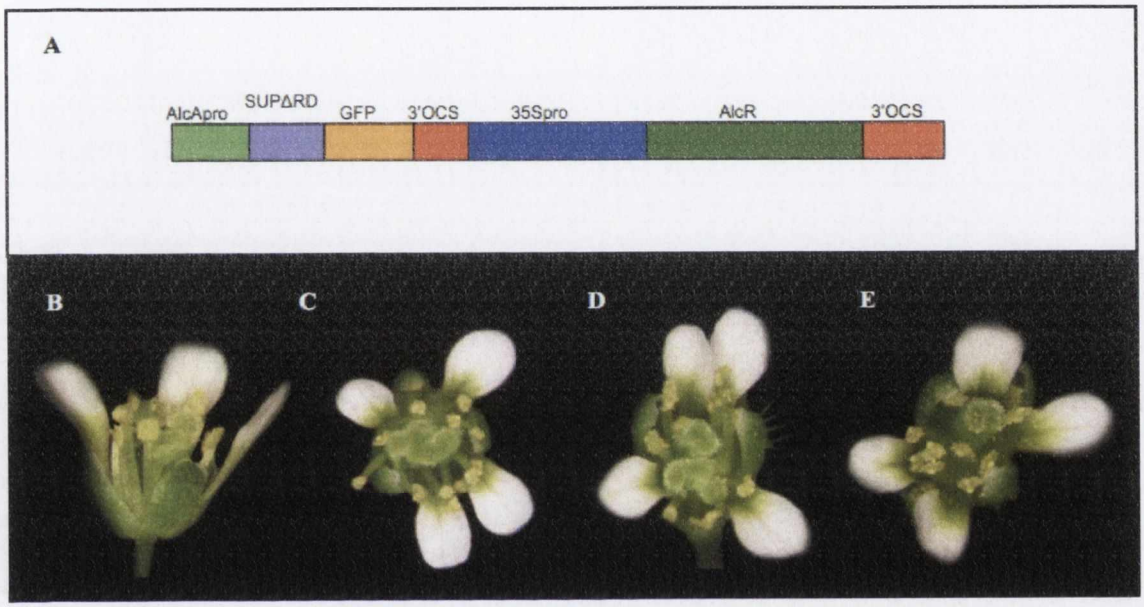

Figure 4.18: Characterization of lines over-expressing SUPΔRD.

(A) Schematic of the T-DNA insertion carrying a 35S$_{PRO}$:AlcR/AlcA$_{PRO}$:SUPΔRD-GFP (AlcA$_{PRO}$:SUPΔRD-GFP) construct. (B-E) Flowers of AlcA$_{PRO}$:SUPΔRD-GFP plants 10 d after a 24 h treatment with EtOH vapour. Flowers exhibit an increase in stamen number compared to the wild type. Flowers also have an increase in carpel tissue and a disrupted gynoecium similar to flowers of *sup-5*. GFP, Green Fluorescent Protein; 3`OCS, octopine synthase terminator sequence.

4.2.10 Exogenous cytokinin treatment causes a partial rescue of the *SUP* mutant phenotype

SUP has been hypothesized to be involved in regulating auxin- and cytokinin-dependent processes in *Arabidopsis* and Tobacco (Nibau et al., 2011). This idea is based on the results of constitutive over-expression of *SUP* (35S$_{PRO}$:SUP), which resulted in phenotypes resembling

those of mutants with defects in cytokinin and auxin responses, including the curling of leaves, increased root growth and loss of apical dominance. Furthermore, overexpression of *SUP* using the 35S promoter was seen to activate the expression of cytokinin and auxin responsive promoters (DR5 and ARR6 respectively), driving GUS expression in seedlings (Nibau et al., 2011). Finally, wild-type *Arabidopsis* were also sprayed with cytokinin solution and this resulted in a dose-dependent decrease in fertility and outgrowths from the replum of carpels. To test if *SUP* was involved in the regulation of cytokinin processes as described, *sup-5* mutant plants were treated with 100 μM 6-Benzylaminopurine (BAP), a synthetic cytokinin (Fig. 4.18 C-D). Roughly 14 d after the initial treatment, *sup-5* flowers began to exhibit wild-type stamen numbers and normal carpel architecture in some of the treated flowers. This also resulted in an increase in seed yield from treated plants. After another week, flowers gradually reverted back to *sup-5* phenotypes likely because these flowers had been initiated after the BAP treatment took place.

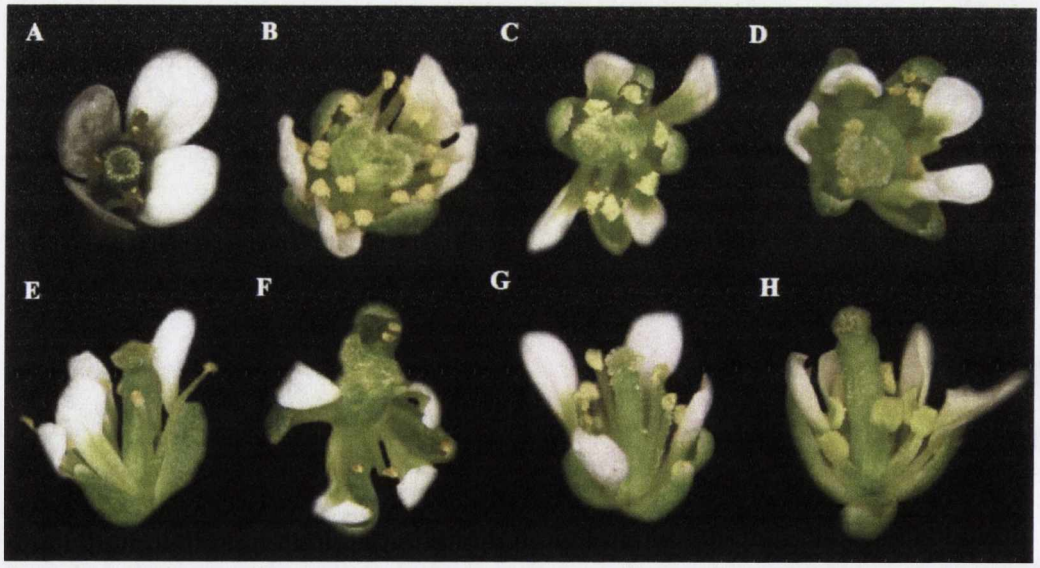

Figure 4.19: Exogenous cytokinin treatment causes a partial rescue of the *sup-5* mutant phenotype.

(A) A wild-type flower. (B) *sup-5* mutant flower. (C-H) Flowers of *sup-5* mutant plants 2 weeks after treatment with 100 μM BAP. Stamen number is rescued in majority of flowers. (G-H) Carpel architecture is restored to near wild-type levels in some flowers.

Figure 4.20: Exogenous cytokinin treatment restores carpel growth in *sup-2* and *sup-3* mutant plants.

(A) An untreated *sup-2* mutant flower with extra stamens and no carpel tissue. (B-D) Flowers of *sup-2* 2 weeks after treatment with 100 μM BAP. Stamen number is unaffected but there is a significant restoration of carpel growth when compared to untreated *sup-2*. (E) An untreated *sup-3* flower with extra stamens and no carpel tissue. (F-H) *Sup-2* flowers 2 weeks after treatment with 100 μM BAP. Stamen number is unaffected or increased relative to untreated *sup*-2, but carpel development is partially restored.

To test if this was the case in other available alleles of *SUP*, *sup-2* and *sup-3* mutant plants were treated with 100 μM BAP. Plants were checked for their floral phenotypes after 2 weeks and were noticeably different to their *sup-5* BAP-treated counterparts. The *sup-2* treated plants (Fig. 4.19 B-D) still had high numbers of stamens similar to untreated *sup-2* mutant

plants. This was also the case for *sup-3* BAP-treated plants. However, there was an increase in carpel tissue in both alleles compared to their them being untreated (Fig. 4.19 B-D; F-H).

In conclusion the partial rescue of the *sup* mutant phenotypes indicates that *SUP* is involved in regulating cytokinin processes in flower development. As the phenotypes were different between the alleles this suggests that cytokinin can stimulate or suppresses cell division in the absence of *SUP*.

4.2.11 Partial rescue of *sup* by overexpression of a known cytokinin biosynthesis gene

The *ISOPENTENYLTRANSFERASES* (*IPT*) genes are known to encode cytokinin synthases, catalysing a rate-limiting step in the biosynthesis of cytokinin (Cheng et al., 2013). Inducible overexpression of *IPT8* from an estradiol-inducible promoter system has been shown to increase endogenous cytokinin levels in *Arabidopsis* (Wang et al., 2015). It was hypothesized that an increase in endogenous cytokinin may result in a rescue of the *sup* mutant phenotype similar to exogenous cytokinin treatments. With the help of an undergraduate student, Aistis Balciunas, *IPT8* was cloned and put under the $35S_{PRO}$:LhG4-GR/6xOP_{PRO} inducible promoter system. A *sup-5* heterozygous population was transformed with this construct and 7 independent transformations were obtained. Mutant lines isolated hetrozygous for *sup-5* and the T-DNA were then obtained through PCR genotyping, and segregation analysis through BASTA selection, respectively. With the help of an undergraduate student, Mr. Cathal Meehan, homozygous lines were isolated plants and treated with 10 μM dexamethasone. Plants were phenotyped 2 weeks after the initial treatment. Some *sup-5* mutant flowers showed a restoration of stamen number to wild-type levels (Fig. 4.20 B-D). Furthermore, a

few flowers also exhibited a wild-type gynoecium (E-F). Due to time constraints these lines have not been fully characterized, but will be in the future.

In conclusion, as originally hypothesized from the results of the initial BAP treatments, the results of the additional experiment strongly suggest that cytokinin has the ability to (partially) restore the *sup* mutant phenotype.

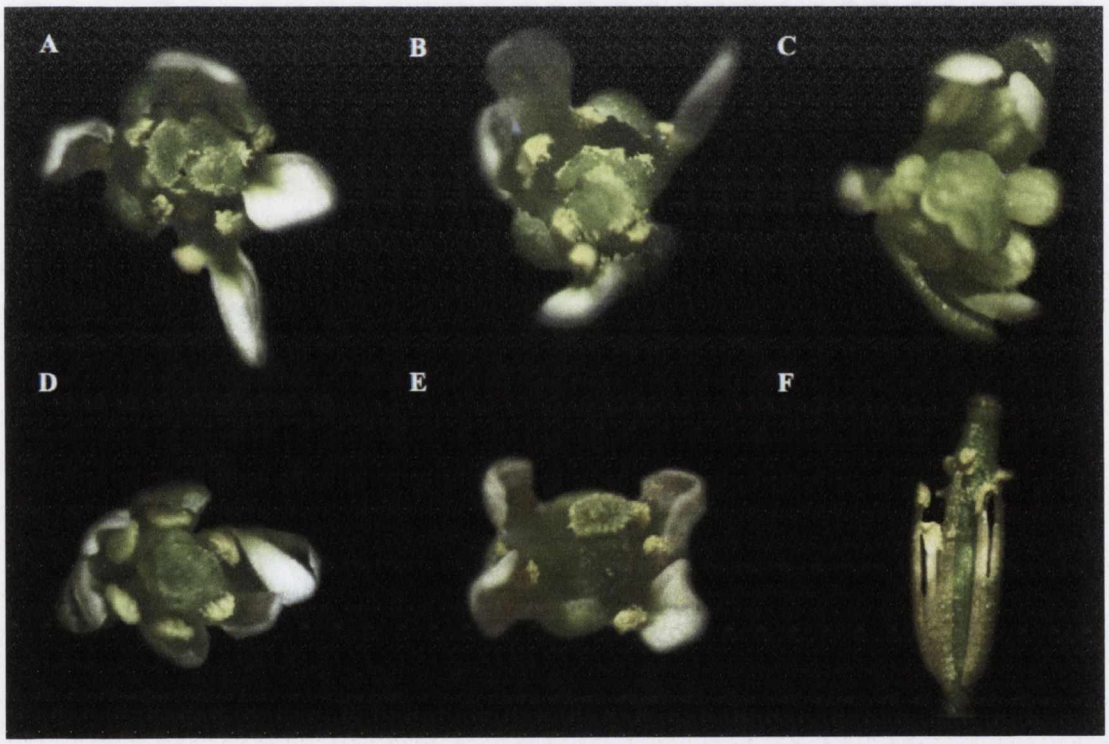

Figure 4.21: Overexpression of *ISOPENTENYLTRANSFERASES8* (*IPT8*) results in a partial rescue of the *sup-5* mutant phenotype.

(A) A *sup-5* mutant flower. (B-F) Flowers of $35S_{PRO}$:LhG4-GR/$6xOP_{PRO}$:IPT8 *sup-5* plants 2 weeks after treatment with 10 μM dexamethasone. Stamen number is restored to near wild-type levels. (E-F) Carpel architecture is restored in some flowers. In (F), petals and sepals were removed to expose the reproductive floral organs.

4.3 Discussion

4.3.1 The role of *SUP* in flower development

It has been over 25 years since the first *sup* mutant allele was identified (Schultz et al., 1991) and since then the exact molecular function of the *SUP* gene has remained unknown. From the analysis of different *sup* mutant alleles its involvement in the regulation of the third and fourth whorl boundary, and the regulation of cell cycle processes, has been hypothesised. However the variability between different *sup* alleles has led to considerable confusion in what processes are regulated by *SUP,* and several different working models for its role in flower development have been proposed over the years (Breuil-Broyer et al., 2016; Gasier et al., 1995 Hiratsu et al., 2002; Sakai et al., 2000; Sakai et al., 1995)

In this study an analysis of the available *sup* mutant alleles was carried out. The *sup-5* allele contains a deletion spanning most of the gene, which should result in a complete loss of function. Flowers of this mutant possess supernumerary stamens, and exhibit an increased proliferation of carpel tissue in the centre of the flower (Fig. 4.1 C-F). The increase in stamen number, carpel tissue, and indeterminacy of the floral meristem, supports the model that *SUP* controls the balance of cell proliferation, and possibly the differentiation of cells, at the boundary between the third and fourth whorl in the floral meristem (Sakai et al., 2000). Conversely, *sup-1* (data not shown), *sup-2*, and *sup-3* have a different floral phenotype to that of *sup-5*. The *sup-1* and *sup-2* alleles have mutations just after the transcriptional start site,

creating premature stop codons, while *sup-3* has a mutation in its DNA binding domain, the zinc-finger domain, presumably rendering it non-functional. The increase in stamen number, with very little carpel tissue forming in the centre of the flower, is a phenotype that all of these alleles have in common (Fig. 2 A-F). The loss of carpel tissue, thought to be a consequence of extra stamen formation in these alleles, is what differentiates these alleles from *sup-5*. These observations led to the hypothesis that *SUP* is a cadastral gene, such that it controls the boundary between the fourth and third whorls. This is supported by the observed expansion of *AP3* expression into the centre of the flower in *sup* mutant flowers (Sakai et al., 2000).

To gain further insight into a full knockdown of *SUP*, and to assess its role at different developmental stages, amiRNAs targeting *SUP* mRNA were designed. To test whether these amiRNAs efficiently knock down *SUP*, constitutive overexpression lines were generated and characterized with regard to their floral phenotypes. Upon selecting a functional SUP-amiRNA, this amiRNA was placed under an inducible promoter system to allow a stage-specific perturbation of *SUP* function. A knockdown of *SUP* was found to be sufficient to cause the development of extra stamens as well as an abnormally shaped gynoecium in flowers two weeks after treatment (Fig. 4.6 A-E). On the other hand, flowers that were at an earlier developmental stage at the time of *SUP* perturbation exhibited an increase in stamen number as well as a complete loss of carpel tissue (Fig. 4.6 F-J). Interestingly, the latter phenotype resembled those of the *sup-1* or *sup-2* mutant alleles and not that of the deletion allele *sup-5*, which is characterized by an increase in carpel tissue in the centre of the flower.

Analysis of this line will provide further insights into which developmental processes *SUP* regulates, at specific stages of flower development. This will be done by perturbing *SUP* activity in the background of the floral induction system and by subsequently analysing differentially expressed genes through transcriptomics approaches.

4.3.2 Genes and processes regulated by SUP

Microarray analysis is a powerful tool to determine differential expression of genes across varying samples at a genome-wide scale. In order to identify the genes and different processes regulated by SUP, the gene expression profiles of homozygous *sup* mutant plants were compared to a pooled wild-type, and heterozygous, population in the floral induction system. By comparing the different transcriptomes of the two populations at different time-points a genome-wide view of the processes and genes acting downstream of SUP was obtained. From these experiments, after statistical analysis across all time points, 366 genes were judged to be down-regulated and 197 were up-regulated. The distribution and directionality of these gene expression changes is overall consistent with the idea of SUP functioning as a repressor and activator (Hiratsu et al., 2002). As more genes than expected were differentially expressed at the 0 day time-point (Fig. 4.8 A) it appears possible that the original microarray dataset is affected by the presence of artifacts. However, with the addition of the 3.5 day time-point and the repeated 5 day time-point (which will be analysed in the near future) hopefully a clearer picture will emerge of which genes are regulated by SUP. Nevertheless, the results obtained thus far gave an interesting selection of candidate genes which have known functions consistent with SUP's hypothesised role in early flower development (Table 4.1). Genes such as *PI*, *VDD,* and the *SHP*s, which are involved in carpel and ovule development respectively,

were found to be differentially expressed. Moreover, genes involved in boundary formation, such as *CRC*, *JLO*, and members of the *LBD* family, were also among the differentially expressed. Consistent with SUP's known involvement in regulating cell cycle processes, genes were also identified that are involved in regulation of the floral meristem, such as *KNU* and *CLV3*. Other groups of genes such as WRKY-domain, WOX-domain, and *ARGONAUTE* genes, were differentially expressed and these genes are known to play roles in the pathogen defence (Eulgem et al., 2000), maintaining stem cell niches (Haecker et al., 2000), and RNA silencing (Garcia-Ruiz et al., 2015) respectively, and these genes will be interesting to investigate further.

Lastly, the results of genetic analyses with mutant alleles for *DRN* and its paralog *DRNL* strongly suggest that the mis-expression of these genes may be in part responsible for the floral phenotypes of *sup* mutants. From the microarray analysis *DRNL* was seen to be up-regulated in both the 3.5 and 5 day time-points, suggesting that SUP may negatively regulate the expression of this gene (Fig. 4.10). As mutants of *DRN* and *DRNL* have minor defects in organogenesis, one hypothesis would be that an up-regulation of these genes may lead to some, or all, of the *sup* mutant phenotype. To test whether this is the case the *drn-1* and *drnl-1* alleles were crossed into the *sup* mutant background. It was found that the resulting double mutants had stamen numbers that were much lower than those in *sup* mutants and similar to those of wild-type plants. Moreover, the carpel tissue defects of *sup* mutants were sometimes partially restored (Fig. 4.11 and 4.12). This partial rescue of the *sup* mutant phenotype suggests that up-regulation of *DRN* and *DRNL* is in part responsible for the *sup* mutant phenotype. With the use of the GFP-tagged SUP expressing lines generated in this thesis,

ChIP experiments will be carried out in the near future to test if the SUP transcription factor directly binds to the promoter regions of either of these genes to regulate their expression.

4.2.3 SUP's role in regulating phytohormone-dependent processes

More recently SUP has been hypothesised to have a role in regulating cytokinin- and auxin-related processes in *Arabidopsis* and Tobacco (Nibau et al., 2011). Constitutive over-expression of *SUP* has been reported to mimic cytokinin-like and auxin-like developmental defects. These phenotypes range from curling of leaves, increased root growth, loss of apical dominance, and severe dwarfism of plants (Hiratsu et al., 2002; Nibau et al., 2011). As cytokinin is known to be a regulator of the rate of cell division by affecting the expression of cell cycle genes (Coenen and Lomax, 1997), a hypothesis would be that *SUP* is controlling processes relating to cytokinin signalling or biosynthesis and hence regulating the cell cycle process in the floral meristem. Other C2H2 zinc-finger domain transcription factors such as *KNU* and *JAGGED* (*JAG*) have proposed functions in stem cell maintenance by controlling cell proliferation (Ohno et al., 2004; Payne et al., 2004). More recently, *JAG* has been shown to control floral organ patterning by repressing genes involved in controlling entry into DNA replication, known as the Kip-related cell cycle inhibitors (Schiessl et al., 2014). Furthermore, confocal imaging has shown that that the floral stem cells in *sup* mutant flowers proliferate for longer than in wild-type allowing for the production of more floral organs (unpublished data and personal communication by Dr. Nathanael Prunet, Meyerowitz group, California Institute of Technology).

The analysis of our microarray data showed differential expression of known genes involved in cytokinin response, known as *ARABIDOPSIS REPSONSE REGULATORs* (*ARR*). Furthermore, qPCRs on RNA used in the repeated 5 day time-point showed down-regulation of *ARR6*, similar to the 3.5 day time-point, and up-regulation of *ARR5* and *CKX6,* a gene known to be involved in the catabolism of cytokinin (Steiner et al., 2012). One interpretation of this data is that cytokinin levels are disrupted in the floral meristem in *sup* mutant flowers. To test whether a reduction in cytokinin levels or response may lead to the phenotypic defects found in *sup* mutant flowers, *sup-5* plants were subjected to exogenous cytokinin treatments. Roughly two weeks after the treatment, flowers began to exhibit a reduction in stamen number as well as a partial restoration of the gynoecium (Fig. 4.18 C-H). Conversely, in *sup-2* and *sup-3* mutant plants, cytokinin resulted in an increase in stamen number and a rescue of carpel tissue in the centre of the flower. Furthermore, activation of a cytokinin biosynthesis gene *IPT8* was able to rescue stamen numbers in developing flowers (Fig. 4.20).

In conclusion, the hypothesis that SUP is involved in regulating cell proliferation through cytokinin synthesis or signalling in the floral meristem has gained more experimental support through this study. However, the phenotypes observed for different *sup* alleles were different, suggesting that cytokinin can stimulate or suppresses cell division in the absence of *SUP* function. It appears possible that this may be due to different cell types having different sensitivities to cytokinin.

Chapter 5 – General discussion and future work

The hypothesis that flowers are in essence modified leaves dates back to the late 18th century (von Goethe, 1790), and has intrigued plant scientists ever since. In recent decades, this hypothesis has been re-addressed, and largely confirmed, through the use of a wide range of experimental approaches. Understanding how leaves evolved into floral organs is a question of growing interest in the plant research community and it is clear that the floral organ identity genes are of central importance for solving this mystery. These genes are known to be essential for flower development, regulating and fine-tuning an array of genes involved in the formation of the various tissues and cell-types found in the different types of floral organs (Sablowski et al., 2010). One question, however, which has remained largely unanswered, is how these master regulators modify the underlying leaf development program, or alternatively, suppress it and then subsequently activate sets of genes with specific roles in floral organ development.

Recent work has opened up a new avenue for exploring this question by using trichome initiation in flowers as a proxy for the leaf developmental program (O'Maoileidigh et al., 2013). In this thesis, I focused mainly on the role that the floral organ identity factor AG plays in suppressing trichome initiation on the reproductive floral organs (see Chapter 3). This work showed that this process is mediated by complex interactions between several genes and pathways, which act either independently from each other or have partially overlapping activities. Specifically, I found that *AG* controls trichome initiation together with other related MADS-box genes. These include the *SHP* genes, which are paralogs of *AG*, and

suppress trichome formation on carpel valves together with AG. Furthermore, I found that *AG* acts with the B function regulators *PI/AP3* to control trichome initiation on the anthers of stamens.

My work further revealed that the SPL transcription factors repress trichome formation in parallel with *AG*. As the plant ages, trichome numbers decrease on each successive leaf and trichome initiation shifts from the adaxial to the abaxial side. This process is thought to be a consequence of increased SPL activity caused by a decrease in the expression of miR156 miRNAs, which target many members of the *SPL* family. Thus, the suppression of trichome formation in flowers seems to involve the coupling of the age-dependent pathway of the plant to flower-specific inputs provided by the floral organ identity genes. Lastly, the regulation of cytokinin response or synthesis was demonstrated here to be essential for suppressing the formation of trichomes on floral organs as well as for the regulation of carpel patterning. In that context, our discovery showing the involvement of *MYB* trichome repressor genes in regulating the latter process was unexpected because these genes have been intensely studied in the past but no link to floral organ development has been made prior to this study. Therefore, the role of these *MYB* genes in carpel patterning will be an exciting area for future research and may reveal how known regulators of leaf development have acquired new functions during the course of evolution to regulate flower-specific processes.

Another avenue for future research should aim at exploring in depth the roles and the regulation of known leaf polarity regulators, such as *KAN1*, during flower development. Work described in this thesis suggests that KAN1 has functions that go beyond its known involvement in polarity specification. Yet, these genes are instrumental for determining and

modifying organ shape in plants, and thus elucidating their functions specifically in flowers should add greatly to our understanding of the evolutionary processes that led to the formation of floral organs from leaves. In this context, it is noteworthy that the floral organ identity factors appear to directly target some of these polarity regulators (O'Maoileidigh et al., 2013; Wuest et al., 2012). Thus, they may act through mechanisms that are similar to those we have identified for the control of regulators of trichome initiation.

Taken together, the combined results from the work described above should provide detailed insights into the evolution of flower development and help explain the emergence of the many different floral organ morphologies found among the large number of extant angiosperm species.

In the second part of this thesis (see Chapter 4), I investigated genes and processes regulated by the C2H2 zinc-finger domain transcription factor SUP. *SUP* was originally identified in the early 1990s with a distinct phenotype of supernumerary stamens, and either an increase or decrease in carpel tissue depending on the allele. The involvement of *SUP* regulating cell division and the boundary between the third and fourth whorl was hypothesised early on. However, how *SUP* molecularly exerts its function remains unknown. The results of inducible perturbation experiments showed that SUP regulates cell division, or differentiation, in the floral meristem. This was evident with the appearance of extra stamens, and depending on the stage of flowers treated, a loss of carpel tissue. However, how it does this is still not known. One promising link is the regulation of cytokinin-dependent processes by SUP, which have been recently described (Nibau et al., 2011). In this thesis, microarray analyses revealed genes involved in the regulation of the floral meristem, such as *CLV3* and *KNU*, to be downstream

of SUP. In addition, cytokinin response genes such as the *ARR*s were found to be differentially regulated, and genes involved in cytokinin catabolism were up-regulated in response to *SUP* perturbation. Results showing that the addition of cytokinin to *sup* mutant plants caused a partial rescue of the organ number defects in the different alleles further strengthen the idea that *SUP* regulates cytokinin-dependent processes (Fig. 4.19). Interestingly, the rescue of *sup-5* seen with *drn-1* and *drnl-1* may be one link between *SUP* and phytohormone regulation (Fig 4.12 and Fig. 4.13). These two genes are known to be involved in auxin response and are regulated in part by it (Chandler et al., 2007). More recently, auxin and cytokinin crosstalk has been identified as an essential factor in pivotal developmental processes (reviewed in: Chandler and Werr, 2015) and it is attractive to speculate that such a crosstalk is also at the core of SUP function. To investigate this further, the lines that were generated as part of this study and that express different versions of (epitope-tagged) SUP can be used. They will hopefully allow us to determine, on a genome-wide scale, the genes and processes that SUP is directly regulating. Furthermore, with the advent of advanced genome-editing approaches such as CRISPR/Cas9 in plants, it will be possible to finally determine what the true loss-of-function phenotype of *SUP* is.

References

Alvarez, J. & Smyth, D.R., 1999. CRABS CLAW and SPATULA, two Arabidopsis genes that control carpel development in parallel with AGAMOUS. *Development*, 126(11), pp.2377–86.

Alves-Ferreira, M. et al., 2007. Global expression profiling applied to the analysis of Arabidopsis stamen development. *Plant physiology*, 145(3), pp.747–62.

Armbruster WS (2014) Floral specialization and angiosperm diversity: phenotypic divergence, fitness trade-offs and realized pollination accuracy. *AoB Plants* 6, plu003.

Barski, A. et al., 2007. High-resolution profiling of histone methylations in the human genome. *Cell*, 129(4), pp.823–37.

Bartel, B. & Bartel, D.P., 2003. MicroRNAs: At the Root of Plant Development? *Plant physiology*, 132(2), pp.709–717.

Bartrina, I. et al., 2011. Cytokinin regulates the activity of reproductive meristems, flower organ size, ovule formation, and thus seed yield in Arabidopsis thaliana. *The Plant cell*, 23(1), pp.69–80.

Bastow, R. et al., 2004. Vernalization requires epigenetic silencing of FLC by histone methylation. *Nature*, 427(6970), pp.164–167

Beilstein, M.A., Al-Shehbaz, I.A. & Kellogg, E.A., 2006. Brassicaceae phylogeny and trichome evolution. *American Journal of Botany*, 93(4), pp.607–619.

Bereterbide, A. et al., 2001. Inhibition of cell proliferation, cell expansion and differentiation by the Arabidopsis SUPERMAN gene in transgenic tobacco plants. *Planta*, 214(1), pp.22–9.

Bernhardt, C. et al., 2005. The bHLH genes GL3 and EGL3 participate in an intercellular regulatory circuit that controls cell patterning in the Arabidopsis root epidermis. *Development*, 132(2), pp.291–8.

Bhaya, D., Davison, M. & Barrangou, R., 2011. CRISPR-Cas systems in bacteria and archaea: versatile small RNAs for adaptive defense and regulation. *Annual review of genetics*, 45, pp.273–97.

Bowman, J.L. & Smyth, D.R., 1999. CRABS CLAW, a gene that regulates carpel and nectary development in Arabidopsis, encodes a novel protein with zinc finger and helix-loop-helix domains. *Development*, 126(11), pp.2387–96

Bowman, J.L. et al., 1992. SUPERMAN, a regulator of floral homeotic genes in Arabidopsis. *Development*, 114(3), pp.599–615.

Bowman, J.L., Smyth, D.R. & Meyerowitz, E.M., 1989. Genes Directing Flower Development in Arabidopsis. *The plant cell online*, 1(1), pp.37–52.

Bowman, J.L., Smyth, D.R. & Meyerowitz, E.M., 1991. Genetic interactions among floral homeotic genes of Arabidopsis. *Development*, 112(1), pp.1–20.

Breuil-Broyer, S. et al., 2016. Analysis of the Arabidopsis superman allelic series and the interactions with other genes demonstrate developmental robustness and joint specification of male-female boundary, flower meristem termination and carpel compartmentalization. *Annals of Botany*, 117(5), pp.905–923.

Busch, M.A. et al., 1999. Activation of a floral homeotic gene in Arabidopsis. *Science*, 285(5427), pp.585–7.

Castillejo, C., Romera-Branchat, M. & Pelaz, S., 2005. A new role of the Arabidopsis SEPALLATA3 gene revealed by its constitutive expression. *The Plant Journal*, 43(4), pp.586–596.

Causier, B. & Davies, B., 2014. Flower Development in the Asterid Lineage. *Methods Mol Biol* 1110, 35–55.

Causier, B., Schwarz-Sommer, Z. & Davies, B., 2010. Floral organ identity: 20 years of ABCs. *Seminars in Cell & Developmental Biology*, 21(1), pp.73–79.

Chae, E. et al., 2008. An Arabidopsis F-box protein acts as a transcriptional co-factor to regulate floral development. *Development*, 135(7), pp.1235–45.

Chandler, J.W. & Werr, W., 2015. Cytokinin-auxin crosstalk in cell type specification. *Trends in plant science*, 20(5), pp.291–300.

Chandler, J.W. et al., 2007. The AP2 transcription factors DORNROSCHEN and DORNROSCHEN-LIKE redundantly control Arabidopsis embryo patterning via interaction with PHAVOLUTA. *Development,* 134(9), pp.1653–62.

Chandler, J.W., 2011. The Hormonal Regulation of Flower Development. *Journal of Plant Growth Regulation*, 30(2), pp.242–254.

Chen, X., 2004. A microRNA as a translational repressor of APETALA2 in Arabidopsis flower development. *Science*, 303(5666), pp.2022–5.

Chen, X., 2005. MicroRNA biogenesis and function in plants. *FEBS letters*, 579(26), pp.5923–31.

Cheng, Y. & Zhao, Y., 2007. A Role for Auxin in Flower Development. *Journal of Integrative Plant Biology*, 49(1), pp.99–104.

Cheng, Z.J. et al., 2013. Pattern of auxin and cytokinin responses for shoot meristem induction results from the regulation of cytokinin biosynthesis by AUXIN RESPONSE FACTOR3. *Plant physiology*, 161(1), pp.240–51.

Clark, S.E., Running, M.P. & Meyerowitz, E.M., 1995. CLAVATA3 is a specific regulator of shoot and floral meristem development affecting the same processes as CLAVATA1. *Development*, 121(7).

Coen, E.S. & Meyerowitz, E.M., 1991. The war of the whorls: genetic interactions controlling flower development. *Nature*, 353(6339), pp.31–37.

Coenen, C. & Lomax, T.L., 1997. Auxin-cytokinin interactions in higher plants: old problems and new tools. *Trends in plant science*, 2(9), pp.351–6.

Colombo, L. et al., 1995. The petunia MADS box gene FBP11 determines ovule identity. *The Plant cell*, 7(11), pp.1859–68.

Colombo, M. et al., 2010. A new role for the SHATTERPROOF genes during Arabidopsis gynoecium development. *Developmental biology*, 337(2), pp.294–302.

Cong, L. et al., 2013. Multiplex genome engineering using CRISPR/Cas systems. *Science*, 339(6121), pp.819–23.

Czechowski, T. et al., 2005. Genome-wide identification and testing of superior reference genes for transcript normalization in Arabidopsis. *Plant physiology*, 139(1), pp.5–17.

Dathan, N. et al., 2002. The Arabidopsis SUPERMAN protein is able to specifically bind DNA through its single Cys2-His2 zinc finger motif. *Nucleic Acids Research*, 30(22), pp.4945–4951.

Di Cristina, M. et al., 1996. The Arabidopsis Athb-10 (GLABRA2) is an HD-Zip protein required for regulation of root hair development. *Plant Journal*, 10(3), pp.393–402.

Ditta, G. et al., 2004. The SEP4 gene of Arabidopsis thaliana functions in floral organ and meristem identity. *Current biology: CB*, 14(21), pp.1935–40.

Esch, J.J. et al., 2003. A contradictory GLABRA3 allele helps define gene interactions controlling trichome development in Arabidopsis. *Development*, 130(24), pp.5885–94.

Favaro, R. et al., 2003. MADS-box protein complexes control carpel and ovule development in Arabidopsis. *The Plant cell*, 15(11), pp.2603–11.

Ferrándiz, C. et al., 2000. Redundant regulation of meristem identity and plant architecture by FRUITFULL, APETALA1 and CAULIFLOWER. *Development*, 127(4), pp.725–34.

Flanagan, C.A., Hu, Y. & Ma, H., 1996. Specific expression of the AGL1 MADS-box gene suggests regulatory functions in Arabidopsis gynoecium and ovule development. *The Plant journal: for cell and molecular biology*, 10(2), pp.343–53.

Fonfara, I. et al., 2016. The CRISPR-associated DNA-cleaving enzyme Cpf1 also processes precursor CRISPR RNA. *Nature*, 532(7600), pp.517–21.

Gaiser, J.C., Robinson-Beers, K. & Gasser, C.S., 1995. The Arabidopsis SUPERMAN Gene Mediates Asymmetric Growth of the Outer Integument of Ovules. *Plant Cell*, 7(3), pp.333–345.

Galway, M.E. et al., 1994. The TTG gene is required to specify epidermal cell fate and cell patterning in the Arabidopsis root. *Developmental biology*, 166(2), pp.740–54.

Gan, L. et al., 2011. Functional characterization of TRICHOMELESS2, a new single-repeat R3 MYB transcription factor in the regulation of trichome patterning in Arabidopsis. *BMC Plant Biology*, 11(1), p.176.

Gan, Y. et al., 2007. Integration of cytokinin and gibberellin signalling by Arabidopsis transcription factors GIS, ZFP8 and GIS2 in the regulation of epidermal cell fate. *Development*, 134, pp.2073–2081.

Garcia-Ruiz, H. et al., 2015. Roles and programming of Arabidopsis ARGONAUTE proteins during Turnip mosaic virus infection. *PLoS pathogens*, 11(3), p.e1004755.

Goethe, J., 1790. *J. W. von Goethe ... Versuch die Metamorphose der Pflanzen zu erklären.*, Gotha by Carl Wilhelm Ettinger. 1790.

Gómez-Mena, C. et al., 2005. Transcriptional program controlled by the floral homeotic gene AGAMOUS during early organogenesis. *Development*, 132(3), pp.429–38.

Gonzalez, D. et al., 2007. The transcription corepressor LEUNIG interacts with the histone deacetylase HDA19 and mediator components MED14 (SWP) and CDK8 (HEN3) to repress transcription. *Molecular and cellular biology*, 27(15), pp.5306–15.

Gramzow, L. et al., 2010. A hitchhiker's guide to the MADS world of plants. *Genome Biology*, 11(6), p.214.

Green, K.A. et al., 2005. CORONA, a member of the class III homeodomain leucine zipper gene family in Arabidopsis, regulates stem cell specification and organogenesis. *The Plant cell*, 17(3), pp.691–704.

Gremski, K., Ditta, G. & Yanofsky, M.F., 2007. The HECATE genes regulate female reproductive tract development in Arabidopsis thaliana. *Development*, 134(20), pp.3593–3601.

Gustafson-Brown, C., Savidge, B. & Yanofsky, M.F., 1994. Regulation of the Arabidopsis floral homeotic gene APETALA1. *Cell*, 76(1), pp.131–143.

Gutierrez-Cortines, M.E. & Davies, B., 2000. Beyond the ABCs: ternary complex formation in the control of floral organ identity. *Trends in Plant Science*, 5(11), pp.471–476.

Haecker, A. et al., 2004. Expression dynamics of WOX genes mark cell fate decisions during early embryonic patterning in Arabidopsis thaliana. *Development*, 131(3):657-68.

Hanley, M.E. et al., 2007. Plant structural traits and their role in anti-herbivore defence. *Perspectives in Plant Ecology, Evolution and Systematics*, 8(4), pp.157–178.

Hawkins, C. & Liu, Z., 2014. A model for an early role of auxin in Arabidopsis gynoecium morphogenesis. *Frontiers in plant science*, 5, p.327.

Heisler, M.G. et al., 2001. SPATULA, a gene that controls development of carpel margin tissues in Arabidopsis, encodes a bHLH protein. *Development*, 128(7), pp.1089–98.

Hirano, H.-Y., Tanaka, W. & Toriba, T., 2014. Grass Flower Development. *Methods Mol Biol 1110, 57–84.*

Hiratsu, K. et al., 2002. The SUPERMAN protein is an active repressor whose carboxy-terminal repression domain is required for the development of normal flowers. *FEBS Letters*, 514(2-3), pp.351–354.

Hiratsu, K. et al., 2004. The petunia ortholog of Arabidopsis SUPERMAN plays a distinct role in floral organ morphogenesis. The Plant cell, 16(4), pp.920-932.

Honma, T. & Goto, K., 2001. Complexes of MADS-box proteins are sufficient to convert leaves into floral organs. *Nature*, 409(6819), pp.525–9.

Huang, T. et al., 2014. Arabidopsis KANADI1 acts as a transcriptional repressor by interacting with a specific cis-element and regulates auxin biosynthesis, transport, and signaling in opposition to HD-ZIPIII factors. *The Plant cell*, 26(1), pp.246–62.

Hyun, Y. et al., 2015. Site-directed mutagenesis in Arabidopsis thaliana using dividing tissue-targeted RGEN of the CRISPR/Cas system to generate heritable null alleles. *Planta*, 241(1), pp.271–84.

Lam, W.K. & Pedigo, L.P., 2001. Effect of trichome density on soybean pod feeding by adult bean leaf beetles (Coleoptera: Chrysomelidae). *Journal of economic entomology*, 94(6), pp.1459–63.

Isernia, C. et al., 2003. NMR structure of the single QALGGH zinc finger domain from the Arabidopsis thaliana SUPERMAN protein. *Chembiochem: A European journal of chemical biology*, 4(2-3), pp.171–80.

Ishida, T. et al., 2008. A genetic regulatory network in the development of trichomes and root hairs. *Annual review of plant biology*, 59, pp.365–86.

Ito T, Sakai H, Meyerowitz EM. 2003. Whorl-specific expression of the SUPERMAN gene of Arabidopsis is mediated by cis elements in the transcribed region. *Current Biology* 13, 1524–1530.

Ito, T. et al., 2004. The homeotic protein AGAMOUS controls microsporogenesis by regulation of SPOROCYTELESS. *Nature*, 430(6997), pp.356–360.

Ito, T. et al., 2007. The homeotic protein AGAMOUS controls late stamen development by regulating a jasmonate biosynthetic gene in Arabidopsis. *The Plant cell*, 19(11), pp.3516–29.

Jack, T., 2004. Molecular and Genetic Mechanisms of Floral Control. *THE PLANT CELL ONLINE*, 16, pp.S1–S17.

Jetha, K., Theissen, G. & Melzer, R., 2014. Arabidopsis SEPALLATA proteins differ in cooperative DNA-binding during the formation of floral quartet-like complexes. *Nucleic Acids Research*, 42(17), pp.10927–10942.

Jinek, M. et al., 2012. A programmable dual-RNA-guided DNA endonuclease in adaptive bacterial immunity. *Science*, 337(6096), pp.816–21.

Jinek, M. et al., 2013. RNA-programmed genome editing in human cells. *eLife*, 2, pp.273–297.

Kaufmann, K. et al., 2009. Target Genes of the MADS Transcription Factor SEPALLATA3: Integration of Developmental and Hormonal Pathways in the Arabidopsis Flower D. Weigel, ed. *PLoS Biology*, 7(4), p.e1000090.

Kaufmann, K. et al., 2010. Chromatin Immunoprecipitation (ChIP) of plant transcription factors followed by sequencing (ChIP-SEQ) or hybridization to whole genome arrays (ChIP-CHIP). *Nature Protocols*, 5(3), pp.457–472.

Kerstetter, R. a et al., 2001. KANADI regulates organ polarity in Arabidopsis. *Nature*, 411(June), pp.706–709.

Kirik, V. et al., 2004. The ENHANCER OF TRY AND CPC1 gene acts redundantly with TRIPTYCHON and CAPRICE in trichome and root hair cell patterning in Arabidopsis. *Developmental biology*, 268(2), pp.506–13.

Komeda, Y., 2004. GENETIC REGULATION OF TIME TO FLOWER IN *ARABIDOPSIS THALIANA*. *Annual Review of Plant Biology*, 55(1), pp.521–535

Kozomara, A. & Griffiths-Jones, S., 2011. miRBase: integrating microRNA annotation and deep-sequencing data. *Nucleic acids research*, 39, pp.D152–7.

Kramer, U., 2015. Planting molecular functions in an ecological context with Arabidopsis thaliana. *eLife*, 2015(4).

Krizek, B.A. & Meyerowitz, E.M., 1996. The Arabidopsis homeotic genes APETALA3 and PISTILLATA are sufficient to provide the B class organ identity function. *Development*, 122(1), pp.11–22.

Krizek, B.A., Lewis, M.W. & Fletcher, J.C., 2006. RABBIT EARS is a second-whorl repressor of AGAMOUS that maintains spatial boundaries in Arabidopsis flowers. *The Plant journal: for cell and molecular biology*, 45(3), pp.369–83.

Krogan, N.T. et al., 2012. APETALA2 negatively regulates multiple floral organ identity genes in Arabidopsis by recruiting the co-repressor TOPLESS and the histone deacetylase HDA19. *Development,* 139(22), pp.4180–90.

Krogan, N.T., Hogan, K. & Long, J.A., 2012. APETALA2 negatively regulates multiple floral organ identity genes in Arabidopsis by recruiting the co-repressor TOPLESS and the histone deacetylase HDA19. *Development*, 139(22).

Laux, T. et al., 1996. The WUSCHEL gene is required for shoot and floral meristem integrity in Arabidopsis. *Development*, 122(1), pp.87–96

Lee, J.-Y. et al., 2005. Activation of CRABS CLAW in the Nectaries and Carpels of Arabidopsis. *The Plant cell*, 17(1), pp.25–36.

Lee, M.M. & Schiefelbein, J., 2002. Cell pattern in the Arabidopsis root epidermis determined by lateral inhibition with feedback. *The Plant cell*, 14(3), pp.611–8.

Lee, T.I., Johnstone, S.E. & Young, R.A., 2006. Chromatin immunoprecipitation and microarray-based analysis of protein location. *Nature protocols*, 1(2), pp.729–48.

Lenhard, M. et al., 2001. Termination of Stem Cell Maintenance in Arabidopsis Floral Meristems by Interactions between WUSCHEL and AGAMOUS. *Cell*, 105(6), pp.805–814.

Levin, J.Z. & Meyerowitz, E.M., 1995. UFO: An Arabidopsis gene involved in both floral meristem and floral organ development. *The Plant cell*, 7(5), pp.529–48.

Li, J.-F. et al., 2013. Multiplex and homologous recombination-mediated genome editing in Arabidopsis and Nicotiana benthamiana using guide RNA and Cas9. *Nature biotechnology*, 31(8), pp.688–91.

Liljegren, S.J. et al., 1999. Interactions among APETALA1, LEAFY, and TERMINAL FLOWER1 Specify Meristem Fate. *The Plant Cell Online*, 11(6), pp.1007–1018.

Liljegren, S.J. et al., 2000. SHATTERPROOF MADS-box genes control seed dispersal in Arabidopsis. *Nature*, 404(6779), pp.766–770.

Lin, Q., Qing, L. & Aoyama, T., 2012. Pathways for epidermal cell differentiation via the homeobox gene GLABRA2: update on the roles of the classic regulator. *Journal of integrative plant biology*, 54(10), pp.729–37.

Lohmann, J.U. & Weigel, D., 2002. Building beauty: the genetic control of floral patterning. *Developmental cell*, 2(2), pp.135–42.

Lohmann, J.U. et al., 2001. A Molecular Link between Stem Cell Regulation and Floral Patterning in Arabidopsis. *Cell*, 105(6), pp.793–803.

Ma, H., Yanofsky, M.F. & Meyerowitz, E.M., 1991. AGL1-AGL6, an Arabidopsis gene family with similarity to floral homeotic and transcription factor genes. *Genes & development*, 5(3), pp.484–95.

Maes, L., Inzé, D. & Goossens, A., 2008. Functional specialization of the TRANSPARENT TESTA GLABRA1 network allows differential hormonal control of laminal and marginal trichome initiation in Arabidopsis rosette leaves. *Plant physiology*, 148(3), pp.1453–64.

Mali, P. et al., 2013. RNA-guided human genome engineering via Cas9. *Science (New York, N.Y.)*, 339(6121), pp.823–6.

Mallory, A.C., Elmayan, T. & Vaucheret, H., 2008. MicroRNA maturation and action—the expanding roles of ARGONAUTEs. *Current Opinion in Plant Biology*, 11(5), pp.560–566.

Mandel, A. et al., 1992. Molecular characterization of the Arabidopsis floral homeotic gene APETALA1. *Nature*, 360(6401), pp.273–277.

Mantegazza, O. et al., 2014. Analysis of the arabidopsis REM gene family predicts functions during flower development. *Annals of botany*, 114(7), pp.1507–15.

Matias-Hernandez, L. et al., 2010. VERDANDI is a direct target of the MADS domain ovule identity complex and affects embryo sac differentiation in Arabidopsis. *The Plant cell*, 22(6), pp.1702–15.

Matías-Hernández, L. et al., 2016. TEMPRANILLO Reveals the Mesophyll as Crucial for Epidermal Trichome Formation. *Plant physiology*, 170(3), pp.1624–39.

Mayer, K.F.. et al., 1998. Role of WUSCHEL in Regulating Stem Cell Fate in the Arabidopsis Shoot Meristem. *Cell*, 95(6), pp.805–815.

McBride, K.E. & Summerfelt, K.R., 1990. Improved binary vectors for Agrobacterium-mediated plant transformation. *Plant Molecular Biology*, 14(2), pp.269–276.

Mendes, M.A. et al., 2013. MADS domain transcription factors mediate short-range DNA looping that is essential for target gene expression in Arabidopsis. *The Plant cell*, 25(7), pp.2560–72.

Meyerowitz, E.M. & Pruitt, R.E., 1985. Arabidopsis thaliana and Plant Molecular Genetics. *Science*, 229(4719), pp.1214–8.

Meyerowitz, E.M., Smyth, D.R. & Bowman, J.L., 1989. Abnormal flowers and pattern formation in floral. *Development*, 106(2), pp.209–217.

Mi, S. et al., 2008. Sorting of Small RNAs into Arabidopsis Argonaute Complexes Is Directed by the 5′ Terminal Nucleotide. *Cell*, 133(1), pp.116–127.

Mizzotti, C. et al., 2014. SEEDSTICK is a Master Regulator of Development and Metabolism in the Arabidopsis Seed Coat R. G. Franks, ed. *PLoS Genetics*, 10(12), p.e1004856

Nag, A., Yang, Y. & Jack, T., 2007. DORNRÖSCHEN-LIKE, an AP2 gene, is necessary for stamen emergence in Arabidopsis. *Plant Molecular Biology*, 65(3), pp.219–232.

Nekrasov, V. et al., 2013. Targeted mutagenesis in the model plant Nicotiana benthamiana using Cas9 RNA-guided endonuclease. *Nature biotechnology*, 31(8), pp.691–3.

Nibau, C. et al., 2011. Arabidopsis and Tobacco SUPERMAN regulate hormone signalling and mediate cell proliferation and differentiation. *Journal of Experimental Botany*, 62(3), pp.949–961.

O'Maoiléidigh, D.S. & Wellmer, F., 2014. A floral induction system for the study of early Arabidopsis flower development. *Methods in molecular biology (Clifton, N.J.)*, 1110, pp.307–14.

Ó'Maoiléidigh, D.S. et al., 2013. Control of reproductive floral organ identity specification in Arabidopsis by the C function regulator AGAMOUS. *The Plant cell*, 25(7), pp.2482–503.

Ó'Maoiléidigh, D.S. et al., 2015. Gene network analysis of *Arabidopsis thaliana* flower development through dynamic gene perturbations. *The Plant Journal*, 83(2), pp.344–358.

Ohno, C.K. et al., 2004. The Arabidopsis JAGGED gene encodes a zinc finger protein that promotes leaf tissue development. *Development*, 131(5), pp.1111–22.

Ohno, C.K. et al., 2004. The Arabidopsis JAGGED gene encodes a zinc finger protein that promotes leaf tissue development. *Development*, 131(5), pp.1111–1122.

Olsson, M.E. et al., 2009. Localization of enzymes of artemisinin biosynthesis to the apical cells of glandular secretory trichomes of Artemisia annua L. *Phytochemistry*, 70(9), pp.1123–8.

Oppenheimer, D.G. et al., 1991. A myb gene required for leaf trichome differentiation in Arabidopsis is expressed in stipules. *Cell*, 67(3), pp.483–493.

Ossowski, S., Schwab, R. & Weigel, D., 2008. Gene silencing in plants using artificial microRNAs and other small RNAs. *The Plant Journal*, 53(4), pp.674–690.

Pajoro, A. et al., 2014. The (r)evolution of gene regulatory networks controlling Arabidopsis plant reproduction: a two-decade history. *Journal of experimental botany*, 65(17), pp.4731–45.

Parcy, F. et al., 1998. A genetic framework for floral patterning. *Nature*, 395(6702), pp.561–6.

Parenicova, L. et al., 2003. Molecular and Phylogenetic Analyses of the Complete MADS-Box Transcription Factor Family in Arabidopsis: New Openings to the MADS World. *THE PLANT CELL ONLINE*, 15(7), pp.1538–1551.

Park, P.J., 2009. ChIP-seq: advantages and challenges of a maturing technology. *Nature reviews. Genetics*, 10(10), pp.669–80.

Pattanaik, S. et al., 2014. An overview of the gene regulatory network controlling trichome development in the model plant, Arabidopsis. *Frontiers in plant science*, 5, p.259.

Payne, C.T., Zhang, F. & Lloyd, A.M., 2000. GL3 encodes a bHLH protein that regulates trichome development in Arabidopsis through interaction with GL1 and TTG1. *Genetics*, 156(3), pp.1349–62.

Payne, T., Johnson, S.D. & Koltunow, A.M., 2004. KNUCKLES (KNU) encodes a C2H2 zinc-finger protein that regulates development of basal pattern elements of the Arabidopsis gynoecium. *Development*, 131(15).

Pelaz, S. et al., 2001. Conversion of leaves into petals in Arabidopsis. *Current Biology* 11, 182-4.

Perazza, Vachon & Herzog, 1998. Gibberellins promote trichome formation by Up-regulating GLABROUS1 in Arabidopsis. *Plant physiology*, 117(2), pp.375–83.

Pinyopich, A. et al., 2003. Assessing the redundancy of MADS-box genes during carpel and ovule development. *Nature*, 424(6944), pp.85–88.

Prunet, N. & Jack, T.P., 2014. Flower development in Arabidopsis: there is more to it than learning your ABCs. *Methods in molecular biology*, 1110, pp.3–33.

Prunet, N. & Meyerowitz, E.M., 2016. Genetics and plant development. *Comptes Rendus Biologies*, 339, pp.240–246.

Prunet, N. et al., 2008. REBELOTE, SQUINT, and ULTRAPETALA1 function redundantly in the temporal regulation of floral meristem termination in Arabidopsis thaliana. *The Plant cell*, 20(4), pp.901–19.

Qi, L.S. et al., 2013. Repurposing CRISPR as an RNA-Guided Platform for Sequence-Specific Control of Gene Expression. *Cell*, 152(5), pp.1173–1183.

Qi, T. et al., 2011. The Jasmonate-ZIM-domain proteins interact with the WD-Repeat/bHLH/MYB complexes to regulate Jasmonate-mediated anthocyanin accumulation and trichome initiation in Arabidopsis thaliana. *The Plant cell*, 23(5), pp.1795–814.

Riechmann, J.L. & Wellmer, F. eds., 2014. *Flower Development*, New York, NY: Springer New York.

Riechmann, J.L., Krizek, B.A. & Meyerowitz, E.M., 1996. Dimerization specificity of Arabidopsis MADS domain homeotic proteins APETALA1, APETALA3, PISTILLATA, and AGAMOUS. *Proceedings of the National Academy of Sciences of the United States of America*, 93(10), pp.4793–8.

Ripoll, J. et al., 2015. microRNA regulation of fruit growth. *Nature Plants*, 1(4), p.15036.

Roslan, H.A. et al., 2001. Characterization of the ethanol-inducible alc gene-expression system in Arabidopsis thaliana. *The Plant journal: for cell and molecular biology*, 28(2), pp.225–35.

Sablowski, R., 2010. Genes and functions controlled by floral organ identity genes. *Seminars in Cell and Developmental Biology*, 21(1), pp.94–99.

Sakai, H. et al., 2000. Regulation of SUP expression identifies multiple regulators involved in Arabidopsis floral meristem development. *The Plant cell*, 12(9), pp.1607–18.

Sakai, H., Medrano, L.J. & Meyerowitz, E.M., 1995. Role of SUPERMAN in maintaining Arabidopsis floral whorl boundaries. *Nature*, 378(6553), pp.199–203.

Samach, A. et al., 1999. The UNUSUAL FLORAL ORGANS gene of Arabidopsis thaliana is an F-box protein required for normal patterning and growth in the floral meristem. *The Plant journal: for cell and molecular biology*, 20(4), pp.433–45.

Savidge, B., Rounsley, S.D. & Yanofsky, M.F., 1995. Temporal relationship between the transcription of two Arabidopsis MADS box genes and the floral organ identity genes. *The Plant cell*, 7(6), pp.721–33.

Schellmann, S. et al., 2002. TRIPTYCHON and CAPRICE mediate lateral inhibition during trichome and root hair patterning in Arabidopsis. *The EMBO Journal*, 21(19), pp.5036–5046.

Schiefthaler, U. et al., 1999. Molecular analysis of NOZZLE, a gene involved in pattern formation and early sporogenesis during sex organ development in Arabidopsis thaliana. *PNAS*, 96(20), pp.11664–9.

Schiessl, K., Muiño, J.M. & Sablowski, R., 2014. Arabidopsis JAGGED links floral organ patterning to tissue growth by repressing Kip-related cell cycle inhibitors. *PNAS*, 111(7), pp.2830–5.

Schilmiller, A.L., Last, R.L. & Pichersky, E., 2008. Harnessing plant trichome biochemistry for the production of useful compounds. *The Plant Journal*, 54(4), pp.702–711.

Schnittger, A. et al., 1999. Generation of a spacing pattern: the role of triptychon in trichome patterning in Arabidopsis. *The Plant cell*, 11(6), pp.1105–16.

Schultz, E.A., Pickett, F.B. & Haughn, G.W., 1991. The FLO10 Gene Product Regulates the Expression Domain of Homeotic Genes AP3 and PI in Arabidopsis Flowers. *The Plant cell*, 3(11), pp.1221–1237.

Schwab, R. et al., 2006. Highly specific gene silencing by artificial microRNAs in Arabidopsis. *The Plant cell*, 18(5), pp.1121–33.

Schwarz, S. et al., 2008. The microRNA regulated SBP-box genes SPL9 and SPL15 control shoot maturation in Arabidopsis. *Plant Molecular Biology*, 67(1-2), pp.183–195.

Searle, I. et al., 2006. The transcription factor FLC confers a flowering response to vernalization by repressing meristem competence and systemic signaling in Arabidopsis. *Genes & Development*, 20(7), pp.898–912.

Seeliger, I. et al., 2016. The AP2-type transcription factors DORNRÖSCHEN and DORNRÖSCHEN-LIKE promote G1/S transition. *Molecular Genetics and Genomics*, 291(5), pp.1835–1849.

Shan, Q. et al., 2013. Targeted genome modification of crop plants using a CRISPR-Cas system. *Nature biotechnology*, 31(8), pp.686–8.

Shuai, B., Reynaga-Peña, C.G. & Springer, P.S., 2002. The lateral organ boundaries gene defines a novel, plant-specific gene family. *Plant physiology*, 129(2), pp.747–61.

Sieber, P. et al., 2004. Organ polarity in Arabidopsis. NOZZLE physically interacts with members of the YABBY family. *Plant physiology*, 135(4), pp.2172–85.

Simonini, S. et al., 2012. Basic pentacysteine proteins mediate MADS domain complex binding to the DNA for tissue-specific expression of target genes in Arabidopsis. *The Plant cell*, 24(10), pp.4163–72.

Smaczniak, C. et al., 2012. Characterization of MADS-domain transcription factor complexes in Arabidopsis flower development. *PNAS*, 109(5), pp.1560–1565.

Smyth, D.R., Bowman, J.L. & Meyerowitz, E.M., 1990. Early flower development in Arabidopsis. *The Plant cell*, 2(8), pp.755–67.

Soltis PS & Soltis DE (2014) Flower diversity and angiosperm diversification. *Methods*
Sridhar VV, Surendrarao A, Gonzalez D, Conlan RS & Liu Z (2004) Transcriptional repression of target genes by LEUNIG and SEUSS, two interacting regulatory proteins for Arabidopsis flower development. *PNAS* USA 101, 11494–11499.

Stahle, M.I. et al., 2009. YABBYs and the transcriptional corepressors LEUNIG and LEUNIG_HOMOLOG maintain leaf polarity and meristem activity in Arabidopsis. *The Plant cell*, 21(10), pp.3105–18.

Steiner, E. et al., 2012. The Arabidopsis O-linked N-acetylglucosamine transferase SPINDLY interacts with class I TCPs to facilitate cytokinin responses in leaves and flowers. *The Plant cell*, 24(1), pp.96–108.

Sternberg, S.H. et al., 2014. DNA interrogation by the CRISPR RNA-guided endonuclease Cas9. *Nature*, 507(7490), pp.62–7.

Stewart, D., Graciet, E. & Wellmer, F., 2016. Molecular and regulatory mechanisms controlling floral organ development. *The FEBS Journal*, 283(10), pp.1823–1830.

Sun, B. & Ito, T., 2010. Floral stem cells: from dynamic balance towards termination. *Biochemical Society transactions*, 38(2), pp.613–6.

Sun, B. et al., 2010. Floral stem cells: from dynamic balance towards termination. *Biochemical Society transactions*, 38(2), pp.613–6.

Szymanski, D.B. et al., 1998. Control of GL2 expression in Arabidopsis leaves and trichomes. *Development*, 125(7), pp.1161–71.

Szymanski, D.B., Lloyd, A.M. & Marks, M.D., 2000. Progress in the molecular genetic analysis of trichome initiation and morphogenesis in Arabidopsis. *Trends in plant science*, 5(5), pp.214–9.

Telfer, A., Bollman, K.M. & Poethig, R.S., 1997. Phase change and the regulation of trichome distribution in Arabidopsis thaliana. *Development*, 124(3), pp.645–54.

The Arabidopsis Genome Initiative, 2000. Analysis of the genome sequence of the flowering plant Arabidopsis thaliana. *Nature*, 408(6814), pp.796–815.

Theißen, G., 2001. Development of floral organ identity: stories from the MADS house. *Current Opinion in Plant Biology*, 4(1), pp.75–85.

Traw, M.B. & Bergelson, J., 2003. Interactive Effects of Jasmonic Acid, Salicylic Acid, and Gibberellin on Induction of Trichomes in Arabidopsis. *Plant physiology*, 133(3), pp.1367–1375.

Tzeng, T.Y. et al., 2009. Overexpression of the lily p70(s6k) gene in Arabidopsis affects elongation of flower organs and indicates TOR-dependent regulation of AP3, PI and SUP translation. *Plant & cell physiology*, 50(9), pp.1695–1709.

Urbanus, S.L. et al., 2010. Intercellular transport of epidermis-expressed MADS domain transcription factors and their effect on plant morphology and floral transition. *The Plant journal: for cell and molecular biology*, 63(1), pp.60–72.

Valouev, A. et al., 2008. Genome-wide analysis of transcription factor binding sites based on ChIP-Seq data. *Nature methods*, 5(9), pp.829–34.

Villanueva, J.M. et al., 1999. INNER NO OUTER regulates abaxial- adaxial patterning in Arabidopsis ovules. *Genes & development*, 13(23), pp.3160–9.

Wada, T. et al., 1997. Epidermal cell differentiation in Arabidopsis determined by a Myb homolog, CPC. *Science*, 277(5329), pp.1113–6.

Wada, T. et al., 2002. Role of a positive regulator of root hair development, CAPRICE, in Arabidopsis root epidermal cell differentiation. *Development*, 129(23), pp.5409–19.

Wagner, D., Sablowski, R.W. & Meyerowitz, E.M., 1999. Transcriptional activation of APETALA1 by LEAFY. *Science*, 285(5427), pp.582–4.

Wang, J.-W. et al., 2008. Dual Effects of miR156-Targeted SPL Genes and CYP78A5/KLUH on Plastochron Length and Organ Size in Arabidopsis thaliana. *The plant cell online*, 20(5), pp.1231–1243.

Wang, S. et al., 2007. TRICHOMELESS1 regulates trichome patterning by suppressing GLABRA1 in Arabidopsis. *Development*, 134(21), pp.3873–82.

Wang, Y. et al., 2015. Endogenous Cytokinin Overproduction Modulates ROS Homeostasis and Decreases Salt Stress Resistance in Arabidopsis Thaliana. *Frontiers in plant science*, 6 (November), p.1004

War, A.R. et al., 2012. Mechanisms of plant defense against insect herbivores. *Plant signaling & behavior*, 7(10), pp.1306–20.

Weigel, D. & Nilsson, O., 1995. A developmental switch sufficient for flower initiation in diverse plants. *Nature*, 377(6549), pp.495–500.

Weigel, D. et al., 1992. LEAFY controls floral meristem identity in Arabidopsis. *Cell*, 69(5), pp.843–59.

Wellmer, F. & Riechmann, J.L., 2005. Gene network analysis in plant development by genomic technologies. *The International Journal of Developmental Biology*, 49(5-6), pp.745–759.

Wellmer, F. & Riechmann, J.L., 2010. Gene networks controlling the initiation of flower development. *Trends in Genetics*, 26(12), pp.519–527.

Wellmer, F. et al., 2004. Genome-wide analysis of spatial gene expression in Arabidopsis flowers. *The Plant cell*, 16(5), pp.1314–26.

Wellmer, F. et al., 2006. Genome-Wide Analysis of Gene Expression during Early Arabidopsis Flower Development. *PLoS Genetics*, 2(7), p.e117.

Werner, T. et al., 2003. Cytokinin-deficient transgenic Arabidopsis plants show multiple developmental alterations indicating opposite functions of cytokinins in the regulation of shoot and root meristem activity. *The Plant cell*, 15(11), pp.2532–50.

Wilkinson, M.D. & Haughn, G.W., 1995. UNUSUAL FLORAL ORGANS Controls Meristem Identity and Organ Primordia Fate in Arabidopsis. *The Plant cell*, 7(9), pp.1485–1499.

Wuest, S.E. et al., 2012. Molecular basis for the specification of floral organs by APETALA3 and PISTILLATA. *PNAS*, 109(33), pp.13452–7.

Xue, X.-Y. et al., 2014. Interaction between Two Timing MicroRNAs Controls Trichome Distribution in Arabidopsis X. Chen, ed. *PLoS Genetics*, 10(4), p.e1004266.

Yu, N. et al., 2010. Temporal Control of Trichome Distribution by MicroRNA156-Targeted SPL Genes in Arabidopsis thaliana. *The plant cell online*, 22(7), pp.2322–2335.

Zhao, M. et al., 2008. The TTG1-bHLH-MYB complex controls trichome cell fate and patterning through direct targeting of regulatory loci. *Development*, 135(11), pp.1991–9.

Zhou, Z. et al., 2013. Zinc Finger Protein 6 (ZFP6) regulates trichome initiation by integrating gibberellin and cytokinin signaling in *Arabidopsis thaliana*. *New Phytologist*, 198(3), pp.699–708.

Appendix

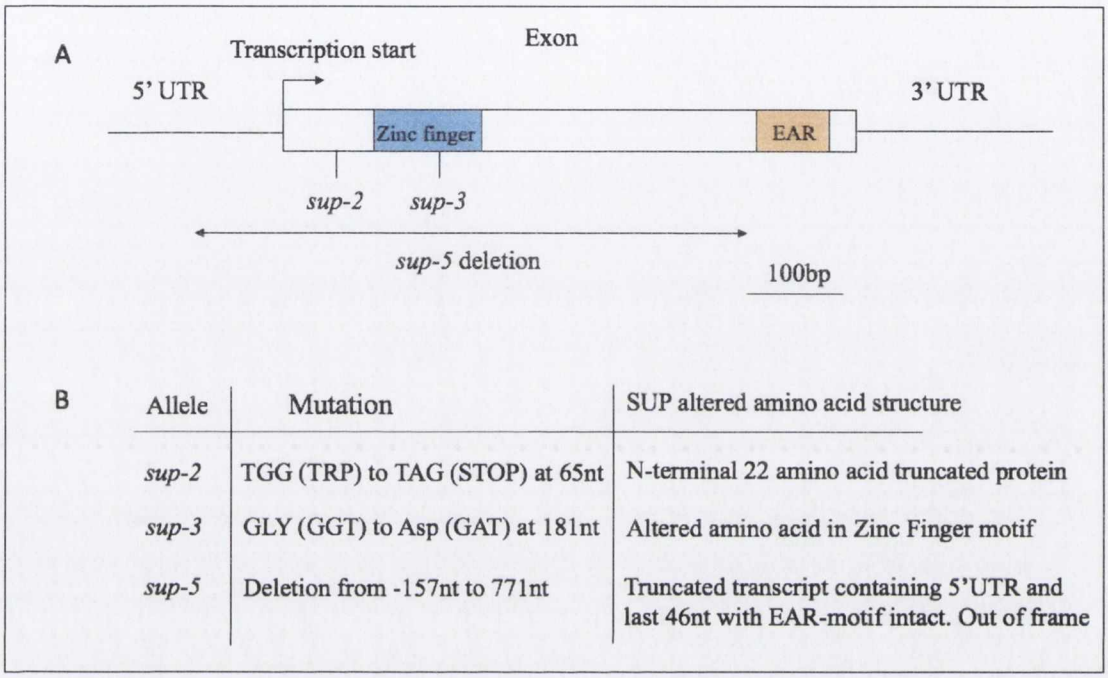

B

Allele	Mutation	SUP altered amino acid structure
sup-2	TGG (TRP) to TAG (STOP) at 65nt	N-terminal 22 amino acid truncated protein
sup-3	GLY (GGT) to Asp (GAT) at 181nt	Altered amino acid in Zinc Finger motif
sup-5	Deletion from -157nt to 771nt	Truncated transcript containing 5'UTR and last 46nt with EAR-motif intact. Out of frame

Supplementary figure 1.1: Schematic of the *SUP* locus depicting mutation sites for the alleles used in this study and their putative protein products.

(A) Diagram of the *SUP* DNA locus with associated mutation locations corresponding to each *sup* allele used in this study. The *sup-2* mutation occurs 65nt after the transcriptional start site and creates a premature stop codon. The *sup-3* mutation is in the the zinc finger DNA binding domain. The mutation in *sup-5* is a deletion spanning from the 5' untranslated region (5' UTR) to just before the EAR motif. (B) Chart showing associated mutations for each *sup* allele and their putative proteins structures.

Supplementary Table 1: List of primers used in this study

pSUP 5'	TGG CGT GGA CGT AAG GTA CCA TAA TG	Cloning
pSUP 5'	TTGGTACCTTGGCAGCGAAACCCAAACGGAGTTCTAG	Cloning
SUP 3'UTR	GGG TTA ACT TAG ATG GTA ATA ACT TTA TCC ATA AAG GAT TCG	Cloning
SUP 3'UTR	CCG GAT CCA GGA ATT CAA TTT GAA GTA GCT AGC AAA TT	Cloning
SUP-5 F in del	AA CAG CAT AGA GTT GAG GAA CAG C	Cloning
SUP-5 R	ACCCAAACGGAGTTCTAGATCC	Cloning
pSUP 5' 1	CCC GAA AGA GAG ATA GTA TGT TTT AGG	Cloning
pSUP 5' 2	CCC GAT TAG TGA CAA CTC ATT TAC TAT GTT	Cloning
psup 5' 3	CCC GTA GCA TAT TTA GAA GAT AAA ACA AGA C	Cloning
psup 5' 4	AAG GAG AAA GGA ACA TCC ACT TTT C	Genotyping
SALK LB	CTTTGACGTTGGAGTCCAC	Cloning
sup-amir1a	gaTCGCCAATAGGATCATGATTAtctctcttttgtattcc	Cloning
sup-amir1b	gaTAATCATGATCCTATTGGCGAtcaaagagaatcaatga	Cloning
sup-amir1c	gaTACTCATGATCCTTTTGGCGTtcacaggtcgtgatatg	Cloning
sup-amir1d	gaACGCCAAAAGGATCATGAGTAtctacatatatattcct	Cloning
sup-amir2a	gaCCGCAAAAGGGAATTCAGATAtctctcttttgtattcc	Cloning
sup-amir2b	gaTATCTGAATTCCCTTTTGCGGtcaaagagaatcaatga	Cloning
sup-amir2c	gaTACCTGAATTCCCATTTGCGGtcacaggtcgtgatatg	Cloning
sup-amir2d	gaCCGCAAATGGGAATTCAGGTAtctacatatatattcct	Cloning
sup-amir3a	gaCCGTGCACGAACTTCACCATAtctctcttttgtattcc	Cloning
sup-amir3b	gaTATGGTGAAGTTCGTGCACGGtcaaagagaatcaatga	Cloning
sup-amir3c	gaTACGGTGAAGTTCCTGCACGGtcacaggtcgtgatatg	Cloning
sup-amir3d	gaCCGTGCAGGAACTTCACCGTAtctacatatatattcct	Cloning
pBJ36	aaGCGGATAACAATTTCACACAGGAA	Seq
6xOP	TGCATATGTCGAGCTCAAGAAATC	Seq
SUP up	AAC TCT ATG CTG TTT GAT CTC TCC	Seq
3'OCS	GGTAAGGATCTGAGCTACACATGCTC	Seq
GL2 F	GATGAGGATCGCACTGTGGAG	Genotyping
GL2 R	TGATCGTCGGAGCATGAAGC	Genotyping
35s:LhG4-GR R	AGGTCGATATGGGAGAGCCT	seq
gl2-1F	CCGATGATCTCCACCTCGAA	genotyping
gl2-1R	TTTCCATTGTCCCTGCGC	genotyping
gl2-1F Mut	GAGGCCCGAAAACTCCAAA	genotyping

SUP_CDS_R	GCC ATA GAA GCT GTT CCT CA	seq
DRNL_F	ATGGAAGAAGCAATCATGAGA	genotyping
DRNL_intR	AACATTCCACCATTTCCGTTC	genotyping
DRNF	ATGGAAAAAGCCTTGAGAAAC	genotyping
DRNR	CTATCCCCACGATCTTCGGCA	genotyping
DRNLCAPS1	TACCGCAAAAGCTGCCTC	genotyping
DRNLCAPS2	AGCGGCGCAGTCATATGCGCAGTCT	genotyping
Spm8	GTTTTGGCCGACACTCCTTAC	genotyping
ITIR3	CTTGCCTTTTTTCTTGTAGTG	genotyping
ipt8 F	CCA CGC GTA TGC AAA ATC TTA CGT	genotyping
ipt8 R	TTC TCG AGA TAA CTC ACA CTT TGT CT	genotyping
PCR-GUS F	AAG GAT CCG GGC CCA TGG	genotyping
PCR-GUS R	TTG GAT CCG AGA GTT GTT GAT TCA TTG TT	genotyping
kan2-1_Fmism	CAACAACAACATCATCATCCT	genotyping
kan2-1_R	AAACCGACTGAAGAATCTCT	genotyping
Crispr_F_SpeI	ATATACTAGTCTAGAGAATGATTAGGCATCGAACCT	cloning
Crispr_R_SpeI	ATGCAGGAAGACAACTAGTCAA	cloning
SUPrgenR1	AAAGAAAGAGCTTGCACATAGTTTTAGAGCTAGAAATAGCAA	cloning
SUPrgenF1	TATGTGCAAGCTCTTTCTTTTCTACAATCACTACTTCGACTCTAGCT	cloning
SUPrgenF2	AGAACTTCACCATGGAGCTAtggGTTTTAGAGCTAGAAATAGCAA	cloning
SUPrgenR2	TAGCTCCATGGTGAAGTTCTTCTACAATCACTACTTCGACTCTAGCT	cloning
crisgenoF	CTCTCTCTCTCTAAGAGACAGACA	cloning
crisgenoR	CATCTAACGCAAGCTTATAGCTTAT	cloning
LBb1.3-salkNEW	ATTTTGCCGATTTCGGAAC	genotyping
Spm1	CTTATTTCAGTAAGAGTGTGGGGTTTTGG	genotyping
gis2-1	AATCATCAAGGCAAATCCGCA	genotyping
gis2-1	TGCTACCACCACCGACATACG	genotypi

		ng
amiRNA A	CTGCAAGGCGATTAAGTTGGGTAAC	cloning
amiRNA B	GCGGATAACAATTTCACACAGGAAACAG	cloning
spl9tdna	TGG TTC CTC CAC TGA GTC ATC	genotyping
spl9tdna	GCT CAT TAT GAC CAG CGA GTC	genotyping
sailLB	GCC TTT TCA GAA ATG GAT AAA TAG CCT TGC TTC C	genotyping
rSPL9F	CGC CTT AAG CTT GTT AAG CAA TCC ACA TCA ACC ACA T	genotyping
rSPL9 R	GCT TAA CAA GCT TAA GGC GCA GTT TGA GTC GCC AAT TC	genotyping
egl3F	CCCCGGAGGAGCGTTATCCAATGGA	genotyping
egl3R	CGGAGTGTATTTATCGTCACTTAAGGG	genotyping
DM242REF1F	AAGCGGTTGTGGAGAACATGATACG	qPCR
DM243REF1R	TGGAGAGCTTGATTTGCGAAATACCG	qPCR
DM_gl1-2_F	GCAAAATTCATCATTACGAGTG3	genotyping
DM_gl1-2_R	TCATCTCAGCAAAAAACTCG3	genotyping
DM_zfp8-1_F	AAAGGAGGATTGATGGGTTTGTT	genotyping
DM_zfp8-1_R	TCGGAGTTATCACCGACGAGC	genotyping
DM_gis2-1_F	TGATGGTAGTTCGACGGGTAG	genotyping
DM_gis2-1_R	TGGTCCGGTACATTCTTCTTG	genotyping
DM_spl9-4_F	TGGTTCCTCCACTGAGTCATC	genotyping
DM_spl9-4_R	GCTCATTATGACCAGCGAGTC	genotyping
DM_spl15-1_F	TGTTGGTGTCTGAAGTTGCTG	genotyping
DM_spl15-1_R	AGGAAGCCAAAACCATAATGG	genotyping
DM_cpc-1_LB	CACATCATCTCATTGATGCTTGGT	genotyping
DM_cpc-1_F	GTATAAACTCGTTGGCGACAG	genotyping
DM_cpc-1_R	AGTAATTCAAGGACAGGTAC	genotyping
DM_try-29760_F	TGATAAACTCCCATTCGATACTGCT	genotyping
DM_try-29760_R	AACATCGTTGAACTTGCATCTG	genotyp

		ng
DM_gl3-1_F	TCAGTACGGAGCCTTTTCCAACAGC	genotyping
DM_gl3-1_R	CTTTAACATTCCTTGTGATGGTGCC	genotyping
DM_tcl1-1_F	TTGCGTCATTTGTGGGAGAA	genotyping
DM_tcl1-1_R	CGTGAGAGTCAGGATCTGTCC	genotyping
DM_shp1-1_F	GTCTACTGATGAGTTGTCACTAGG	genotyping
DM_shp1-1_R	GTGACGGAAGGAGGGTTGACG	genotyping
DM_shp1-1_T-DNA	GATGCACTCGAAATCAGCCAATTTTAGAC	genotyping
DM_shp2-1_F	GAGGATAGAGAACACTACGAATCGTC	genotyping
DM_shp2-1_R	CAGGTCAAGTCAATAGATTCCCTAC	genotyping
DM_SHP2_SalI_F	ATGTCGACTAGAAATGGAGGGTGGTGCGAGT	cloning
DM_SHP2_MluI_R	ACGCGTAGAACAAGTTGCAGAGGTGGTT	cloning
qDS7_ARR5_F	AAGTTACTGTTGTCGATAGTGCGAC	qPCR
qDS8_ARR5_R	CTT CAG ATC CTC AAA TCC AAC CGA A	qPCR
qDS9_ARR6_F	GTCGACGACAGTCACGTTGATCG	qPCR
qDS10_ARR6_R	GCT CTT GTT GCA CTA TCA ACA ACA GT	qPCR
qDS11_ARR6_F	CCGGTATGACTGGATATGAACTCTTG	qPCR
qDS12_ARR6_R	GTT CTC GGA GGA CAT AAT TAC CAC CG	qPCR
qDS13_HEC1_F	ACAGCTTCGATGCTCGATGAAGC	qPCR
qDS14_HEC1_R	CGT CAT TCC ACC TCC ACC GA	qPCR
qDS15_HEC2_F	GGT GGT TAA CGG CGG AGG AAT G	qPCR
qDS16_HEC2_R	GCA TCT GGT GAT GAT CAG ACC GCA TA	qPCR
qDS17_DRNL_F	TTAGCTGACTTCCATGTCGAAGGAA	qPCR
qDS18_DRNL_R	CGT TCT GCT GCA TCT TAG CTG AAT CA	qPCR
qDS19_DRN_F	CCACTGTAACCATCGCCGGA	qPCR
qDS20_DRN_R	ACGAGCCGCAGAGTCGTAAG	qPCR
qDS21_SPL9_F	CAGTGCAGCAGGTTTCATCAGC	qPCR
qDS22_SPL9_R	CAC AGA GAG AGA CGC AGG CT	qPCR
qDS23_SPL8_F	CCA GCA ATG CAG CAG GTT CC	qPCR
qDS24_SPL8_R	CGT TCG GTG ACT TTG GAG TAG TCT	qPCR
qDS25_SPL15_F	AACAATGTAGCAGGTTTCACCAGC	qPCR
qDS26_SPL15_R	GGA GCG ATT CGA GAG TAA TGA GAA G	qPCR
JAGF	GGTTTCCCTATCCGTGGCCC	qPCR

JAGR	TCAGAGCGAGTGATGATCTTGAAACC	qPCR
LOBF	AGGCGAGTGTGG^GTTGTAAGAAG	qPCR
LOBR	AATTTGTGTGGCTCCTCCGGTG	qPCR
JLOF	ACCTCAACCACCACAGGTTC	qPCR
JLOR	TGAAGATGACACCGGAACCTG	qPCR
GL1F	CACAAGCTCCTCGGCAATAG^ATG	qPCR
GL1R	GCTGAGATGAGTGTTCCAGTAGTTC	qPCR
ZFP8F	GCCAAACGCGGTTCCATGAC	qPCR
ZFP8R	TGGTGGTGGTTGTTGAGGAAGC	qPCR
TCL1F	CCAAGTTCACTCATAGCTCTCAAG	qPCR
TCL1R	ATCTCCTTTGCCTCACGTCC	qPCR
CPCF	ATGTATAAACTCGTTGGCGACAGG	qPCR
CPCR	ACGACGCCGTGTTTCATAAGC	qPCR
CKX6F	TTCGTACACAACAGGGAAGATG	qPCR
CKX6R	ATACTTGGTTGGTGCGTATTGG	qPCR
SUPF	GAGGCTGGAGAGGCTACAAG	qPCR
SUPR	AATTAAGCGAAACCCAAACGGAG	qPCR

Supplementary Table 2: SUP-amiRNA target sequences

Name	Sequence	Target in CDS	Phenotype
SUP-amiRNA1	TACTCATGATCCTTTTGGCGT	247nt	None
SUP-amiRNA2	TACCTGAATTCCCATTTGCGG	289nt	None
SUP-amiRNA3	TACGGTGAAGTTCCTGCACGG	355nt	sup-like

Supplementary Table 3: *SUPERMAN* CRISPR/Cas target sequence

Name	Nucleotide targets	Sequence
SUP-CRISPR 1	83	aaagaaagagcttgcacata
SUP-CRISPR 2	153	agaacttcaccatggagcta